

Oxidative Copper-Catalyzed Arylation of sp^3 -Carbon Centers via Decarboxylation

by

Anis Fahandej-Sadi

A thesis submitted in partial fulfillment of the requirements for the degree of

Master of Science

Department of Chemistry
University of Alberta

© Anis Fahandej-Sadi, 2018

Abstract

Transition-metal catalyzed cross-coupling reactions are a broad set of tools that enable the generation of molecular complexity by coupling together molecular pieces. This is done by the use of activating groups on the molecular pieces and a metal-based catalyst. These methods are widely used in synthetic chemistry, including (but not limited to) the production of materials (such as polymers), pharmaceuticals, and agrochemicals. Typical cross-coupling reactions involve the coupling of nucleophilic partners to electrophilic species. Alternatively, oxidative cross-coupling reactions, which enables the coupling of two nucleophilic reactants, have undergone significant developments since their initial discovery over a century ago. The functional group selectivity of these transformations is in complement to established nucleophile-electrophile cross-coupling reactions, due to the reactivity profile of the metal catalyst used and the conditions employed therein. Oxidative cross-couplings to generate carbon-heteroatom bonds are well established. Less work has been conducted into the development of carbon-carbon forming reactions under mild oxidative conditions.

Decarboxylation reactions of carboxylic acids, to generate both carbanions and carbon-based radicals, have been extensively utilized in synthetic chemistry. These reactions have been demonstrated to occur under a variety of conditions, utilizing both metals catalysts and organocatalysts, and undergoing both one and two-electron chemistry. The myriad of initiation methods for the decarboxylation of carboxylic acids makes these functional groups an attractive source of radical and nucleophilic carbon centres. However, typical conditions to initiate decarboxylation are quite harsh, usually consisting of elevated temperatures above 100 °C. This thesis will cover two reactions that merge the areas of decarboxylative chemistry and oxidative cross-coupling reactions, in order to facilitate the arylation reactions of sp^3 -carbon centers.

Organic molecules containing at least one fluorine atom play an important role in the pharmaceutical and agrochemical industries. This is due, in part, to the unique properties that fluorine can impart onto a molecule. These unique properties drive the demand for the development of synthetic methods to generate molecules containing carbon-fluorine bonds. Copper(II) triflate mediated the synthesis of α -aryl- α -fluoro acetates by the oxidative decarboxylative coupling of arylboroxines and arylboronic esters with monofluoro malonate half esters. The reaction proceeded with good to excellent yields across a variety of substrates under mild conditions. Functional group tolerances included electrophilic moieties that would be prone to reactions under traditional coupling conditions, such as aryl halides and Michael acceptors.

Diarylmethanes are found in many biologically active compounds and tailored pharmaceuticals. Recent work into synthesizing these molecular templates focused on the generation of benzyl anions by decarboxylation of *ortho* or *para*-nitrophenyl acetates and their use in palladium-catalyzed cross-coupling reactions. The conditions for this process are quite harsh, utilizing temperatures in excess of 100 °C. With temperatures as low as 35 °C, we have developed a copper(II) acetate mediated reaction to generate diarylmethanes by the oxidative coupling of *ortho*-nitrophenyl acetates and arylboronic esters. This reaction exhibits exceptional chemoselectivity, as it is tolerant towards electrophilic functionalities such as aryl-halides, Michael acceptors, and aldehydes, as well as protic functionalities such as secondary amides and primary alcohols. The utility of these diarylmethane molecules was further exemplified in functionalization work that diversified both the nitroarene and the methylene position of these molecules. We proposed a mechanism for this reaction centered on a decarboxylation event preceding the oxidative carbon-carbon bond formation.

Preface

All of the research conducted for this thesis was performed in collaboration with Rylan Lundgren. Chapter 2 has been published as Fahandej-Sadi, A.; Lundgren, R. J.; “Copper-Mediated Synthesis of Monofluoro Aryl Acetates via Decarboxylative Cross-Coupling” *Synlett*, **2017**, *28*, 2886-2890. Competition studies (Figure 2-19, Figure 2-20, Figure 2-21) and the trifluoroethyl ester example (**2.65**) were carried out by Patrick Moon. The reaction optimization and the remaining scope examples in chapter 2 and the compilation of the supporting information are my original work.

Chapter 3 has been accepted for publication as Moon, P. J.; Fahandej-Sadi, A.; Qian, W. “Decarboxylative Benzylolation of sp^2 -Organoboron Reagents” *Angew. Chem. Int. Ed.* **2018** DOI: 10.1002/anie.201800829. Initial reaction discovery and the optimization of the benzylolation chemistry were carried out by Patrick Moon. Synthesis and isolation of **3.62** was conducted by Emily Willette. Synthesis and isolation of **3.94** was conducted by Patrick Moon. The remaining work, including scope and functionalization investigations, as well as the compilation of the supporting information, are my original work.

Acknowledgements

I have so many people to thank for making this work a reality, and for making my time in Edmonton and at the University of Alberta a memorable experience.

I would like to extend my sincerest thanks to all of the members of the Lundgren group, including both past (Heather Halperin, Jenner Lakusta, Ping Shen, Bryce Thomas, Shengkang Yin) and current members (Chris Cooze, Raphael Dada, Ruohua Gui, Wenyu “Mac” Qian, Zhongyu Wei). A very special thanks goes out to Patrick Moon, for his guidance both in and out of the lab, for encouraging my good ideas and discouraging my bad ones, for putting up with all of my incessant questions and inquiries, and for being the star in way too many Snapchat videos; moms’ spaghetti will always have a warm, noodle-filled place inside my heart. I would also like to extend the warmest acknowledgement to all of those students and post-doctoral fellows within the department that I am honoured to call my friends. I will be forever grateful for the friendship and companionship that you have all provided through this graduate student experience, and I hope that I am just as much a friend to all of you as you all are to me. Special shout-outs to my gym partner Riley Endean, Meagan Oakley for all of the coffee breaks and life advice, and Matthew Michael David Roy for all of the escapades and hilarious stories that we now have. Jose Rodriguez (former undergrad at UofA, currently an exceptional PhD student at the University of Toronto) is acknowledged for being my brother-in-arms through the gauntlet that was Chem 463/563 and for his enduring friendship after that.

I would like to thank all of the individuals that make possible the outstandingly fantastic mass spectrometry and NMR spectroscopy facilities at the University of Alberta. Particular thanks are given to Jing Zheng and Dr. Angelina Morales-Izquierdo for the acquisition of mass-spectrometry data, and Mark Miskolzie for his Wizard-Level proficiency and knowledge in all

things NMR. Thanks for putting up with all of my questions, for your exceptionally entertaining anecdotes, and for the banter. I would also like to thank the members of my committee, Dr. Jillian Buriak and Dr. Ratmir Derda, for their input and guidance throughout my time at the University of Alberta.

I would like to give a huge thank you to Rylan Lundgren for taking me on as a graduate student and seeing me through this dissertation. His guidance, advice, and endless (*endless*) patience throughout have made this an invaluable experience of which I am eternally thankful for.

Thank you Mom and Dad for your endless and tireless support throughout my entire life and through all of my endeavours. Thank you for pushing me to be my best and for always believing in me, especially in those times that I did not believe in myself.

Thanks are extended to my roommates, Kolton Meier and Jordan Birch, as well as their cats Bandit (rest in peace), Comet, and Nova. This was my first time living away from home (and first time living with pets!), and they all made it an enjoyable and memorable experience. I would also like to thank Sarah Parke and Eric Koch; I was good friends with these two before I moved to Edmonton, and their friendship in those early days in Edmonton were a welcome sight in what was to me a new and strange place, full of new and strange faces.

The Government of Alberta and NSERC are thanked for financial support throughout the course of my program.

Table of Contents

Abstract.....	ii
Preface.....	iv
Acknowledgements	v
List of Tables	x
List of Figures.....	xii
Abbreviations	xviii

Chapter 1 – Oxidative Cross-Coupling & Decarboxylation of Carboxylic Acids: Fundamental Aspects and Current Applications

1.1 Metal-Catalyzed Cross-Coupling Reactions.....	1
1.2 Oxidative Cross-Coupling Reactions.....	4
1.2.1 Concept of Oxidative Cross-Coupling.....	4
1.2.2 Representative Examples of Oxidative Cross-Coupling.....	6
1.2.3 Mechanistic Investigations into Oxidative Cross-Coupling	9
1.2.4 Modern Example of Oxidative C-C Bond Formation Catalyzed by Copper.....	19
1.3 Decarboxylation in Metal-Catalyzed Cross-Coupling Reactions.....	21
1.3.1 Fundamental Aspects of a Decarboxylation Reaction	21
1.3.2 Decarboxylation in Nature and Decarboxylative Organocatalysis	22
1.3.3 Decarboxylation in Metal-Catalyzed Reaction	23
1.3.4 Radical Initiated Decarboxylation	25

CHAPTER 2 – Copper-Mediated Synthesis of Monofluoro Aryl Acetates via Decarboxylative Cross-Coupling

2.1 Introduction.....	30
2.1.1 Molecules Containing Carbon-Fluorine Bonds	30

2.1.2 α -Fluorination of Aryl Acetates.....	33
2.1.3 α -Arylation of Monofluoro Acetates.....	37
2.2 Reaction Optimization.....	42
2.3 Reaction Scope.....	47
2.3.1 Scope of Mono-Substituted Arylboroxines.....	48
2.3.2 Scope of Poly-Substituted and Heteroaromatic Arylboroxines and Arylboronic Neopentyl Glycol Esters.....	49
2.3.3 Scope of Ester Substitutions of the Monofluoro Malonate Half Ester.....	52
2.3.4 Unsuccessful Substrates.....	52
2.4 Mechanistic Considerations.....	56
2.5 Summary.....	63
2.6 Procedures and Characterization.....	65
2.6.1 General Considerations.....	65
2.6.2 General Procedures for the Copper Catalyzed Synthesis of Mono-Fluoro Aryl Acetates via Decarboxylative Cross-Coupling.....	66
 CHAPTER 3 – Synthesis of Diarylmethanes <i>via</i> Decarboxylative Benzylation of sp^2- Organoboron Reagents: Scope and Functionalization	
3.1 Introduction.....	80
3.1.1 The Diarylmethane Unit.....	80
3.1.2 Diarylmethane Synthesis by Friedel-Crafts Alkylation.....	82
3.1.3 Nucleophile-Electrophile Cross-Coupling to Synthesize Diarylmethanes.....	84
3.1.4 Diarylmethane Synthesis via Radical Chemistry.....	88

3.1.5 Synthesis of Diarylmethanes by Palladium-Catalyzed Decarboxylative Electrophile Trapping of Nitroaryl Acetates	91
3.2 Reaction Optimization	95
3.3 Reaction Scope	97
3.3.1 Scope of Mono-Substituted Arylboronic Esters	97
3.3.2 Scope of Poly-substituted and Complex Arylboronic Esters.....	100
3.3.3 Scope of Heteroaromatic Arylboronic Esters	104
3.4 Functionalization Studies on Benzylated <i>Ortho</i> -Nitrobenzenes.....	105
3.5 Proposed Mechanism.....	111
3.6 Summary.....	112
3.7 Procedures and Characterization	114
3.7.1 General Considerations.....	114
3.7.2 Synthesis of Starting Materials	115
3.7.3 Oxidative Benzylation Procedures and Characterization Data	116
3.7.4 Functionalization Procedures and Characterization Data	133
REFERENCES.....	138

List of Tables

Table 2-1	Effect on reaction performance of the optimized reaction when compared to the previously employed reaction conditions for the ethyl malonate half ester43
Table 2-2	Effect of the boronic acid/ester on the decarboxylative oxidative arylation of a monofluoro malonate half ester44
Table 2-3	Effect of the copper species on the decarboxylative oxidative arylation of a fluromalonate half ester45
Table 2-4	Effect on the atmosphere on the decarboxylative oxidative arylation of a monofluoro malonate half ester46
Table 2-5	Effect of various parameters on the decarboxylative oxidative arylation of a monofluoro malonate half ester47
Table 2-6	Copper-mediated oxidative decarboxylative arylation of monofluoro malonate half esters using mono-substituted arylboroxines, Part 148
Table 2-7	Copper-mediated oxidative decarboxylative arylation of monofluoro malonate half esters using mono-substituted arylboroxines, Part 249
Table 2-8	Copper-mediated oxidative decarboxylative arylation of monofluoro malonate half esters using polysubstituted and heteroaromatic arylboroxines and arylboronic esters51
Table 2-9	Copper-mediated oxidative decarboxylative arylation of monofluoro malonate half esters with variations on the ester52
Table 2-10	Unsuccessful aryl examples in the copper-mediated oxidative decarboxylative arylation of monofluoro malonate half esters53
Table 2-11	Attempted copper-mediated oxidative arylation of α -fluoro carbonyls55
Table 3-1	Effect of water on the copper-mediated oxidative decarboxylative benzylation of arylboronic esters96
Table 3-2	Effect of modulating the area of atmosphere exposure on the copper-mediated oxidative decarboxylative benzylation of arylboronic esters.....96
Table 3-3	Copper-mediated oxidative decarboxylative benzylation of mono-substituted arylboronic esters with electron-withdrawing groups, Part 198

Table 3-4	Copper-mediated oxidative decarboxylative benzylation of mono-substituted arylboronic esters with electron-withdrawing groups, Part 2	99
Table 3-5	Copper-mediated oxidative decarboxylative benzylation of mono-substituted arylboronic esters with electron-donating groups.....	100
Table 3-6	Copper-mediated oxidative decarboxylative benzylation of poly-substituted arylboronic esters	102
Table 3-7	Copper-mediated oxidative decarboxylative benzylation of complex arylboronic esters with electron-withdrawing groups	103
Table 3-8	Copper-mediated oxidative decarboxylative benzylation of heteroaromatic arylboronic esters	105

List of Figures

Figure 1-1	Generic example of a cross-coupling reaction.....	1
Figure 1-2	(Non-comprehensive) list of nucleophiles and electrophiles used in cross-coupling reactions	2
Figure 1-3	Schematic metal-catalyzed cross-coupling catalytic cycle.....	3
Figure 1-4	Examples of materials and pharmaceuticals that utilize metal-catalyzed cross-coupling in their synthesis	4
Figure 1-5	Schematic oxidative cross-coupling reaction.....	5
Figure 1-6	Schematic metal-catalyzed oxidative cross-coupling catalytic cycle	5
Figure 1-7	Orthogonal reactivity exhibited by palladium and copper.....	6
Figure 1-8	Glaser and Hay alkyne oxidative coupling with copper	7
Figure 1-9	Proposed dinuclear mechanism for alkyne coupling catalyzed by copper	7
Figure 1-10	Schematic Chan-Evan-Lam reaction	8
Figure 1-11	Example of Chan-Evans-Lam oxidative cross-coupling	9
Figure 1-12	Evans proposed pathway for copper-mediated etherification.....	10
Figure 1-13	Stahl mechanism for catalytic Cu(II)-catalyzed oxidative coupling of 4-tolylboronic acid derivatives (Ar-BX' ₂) and MeOH (X, X' = OAc, OMe, OH)...	12
Figure 1-14	Copper-catalyzed phenyl amination reaction with imidazole.....	13
Figure 1-15	(A) Proposed mechanism for imidazole arylation by oxidative copper-catalysis; (B) alternative disproportionation mechanism.....	15
Figure 1-16	(A) structure of arylboronic acid pinacol (Bpin) esters; (B) schematic metal-catalyzed methodologies for Bpin synthesis.....	16
Figure 1-17	Investigated amination of aryl-Bpin reagents, promoted by copper.....	17
Figure 1-18	(A) Activation and deactivation of [Cu(OAc) ₂] ₂ paddlewheel complex; (B) amine promoted Cu(I) oxidation pathway; (C) Cu(I) promoted arylboronic acid decomposition.....	18

Figure 1-19	(A) reversible binding of B(OH) ₃ to pinacol and acetate; (B) effect on reaction selectivity with increased amine stoichiometry; (C) overall optimized copper-catalyzed amination conditions.....	19
Figure 1-20	Aldehyde α-alkenylation by copper and amine catalysis	20
Figure 1-21	Formation and imine trapping of an activated Cu(III) alkene complex.....	20
Figure 1-22	(A) Arylation of malonate derivatives by oxidative coupling; (B) proposed synthesis of aryl acetates by decarboxylative oxidative coupling	21
Figure 1-23	(A) Decarboxylation from a negatively-charged carboxylic acid results in the formation of a carbonation; (B) decarboxylation from an oxygen-based radical on the carboxylic acid results in the formation of a carbon-based radical.....	22
Figure 1-24	Enzymatic decarboxylative carbon-carbon bond forming (ACP = acyl carrier protein, KS = ketosynthase).....	23
Figure 1-25	(A) Biomimetic decarboxylative carbon-carbon bond formation; (B) proposed mechanism	23
Figure 1-26	(A) Schematic palladium-catalyzed Suzuki cross-coupling reaction; (B) examples utilizing aryl-carboxylic acids as the nucleophile equivalent.....	25
Figure 1-27	Decarboxylation and bis(aryl)palladium formation with (A) palladium or (B) silver.....	25
Figure 1-28	(A) Copper-catalyzed decarboxylative alkynylation of α-amino acids; (B) proposed mechanism.....	27
Figure 1-29	Photocatalytic SET generation of a carbon-based radical via decarboxylation coupled to a nickel-catalyzed cross-coupling reaction	28
Figure 1-30	Copper-catalyzed decarboxylative arylation of malonate half-esters.....	29
Figure 1-31	(A) Copper-mediated oxidative decarboxylative arylation of monofluoro malonate half-esters; (B) copper-mediated oxidative decarboxylative arylation of <i>ortho</i> -nitroaryl acetates	29
Figure 2-1	Synthesis of monoaryl acetates by decarboxylative oxidative cross-coupling, utilizing either a malonate or monofluoro malonate half-ester.....	30

Figure 2-2	(A) effect on acidity; (B) effect on the rate of H-D exchange; (C) effect on the nucleophilicity (D) combined effects of α -hydrogen acidity and anion nucleophilicity.....	32
Figure 2-3	Synthetic strategies for the synthesis of monofluoro aryl acetates	32
Figure 2-4	α -fluorination by anodic oxidation	33
Figure 2-5	Copper-catalyzed fluorination of aryl diazoesters using potassium fluoride.....	34
Figure 2-6	(A) Deoxyfluorination reagents utilizing N-heterocyclic scaffolds; (B) nucleophilic deoxyfluorination utilizing <i>Alkylfluor</i> , with proposed O-bound N-heterocycle intermediate	35
Figure 2-7	Electrophilic fluorination and substitution of a metal-ketene-enolate	36
Figure 2-8	S_NAr reaction to generate monofluoro aryl acetic acids	38
Figure 2-9	(A) Palladium-catalyzed and nickel-catalyzed Suzuki cross-coupling to generate aryl fluoro acetates; (B) nickel-catalyzed Hiyama coupling to generate aryl fluoro acetates	39
Figure 2-10	Proposed radical mechanism for nickel-catalyzed Suzuki and Hiyama cross-coupling reactions to generate aryl fluoro acetates.....	40
Figure 2-11	(A) C-H functionalization by iridium photocatalyst for the generation of fluoro-acetate substituted benzoheterocycles ($Ir^{III*} = \text{photoexcited } Ir^{III}$); (B) proposed mechanistic pathway.....	41
Figure 2-12	Copper-mediated decarboxylative oxidative methodology to synthesize monofluoro aryl acetates.....	41
Figure 2-13	Optimized conditions for the copper-mediated decarboxylative oxidative cross-coupling of arylboroxines and monofluoro malonate half esters to synthesize α -fluoro- α -aryl acetates	42
Figure 2-14	Attempted oxidative decarboxylative synthesis utilizing <i>ortho</i> -tolylboroxine (2.82), instead yielding an <i>O</i> -arylated ester (2.84) and further α -arylated product (2.85).....	56
Figure 2-15	Proposed mechanistic pathways for monofluoro aryl acetate synthesis by oxidative cross-coupling	57

Figure 2-16	(A) Effect on the decarboxylation of the α -carboxy product in the presence of DMA (\pm Cu(OTf) ₂) or DCE solvent; (B) NMR evidence for the <i>in situ</i> generation of the α -carboxy intermediate.....	58
Figure 2-17	(A) Migration from carboxylate (17-I) to α -carbon (17-II) binding to copper centre, followed by reductive elimination to yield the α -arylated product prior to decarboxylation; (B) alternative bimolecular mechanism relying on the formation of a copper-bound enolate (17-V).....	59
Figure 2-18	(A) Proposed reaction for generating the <i>O</i> -arylated product (2.84); (B) proposed reaction to form the α -arylated product (2.85)	60
Figure 2-19	Competition study under malonate half ester optimized conditions.....	61
Figure 2-20	Competition study under monofluoro malonate half ester optimized conditions..	62
Figure 2-21	Competition study utilizing trifluoroethyl-ester (2.64) and α -fluoro malonate half ester (2.26)	63
Figure 3-1	Diarylmethane containing molecule with potential uses in treating various conditions.....	81
Figure 3-2	Methodologies for the synthesis of diarylalkanes.....	81
Figure 3-3	Schematic Friedel-Crafts alkylation	82
Figure 3-4	(A) Ferrocenium boronic acid catalyzed FC reaction; (B) proposed formation of carbocation stabilized by solvation interactions and zwitterion formation	83
Figure 3-5	Triflic acid catalyzed FC reaction.....	84
Figure 3-6	(A) Base-mediated coupling of arylboronic acids and benzyl halides; (B) fluoride-mediated coupling of arylboronic acids and benzyl mesylates.....	85
Figure 3-7	Mechanistic steps of arylboronic acid coupling to benzyl halides/mesylates under metal-free conditions	85
Figure 3-8	Schematic synthesis of diarylalkanes (benzylic-substituted diarymethanes)	86
Figure 3-9	Nickel-catalyzed Negishi-arylation to generate diarylalkanes	86
Figure 3-10	Quaternary stereocenters synthesis by nickel-catalyzed cross-coupling	87

Figure 3-11	Catalytic cycle for nickel-catalyzed quaternary-center synthesis (PY ₃ = <i>CyJohnPhos</i>).....	88
Figure 3-12	Copper-mediate cross-dehydrogenative-coupling of electron-rich arenes with toluenes	89
Figure 3-13	Stahl (A) and Liu (B) systems for copper-catalyzed radical synthesis of diarylalkanes	89
Figure 3-14	Catalytic cycle for copper-catalyzed radical synthesis of diarylalkanes (X, Y = <i>t</i> BuO or X = F, Y = N(S(O) ₂ Ph) ₂)	90
Figure 3-15	Example of diarylation of unhindered benzyl positions with electron-deficient arylboronic acids.....	91
Figure 3-16	Nitroaryl acetate decarboxylation and anion resonance	92
Figure 3-17	Palladium-catalyzed decarboxylative cross-coupling of nitrophenyl acetates with activated electrophiles.....	92
Figure 3-18	Catalytic cycle for palladium-catalyzed decarboxylative cross-coupling of nitrophenyl acetates with alkenyl-triflates	93
Figure 3-19	Copper-mediated oxidative decarboxylative coupling of arylboronic esters and nitrophenyl acetates	94
Figure 3-20	Optimized reaction conditions for the oxidative decarboxylative copper-mediated synthesis of diarylmethanes by coupling of arylboronic esters and <i>ortho</i> -nitroaryl acetates	95
Figure 3-21	Cu-carboxylate synthesis of a diarylmethane containing a terminal alcohol	103
Figure 3-22	Nitroaryl acetate decarboxylation and anion resonance	106
Figure 3-23	(A) Zinc metal mediated reduction of a nitroarene (3.94) to an aniline (3.95); (B) S _N Ar byproduct (3.97) generated under aqueous conditions.....	107
Figure 3-24	Deaminoiodination to generate an aryl iodide (3.98) via a diazonium salt intermediate (3.99).....	108
Figure 3-25	Deaminoborylation to generate an aryl-Bpin (3.100) via a diazonium salt intermediate.....	108

Figure 3-26	(A) Palladium-catalyzed Heck-Matsuda reaction to generate a functionalized alkene (3.101) via a diazonium salt intermediate; (B) proposed mechanism of dual-catalysis to generate sub-stoichiometric quantities of aryl-diazonium salt intermediate, coupled to a palladium-catalyzed Heck-Matsuda reaction110
Figure 3-27	Methylene allylation to generate allylated product (3.103)111
Figure 3-28	Proposed mechanisms for the copper-mediated decarboxylative oxidative synthesis of diarylmethanes by coupling of <i>ortho</i> -nitrophenyl acetates and arylboronic esters112

Abbreviations

Å	Ångström
acac	acetylacetone
aq.	aqueous
°C	degrees Celsius
Ar	generic aryl moiety
Bn	benzyl
Bneop	neopentyl glycol boronic ester
Boc	<i>tert</i> -butyloxycarbonyl
BOX	bisoxazoline
Bpin	pinacol boronic ester
bpy	2,2'-bipyridine
cat.	catalytic stoichiometry
CEL	Chan-Evans-Lam
Cy	cyclohexyl
δ	chemical shift
DCE	1,2-dichloroethane
DCM	dichloromethane
DMS	dimethyl sulfide
DMA	<i>N,N</i> -dimethylacetamide
DMF	<i>N,N</i> -dimethylformamide
dme	1,2-dimethoxyethane
DiPPF	1,1'-bis(<i>di-isopropylphosphino</i>)ferrocene

equiv.	equivalents
EPR	electron paramagnetic resonance
FC	Friedel-Crafts
Et	ethyl
Hex	hexane (mixture of isomers)
h ν	light
HFIP	1,1,1,3,3,3-hexafluoroisopropanol
HRMS	high resolution mass-spectroscopy
<i>i</i> Pr	iso-propyl
L	generic ligand
LG	generic leaving group
[M]	generic metal complex
Me	methyl
MeCN	acetonitrile
Ms	methylsulfonyl
NEt ₃	triethylamine
NFSi	<i>N</i> -fluorobenzenesulfonamide
NMR	nuclear magnetic resonance
NMP	<i>N</i> -methylpyrrolidine
OAc	acetate
OTf	triflate
Ph	phenyl
Phen	phenanthroline

ppy	2-phenylpyridyl
R	generic group
rt	room temperature
S _N Ar	bimolecular nucleophilic aromatic substitution
<i>t</i> Bu	<i>tert</i> -butyl
TBS	<i>tert</i> -butyldimethylsilyl
THF	tetrahydrofuran
TLC	thin-layer chromatography
TMEDA	tetramethylethylenediamine
TMS	trimethylsilyl
Tol	tolyl
Ts	4-toluenesulfonyl
UV	ultraviolet
X ⁻	generic anion
XAFS	X-ray absorption fine structure

Chapter 1 – Oxidative Cross-Coupling & Decarboxylation of Carboxylic Acids: Fundamental Aspects and Current Applications

1.1 Metal-Catalyzed Cross-Coupling Reactions

If one wishes to synthesize molecules of increasing complexity, it is necessary to have tools that enable the generation of new molecular bonds in a selective and efficient manner. One way in which new molecular bonds can be synthesized is through a *cross-coupling reaction*.¹ By definition, a cross-coupling reaction is a reaction where two molecules, each with an activating group, are coupled together, with the loss of the activating groups and the generation of a new covalent bond (Figure 1-1). It is important to note that the newly generated bond originates from the atoms previously occupied by the activating groups. Therefore, placement of activating groups serves as a method of dictating the reaction outcome. Typically, a metal-based catalyst mediates these reactions, with these reactions being referred to as *metal-catalyzed cross-coupling reactions*. Pioneering work in this area was predominantly conducted with palladium-based metal catalysts, and these still dominate the area of metal-catalyzed cross-coupling reactions.²⁻⁶

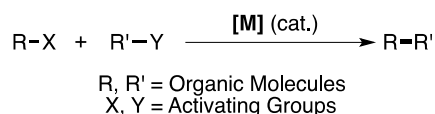


Figure 1-1 Generic example of a cross-coupling reaction

A common form of a metal-catalyzed cross-coupling reaction involves the coupling of a nucleophilic species (typically an organometallic or organoboron) and an electrophilic species (typically a halide or pseudo-halide-containing organic species) (Figure 1-2). For palladium-catalyzed reactions where a nucleophile and electrophile are coupled together, the sequence of

mechanistic events has been well-studied.⁷⁻⁸ The exact details for each step will vary depending on the nature of the nucleophilic and electrophilic species, but a general sequence of events can be provided (Figure 1-3). The first step will be the oxidative addition of the organic electrophile onto the metal center, generating an oxidized metal complex with a new metal–carbon bond. This complex will then react via a transmetalation with an organic nucleophile to generate a metal complex bound to two organic species. The metal center can now undergo a reductive elimination, a process that generates a new covalent bond (and thus the product) and returns the metal center to its original oxidation state; the metal center can now begin the reaction with a new set of substrates.

<u>Nucleophiles</u>		<u>Electrophiles</u>	
R–MgX	<i>Grignard</i>	R–Cl	<i>Organochloride</i>
R–ZnX	<i>Organozinc</i>	R–Br	<i>Organobromide</i>
R–SnR' ₃	<i>Organotin</i>	R–I	<i>Organiodide</i>
R–B(OR') ₂	<i>Organoboron</i>	R–OTf	<i>Organotriflate</i>
R–SiR' ₃	<i>Organosilane</i>	R–OTs	<i>Organotosylate</i>
R–CCH	<i>Alkyne</i>		
R = alkyl, alkenyl, alkynyl, aryl		R = alkyl, alkenyl, aryl	
R' = alkyl, aryl			
X = halide			

Figure 1-2 (Non-comprehensive) list of nucleophiles and electrophiles used in cross-coupling reactions

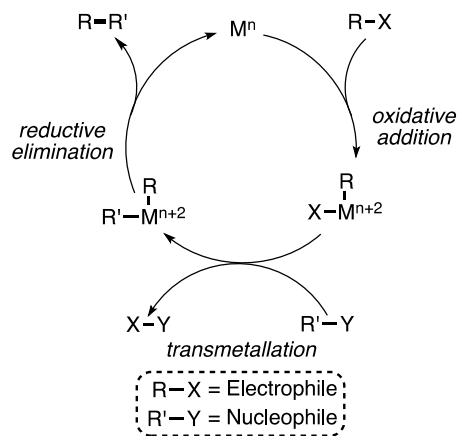


Figure 1-3 Schematic metal-catalyzed cross-coupling catalytic cycle

Metal-catalyzed cross-coupling reactions have been extensively studied for the better part of the last half-century, and have found multiple uses in the areas of materials chemistry and the pharmaceutical industry (Figure 1-4).⁹⁻¹² In addition to the preceding methods that deal with the metal-catalyzed cross-coupling of a nucleophilic species and an electrophilic species, there exists another cross-coupling regime that couples together two nucleophilic partners in an oxidative manner; this concept is referred to as *oxidative cross-coupling*, and is discussed in the next section.

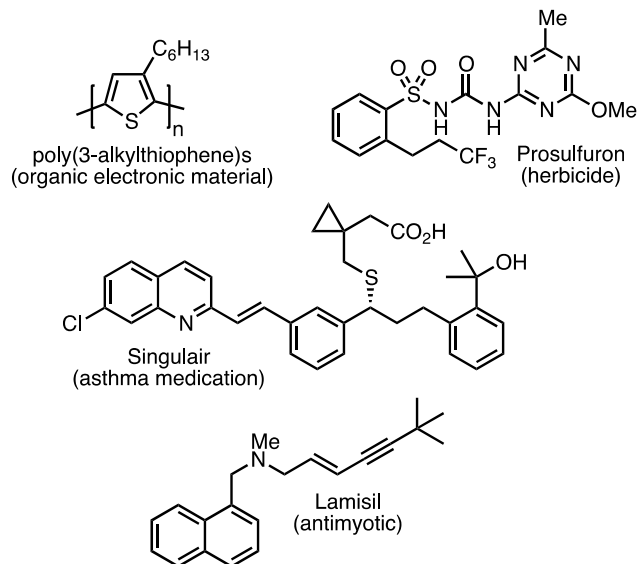


Figure 1-4 Examples of materials and pharmaceuticals that utilize metal-catalyzed cross-coupling in their synthesis

1.2 Oxidative Cross-Coupling Reactions

1.2.1 Concept of Oxidative Cross-Coupling

An oxidative cross-coupling reaction is a cross-coupling reaction where the two reacting species are both nucleophiles (Figure 1-5)¹³⁻¹⁵. At a first glance, this may seem illogical, as two nucleophiles would not typically interact in a bond-forming fashion due to similar polarities; however, with a suitable catalytic system, this reaction can be productive. A scheme of a metal-catalyzed oxidative cross-coupling is provided in Figure 1-6.¹⁶ An oxidized metal center can undergo two sequential transmetalations to generate a metal center bound to two organic species. This species can then undergo reductive elimination to generate a new covalent bond between the two organic fragments and reduce the metal center. The catalytic cycle has not been closed, as the starting point is a metal in the “n+2” oxidation state; in order to regenerate this species, an oxidant is utilized that oxidizes the metal center (hence the term *oxidative* cross coupling).

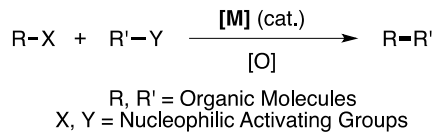


Figure 1-5 Schematic oxidative cross-coupling reaction

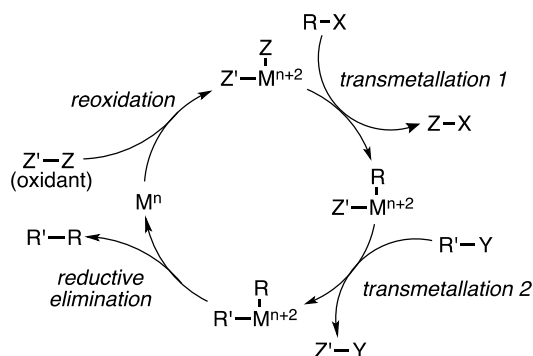


Figure 1-6 Schematic metal-catalyzed oxidative cross-coupling catalytic cycle

Often, oxidative cross-coupling reactions exhibit reactivity profiles orthogonal to nucleophile-electrophile reactions, as they are typically inert to aryl halides and Michael acceptors; this can be explained by considering the metal species utilized in each reaction. To illustrate, consider a palladium-catalyzed cross-coupling reaction and a copper-catalyzed oxidative cross-coupling reaction (Figure 1-7). The starting point for the palladium reaction is typically an electron-rich Pd(0) species, which will readily react with electrophilic substituents such as aryl halides and alkenes in conjugation with electron-withdrawing groups. In opposition, the starting point for a copper-catalyzed oxidative cross-coupling reaction is typically a Cu(II) species, which is electron-poor in comparison to the aforementioned Pd(0); generally, Cu(II) will

preferentially transmetalate with an electron rich species such as an arylboronic acid as opposed to reacting with electrophiles. This discrepancy in reactivity profile is what leads to the chemoselective orthogonality of oxidative cross-coupling reactions.

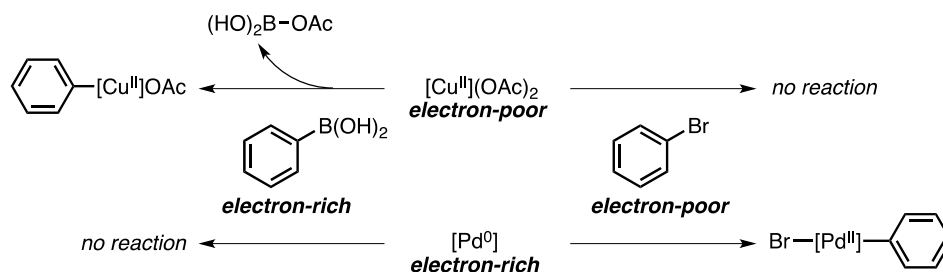


Figure 1-7 Orthogonal reactivity exhibited by palladium and copper

1.2.2 Representative Examples of Oxidative Cross-Coupling

Oxidative cross-coupling reactions involving copper have been known since the 19th century. One of the earliest examples of an oxidative cross-coupling reaction mediated by copper is the homocoupling of acetylenes to generate products like **1.3** (Figure 1-8)¹⁷, first reported by Glaser in 1869,¹⁸ with further improvement by Hay in 1962 with the inclusion of a catalytic TMEDA Cu(I) chloride complex utilizing organic solvents.¹⁹ Mechanistically, Clifford and Waters originally proposed the generation of free-radicals, originating from a copper-acetylide complex such as **1.2**, that would recombine *in situ* to generate the coupled dialkyne product²⁰; however, further studies by Bohlmann found that reactions involving different alkynes generated predominantly homocoupled products, an observation that is not reconcilable with a free radical mechanism.²¹ Instead, based on an observed second order rate dependence on the concentration of alkyne, the authors propose a dinuclear-Cu(I)-acetylide complex that cyclizes directly to the product (Figure 1-9).

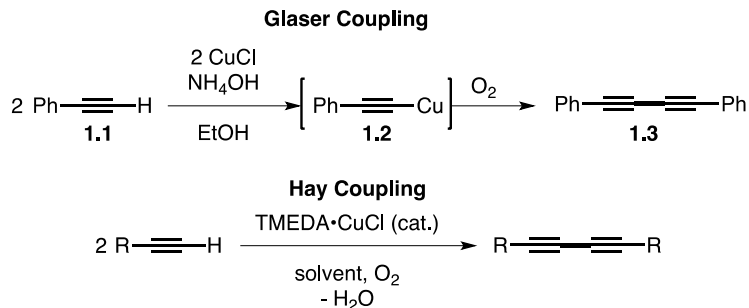


Figure 1-8 Glaser and Hay alkyne oxidative coupling with copper

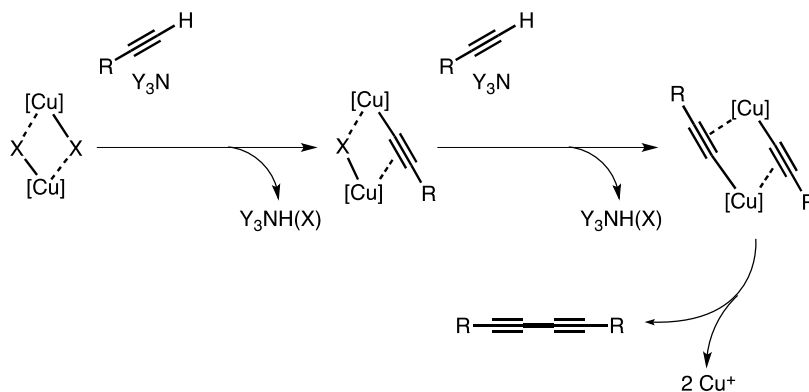


Figure 1-9 Proposed dinuclear mechanism for alkyne coupling catalyzed by copper

A more recent example of an oxidative cross-coupling reaction is the Chan-Evans-Lams (CEL) reaction (Figure 1-10).²²⁻²⁴ This reaction utilizes copper as a mediator or catalyst (depending on the conditions employed) to facilitate an oxidative bond forming reaction between an arylboronic acid and a protic heteroatom. In addition to oxygen and nitrogen heteroatom partners, as illustrated in the original three publications, additional developments have allowed

the use of sulfur²⁵, as well as selenium- and tellurium²⁶, species to form carbon-heteroatom bonds.

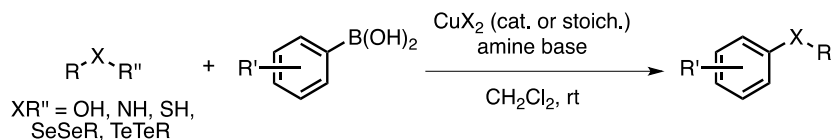


Figure 1-10 Schematic Chan-Evans-Lam reaction

The example presented in Figure 1-11 illustrates the chemoselectivity of this methodology, as a number of functional groups on **1.5** that would be reactive under nucleophilic-electrophilic cross-coupling conditions (such as the electron-poor aryl iodides and the acidic α -C-H of the ester) remain intact to generate the diarylether **1.6**. Other key features are that the reaction was conducted at room temperature and used a weak base (triethylamine). These conditions, and the previously discussed chemoselective orthogonality of oxidative cross-coupling reactions, combine to yield an exceptionally mild method for the formation of new carbon-heteroatom bonds.

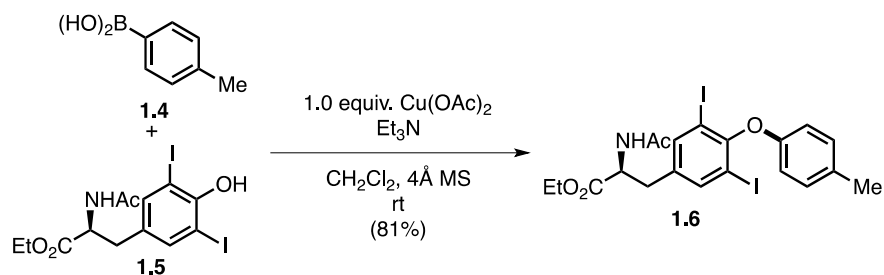


Figure 1-11 Example of Chan-Evans-Lam oxidative cross-coupling

1.2.3 Mechanistic Investigations into Oxidative Cross-Coupling

A complete picture of the mechanistic underpinnings of the CEL reaction have so far been elusive, with a number of investigations having been undertaken to yield various insights into the nature of the reaction. In Evans' early work,²³ specifically in regards to the stoichiometric etherification reaction, speculation was provided towards a transmetalation and phenoxide-trapping sequence of events from the Cu(II) starting material (Figure 1-12). The major uncertainty is to whether reductive elimination to form product occurs from a Cu(II) or Cu(III) species; an increase in product yield is observed when the reaction is exposed to oxygen, implying that an oxidized Cu(III) is the precursor to reductive elimination.

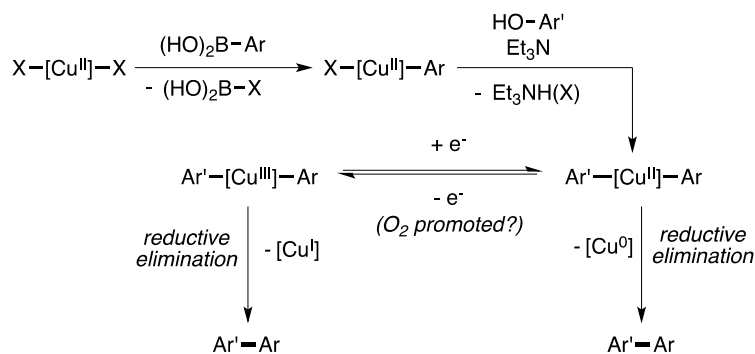


Figure 1-12 Evans proposed pathway for copper-mediated etherification

In two publications published in 2009²⁷ and 2012²⁸, the Stahl group reported their mechanistic investigations into the copper-catalyzed oxidative etherification reaction, utilizing a combination of stoichiometric, kinetic, and spectroscopic techniques. When the reaction is conducted under rigorously anaerobic conditions, a 2:1 Cu(II):product stoichiometry is observed, revealing the single-electron oxidant role of Cu(II); addition of oxygen back into the reaction to reoxidize Cu(I) reveals a 4:1 ratio of Cu(I) to O₂. Kinetic studies revealed a half-order dependence on copper, a zero-order dependence on O₂, and a saturation dependence on the boronic acid. EPR studies were conducted by analyzing liquid-nitrogen frozen aliquots of the active solution, with these indicating the near-complete presence of the copper as an EPR active Cu(II) species, as opposed to an EPR silent [Cu(OAc)₂]₂ paddlewheel-dimer. Addition of arylboronic acid to a solution of Cu(OAc)₂ in methanol generates the appearance of a two distinct EPR signals assigned to two Cu(II) species, implying a reaction between these two components and the formation of some sort of heterobimetallic Cu(II)-boron structure, and thus the generation of a putative aryl-Cu(II) species. This strongly implies that transmetalation is the

rate-limiting step, and transmetalation occurs prior to the oxidation of the copper or the formation of a copper-alkoxide (reaction of the copper with the oxygen coupling partner).

Utilizing this and additional insights, a mechanism for the copper-catalyzed CEL reaction was proposed by the Stahl group. A summary of those results are presented below (Figure 1-13); the reaction is proposed to begin from Cu(II) (**13-I**), which undergoes transmetalation with an arylboronic acid to generate a Cu(II)-aryl (**13-II**). This complex can undergo a disproportionation reaction with another Cu(II) species to become oxidized to Cu(III) (**13-III**). The generated Cu(III)-aryl complex undergoes a C–O reductive elimination with methanol, forming the new carbon-oxygen bond and generating a Cu(I) species (**13-IV**); this Cu(I) and the previous Cu(I) utilized in the oxidation step are both oxidized by molecular oxygen to Cu(II), restarting the cycle. A key point to address is that this mechanism is specifically for the C–O bond forming CEL reaction, and that this reaction was conducted with one of the reactive partners (methanol) as the solvent. As such, these studies do not so much as provide a rigorous mechanism for the general CEL reaction, but a set of tools that can be utilized to study related carbon-heteroatom bond-forming reaction utilizing copper.

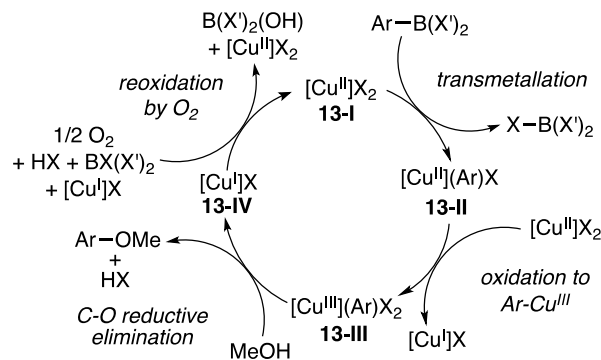


Figure 1-13 Stahl mechanism for catalytic Cu(II)-catalyzed oxidative coupling of 4-tolylboronic acid derivatives (Ar-BX'₂) and MeOH (X, X' = OAc, OMe, OH)

Mechanistic studies have also been undertaken into the related copper-catalyzed amination reaction utilizing arylboron reagents and protic amines. A 2010 study published by the Tromp group reported their mechanistic investigations into a copper-catalyzed amination reaction (Figure 1-14) involving the coupling of imidazoles (**1.8**) with arylboronic acids (**1.7**).²⁹ A number of *in situ* and time-resolved spectroscopic techniques, including X-ray absorption fine structure (XAFS), UV-vis, EPR, and NMR, were utilized. The conditions for this reaction vary considerably from the standard CEL reaction; no base is utilized, there is presence of a significant amount of water as part of the solvent, and oxygen is not required for catalytic turnover. However, as this is a conceptually related oxidative copper-catalyzed amination reaction, insights into the mechanism are nonetheless relevant.

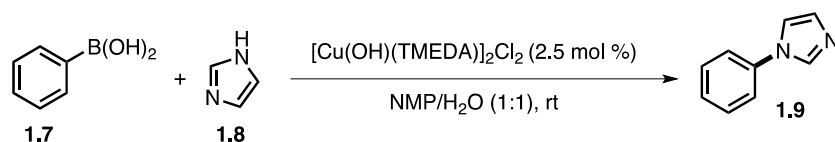


Figure 1-14 Copper-catalyzed phenyl amination reaction with imidazole

Firstly, as the oxygen is not required for catalytic turnover, the use of another oxidant within the reaction is implied. The addition of phenylboronic acid alone in a stoichiometric reaction with the copper dimer results in the fast formation of the biphenyl byproduct. If imidazole is added before the boronic acid, a cross-coupling reaction is observed, with both product and imidazole inhibition being reported. This implies that the imidazole interacts with the copper first, followed by the arylboron reagents, and that the imidazole functionality can act as an inhibitor if in excess quantities. XAFS data indicated that the hydroxide-bridged dimeric copper starting material is still intact in solution, implying that this is the entry point (and resting state) for the catalytic cycle. Stoichiometric studies using ^{11}B NMR indicated the presence of a boron hydride intermediate, $\text{H-B}(\text{OH})_2$, with further reaction in the presence of water to form the boric acid, $\text{B}(\text{OH})_3$. In addition, by EPR studies, phenylboronic acid was demonstrated to be oxidative in nature. As oxygen is not necessary for this reaction but water is essential (reactions conducted in only NMP generated no starting material conversion, but the use of water caused a rapid generation of a $\text{Cu}(\text{I})$ species), both phenylboronic acid and water are most likely involved in the reoxidation step.

A combination of the above data led the authors to propose two potential catalytic cycles. The first proposed cycle (Figure 1-15 A) begins with a base-promoted coordination of the imidazole resulting in the formation of an imidazole- $\text{Cu}(\text{II})$ species (**15-III**) from the bimetallic

hydroxide-bridged copper precursor (**15-I**). This can undergo a water-promoted copper-oxidation and transmetalation sequence that is followed by, through a Cu(III) intermediate (**15-IV**), a reductive elimination to generate the product and a Cu(I) species (**15-V**). This Cu(I) can be reoxidized to the Cu(II) starting material by a combination of water and arylboronic acid. The second mechanism (Figure 1-15 B) depends on a disproportionation pathway between two imidazole-Cu(II) complexes (**15-VI**), with the resulting Cu(III) (**15-VII**) undergoing a formal transmetalation with an arylborate to generate an imidazole-phenyl-Cu(III) complex (**15-IX**), which can reductively eliminate to give the product. As the authors state, further spectroscopic and kinetic studies are required to differentiate between these two cycles.

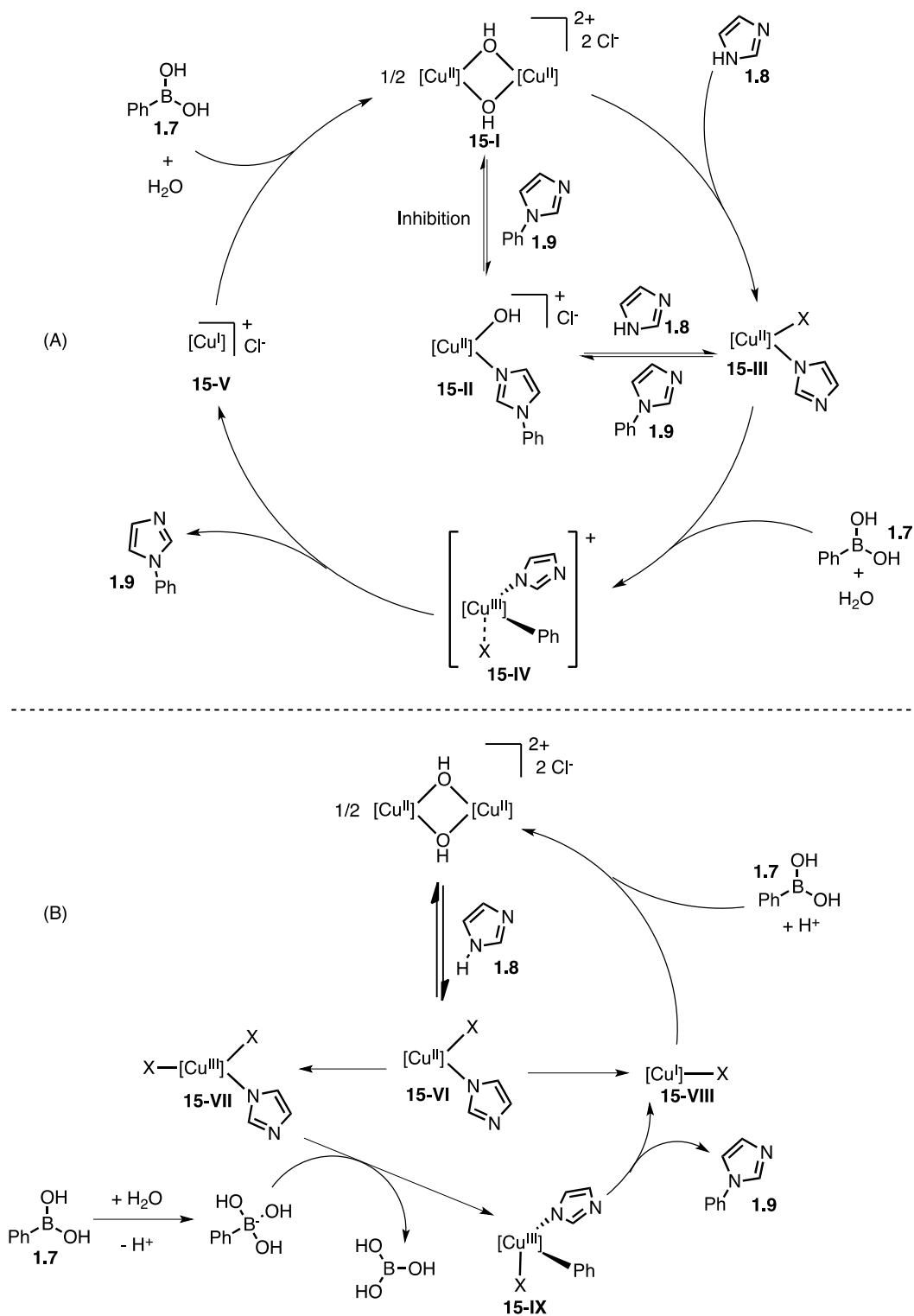


Figure 1-15 (A) Proposed mechanism for imidazole arylation by oxidative copper-catalysis; (B) alternative disproportionation mechanism

One way to increase the scope of CEL amination reactions is to be able to utilize arylboronic acid pinacol (Bpin) esters (**1.11**) (Figure 1-16 A). These reagents are typically more stable towards protodeboronation than their boronic acid counterparts,³⁰ and are readily accessible via various metal-catalyzed borylation reactions (Figure 1-16 B).³¹⁻³⁶ Unfortunately, these reagents typically exhibit reduced reactivity in CEL amination reactions, though solutions (typically through empirical experimentation) have been offered.³⁷⁻⁴¹ In order to provide a more concise and widely applicable solution to the Bpin problem, the Watson group instigated and subsequently reported a rigorous mechanistic investigation of this reaction.⁴²

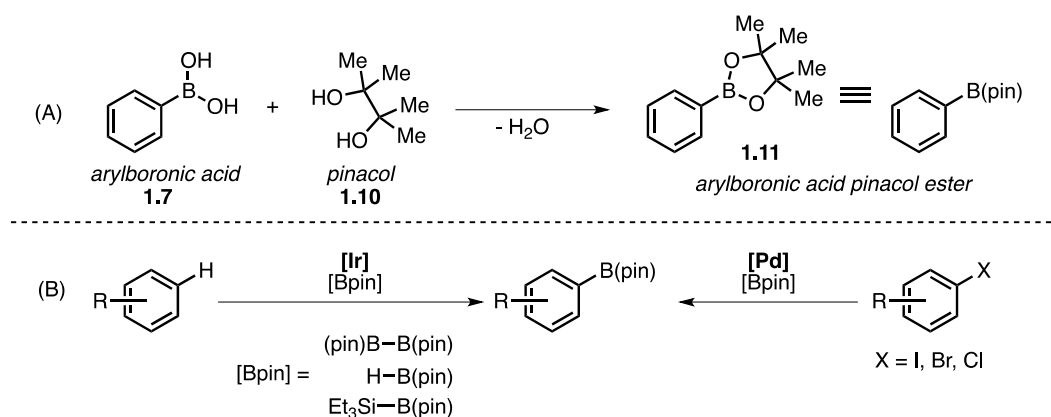


Figure 1-16 (A) structure of arylboronic acid pinacol (Bpin) esters; (B) schematic metal-catalyzed methodologies for Bpin synthesis

Specifically, they investigated and compared the amination of a biphenylboronic neopentyl glycol ester (**1.12**) with both alkyl amines (**1.13**) and anilines (**1.14**). Spectroscopic (EPR, ¹H NMR, and UV-vis) and mass spectrometric techniques (to investigate copper-containing species *in situ*), as well as kinetic and stoichiometric reaction studies, were utilized to investigate the nature of the CEL amination of aryl Bpin reagents (Figure 1-17). Using this

approach, the authors were able to identify a number of pitfalls in the reaction, which they were able to effectively address.

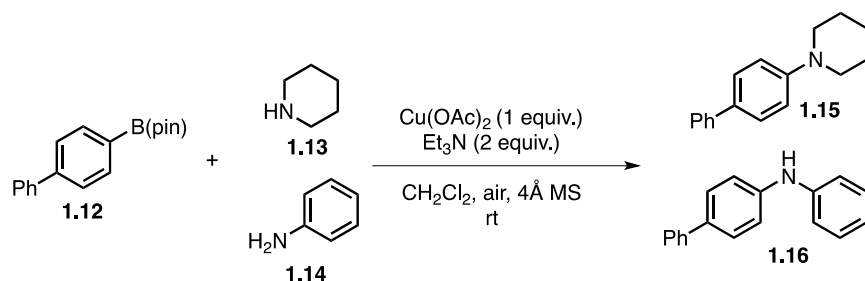


Figure 1-17 Investigated amination of aryl-Bpin reagents, promoted by copper

The amine-coupling partner was found to have an indispensable role, in cooperation with triethylamine, in the dissociation of the inactive $[\text{Cu}(\text{OAc})_2]_2$ paddlewheel complex (**1.18**) to an activated Cu(II) species (**1.19**) (Figure 1-18 A). Excess acetate was found to promote the formation of inactive paddlewheel complex (**1.18**) (Figure 1-18 A). The complexation of pinacol with the paddlewheel Cu(II) complex generates an inactive Cu(II)-diol complex (**1.17**) (Figure 1-18 A). The oxidation of Cu(I) to the activated Cu(II) species (**1.19**) is an amine-promoted event (Figure 1-18 B). A sluggish oxidation of Cu(I) to Cu(II) was established to be a key issue under these conditions, as Cu(I) was found to be efficient at both protodeboronation (**1.22**) and oxidation of the aryl-Bpin reagent (**1.21**) (Figure 1-18 C). As such, reaction modifications were orchestrated in order to (1) promote the oxidation of Cu(I) to Cu(II) and (2) sequester excess pinacol and acetate under the reaction conditions.

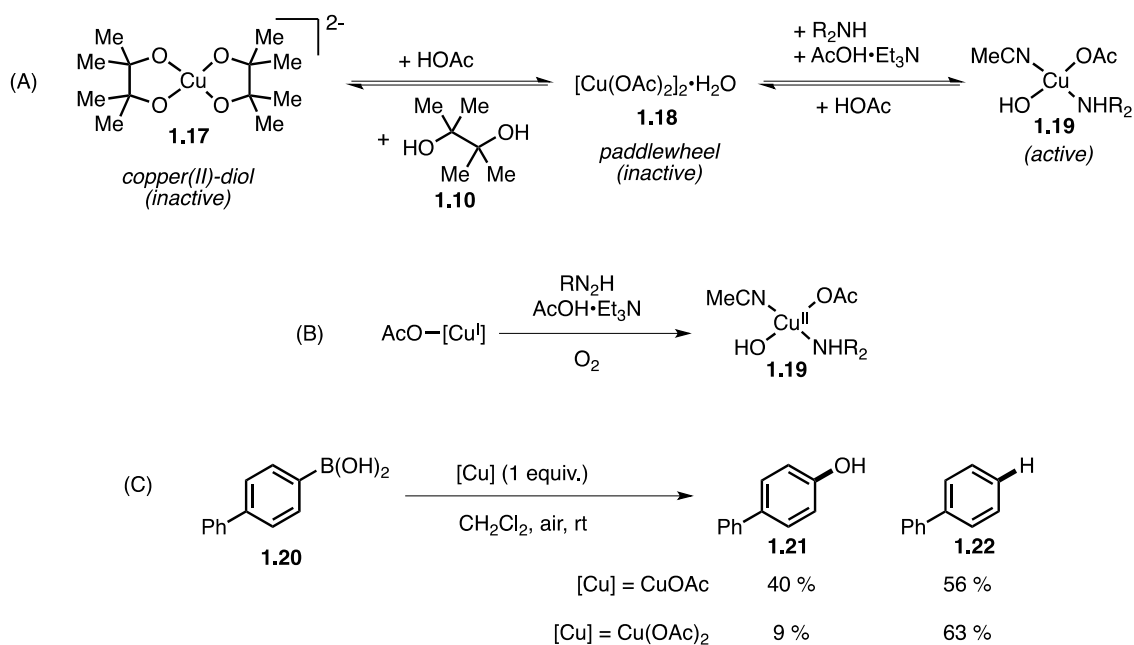


Figure 1-18 (A) Activation and deactivation of $[\text{Cu}(\text{OAc})_2]_2$ paddlewheel complex; (B) amine promoted Cu(I) oxidation pathway; (C) Cu(I) promoted arylboronic acid decomposition

Two major modifications were put in place in order to increase the rate of the productive reaction. The first of these was the inclusion of $\text{B}(\text{OH})_3$ (**1.23**); this reagent can reversibly bind to both acetate (**1.24**) and pinacol (**1.25**) (Figure 1-19 A). Boric acid was shown to promote the oxidation of Cu(I) to Cu(II) in the presence of acetic acid and Et_3N . Since the Cu(I) to Cu(II) oxidation event is amine promoted, increasing the equivalents of the amine coupling partner (**1.13**) was also shown to improve the reaction selectivity for the product (**1.15**) (Figure 1-19 B); these two modifications were fundamental in their optimized, copper-catalyzed and $\text{B}(\text{OH})_3$ mediated reaction conditions (Figure 1-19 C).

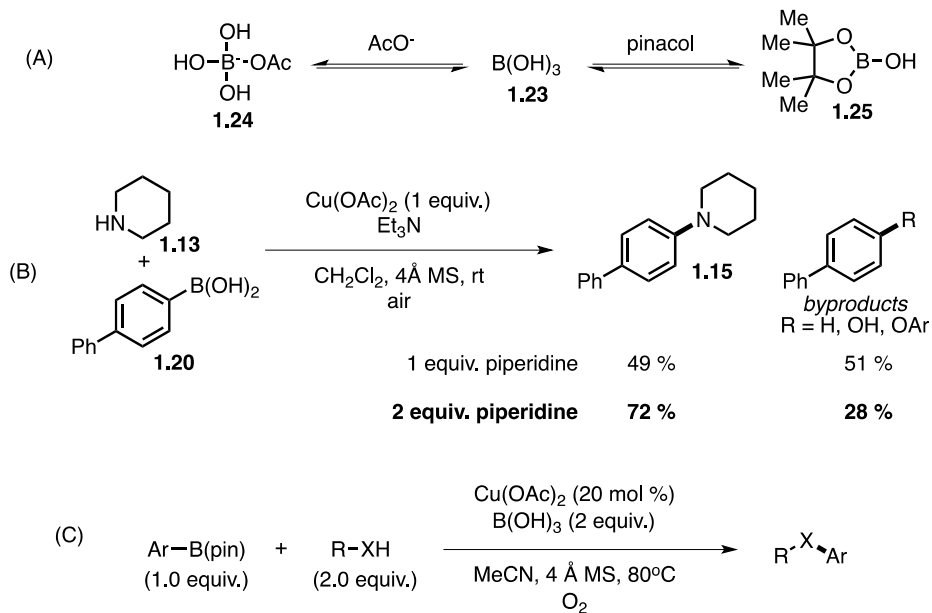


Figure 1-19 (A) reversible binding of B(OH)₃ to pinacol and acetate; (B) effect on reaction selectivity with increased amine stoichiometry; (C) overall optimized copper-catalyzed amination conditions

1.2.4 Modern Example of Oxidative C-C Bond Formation Catalyzed by Copper

Though less well-studied, carbon-carbon bond forming reactions under oxidative copper conditions have been developed; an example of this is the merging of both oxidative copper-catalysis and organocatalysis for the alkenylation of aldehydes (**1.26**) utilizing alkenyl boronic acids (**1.27**) and a chiral amine catalyst (**1.28**) (Figure 1-20).⁴³ This reaction hinges on the use of a Cu(II) acetate that undergoes transmetalation with an alkenyl boronic acid and oxidation by another Cu(II) to generate a Cu(III) alkenyl complex, which acts as an electrophile to trap a chiral amine (Figure 1-21). This reaction demonstrates that copper can be utilized to form carbon-carbon bonds under conditions that mimic the traditional CEL reaction. The scope and mechanistic understanding of these reactions remain underdeveloped.

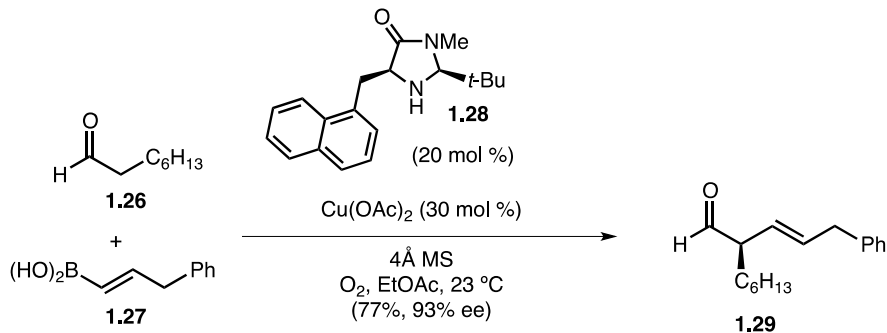


Figure 1-20 Aldehyde α -alkenylation by copper and amine catalysis

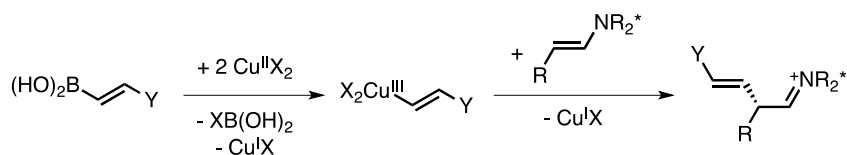


Figure 1-21 Formation and imine trapping of an activated Cu(III) alkene complex

Inspired by the mild conditions of the CEL reaction and the examples that do exist of copper-utilizing oxidative cross-coupling reactions to generate new carbon-carbon bonds, we set out and were successful in developing such a reaction (Figure 1-22 A) that combined arylboron reagents (**1.30**) with activated sp^3 carbon nucleophiles (**1.31**) to generate new carbon-carbon bonds (**1.32**).⁴⁴ Expanding on this work, we hoped to increase the scope of this reaction by incorporating a decarboxylation step into the product, such that we could generate an expanded suite of aryl esters (Figure 1-22 B). As such, it would be pertinent to discuss decarboxylation chemistry, both in how decarboxylation can be stimulated and how it has been utilized within synthetic methodologies.

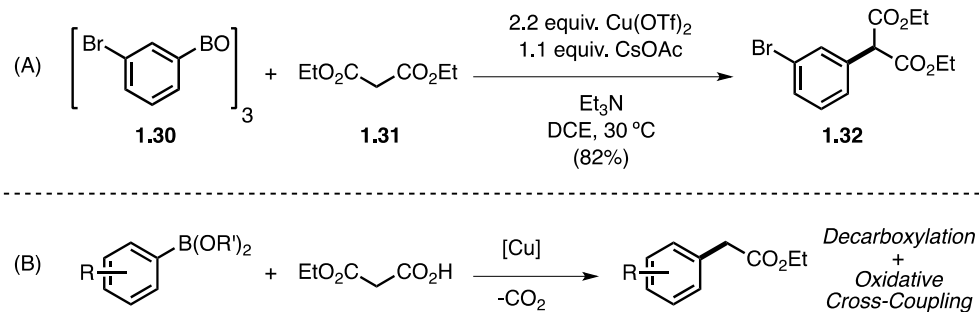


Figure 1-22 (A) Arylation of malonate derivatives by oxidative coupling; (B) proposed synthesis of aryl acetates by decarboxylative oxidative coupling

1.3 Decarboxylation in Metal-Catalyzed Cross-Coupling Reactions

1.3.1 Fundamental Aspects of a Decarboxylation Reaction

A decarboxylation reaction is where a carboxylic acid group is removed from a molecule, liberating CO_2 . There are a number of ways in which this can occur, and the product that is generated will differ depending on the state of the carboxylic acid prior to decarboxylation. If the carboxylic acid is negatively charged (for example, from the abstraction of a proton), a decarboxylation from this intermediate would result in the formation of a carbanion (Figure 1-23 A). If the carboxylic acid is oxidized by a single electron to generate an oxygen-based radical, decarboxylation from this intermediate would result in the formation of a carbon-based radical (Figure 1-23 B). Decarboxylation reactions and their applications to synthesis have been extensively studied.⁴⁵⁻⁴⁸ Methods for the activation of carboxylic acids in a decarboxylative manner, and representative examples, will be discussed in the following sections.

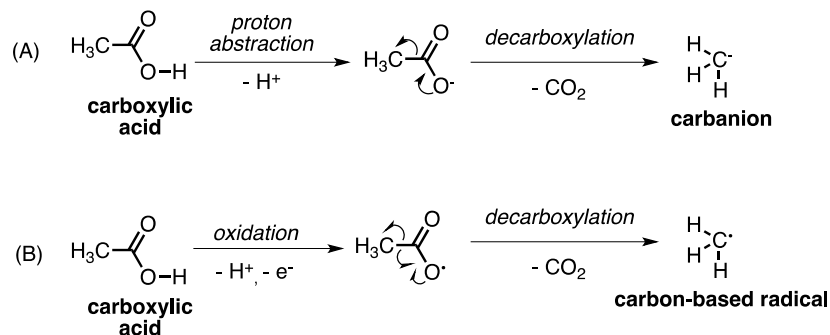


Figure 1-23 (A) Decarboxylation from a negatively-charged carboxylic acid results in the formation of a carbanion; (B) decarboxylation from an oxygen-based radical on the carboxylic acid results in the formation of a carbon-based radical

1.3.2 Decarboxylation in Nature and Decarboxylative Organocatalysis

Nature has already expertly harnessed the decarboxylation reaction to suit its needs, as there exist many enzymes and biological processes that exploit decarboxylative chemistry.⁴⁹⁻⁵¹ An example of an enzyme-facilitated decarboxylative carbon–carbon bond forming reaction is in the synthesis of polyketides, where decarboxylation of an acyl carrier protein-bound malonyl generates a nucleophile that is trapped by a ketosynthase-bound thioester, creating a new carbon–carbon bond (Figure 1-24).⁵² These enzymatic processes have been the source of inspiration for a number of related organocatalytic decarboxylation reactions, including the Nakamura and Shibata decarboxylative enantioselective aldol reaction (Figure 1-25 A) between isatins (**1.33**) and malonic half thioesters (**1.34**) catalyzed by a squaramide derivative (**1.35**). The polyfunctional organocatalyst acts to both stabilize the decarboxylated intermediate and act as a directing group for the subsequent nucleophilic attack (Figure 1-25 B).⁵³⁻⁵⁴ However, the use of a complex organocatalyst and the limits in substrate scope (as specialized substrates are usually required) limits their utility.

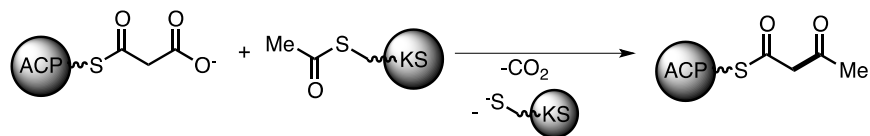


Figure 1-24 Enzymatic decarboxylative carbon-carbon bond forming (ACP = acyl carrier protein, KS = ketosynthase)

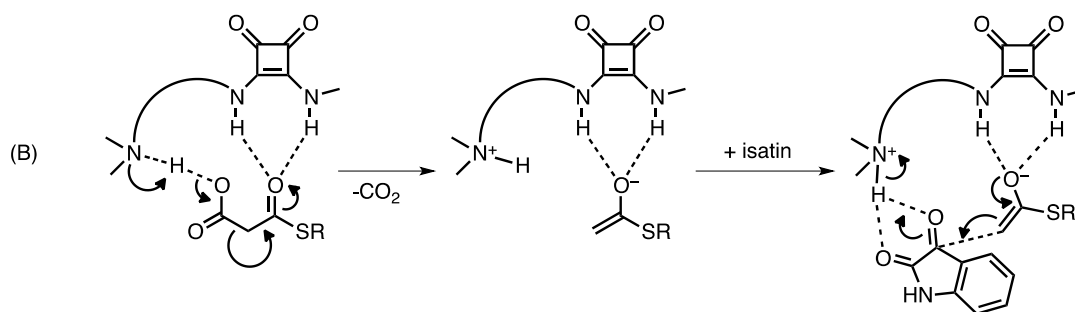
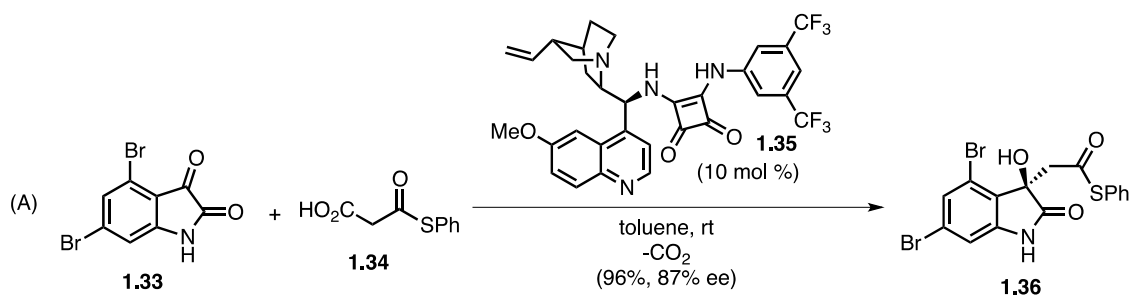


Figure 1-25 (A) Biomimetic decarboxylative carbon-carbon bond formation; (B) proposed mechanism

1.3.3 Decarboxylation in Metal-Catalyzed Reaction

Carboxylic acids can also be utilized as activating groups in metal-catalyzed cross-coupling reactions. In contrast to enzymatic and bio-inspired decarboxylative reactions (which typically occur near and around room temperature), these reactions can require elevated

temperatures in excess of 100 °C. These reactions can provide carboxylic acid based alternatives to traditional cross-coupling reaction partners. For example, the palladium-catalyzed Suzuki reaction is a well-established method to form aryl-aryl bonds (Figure 1-26 A), utilizing an arylboronic acid as the source of nucleophile.² The synthesis of similar biaryl products can be conducted by using electron-deficient aryl carboxylic acids (**1.37** and **1.40**) in place of arylboronic acids as the source of nucleophile, with the presented examples utilizing either a single metal (palladium) or dual metal (palladium and silver) system (Figure 1-26 B).⁵⁵⁻⁵⁶ The key difference between these two systems is upon which metal the decarboxylation occurs. For the palladium only system, the decarboxylation is proposed to occur at the palladium itself (Figure 1-27 A). For the catalytic-in-silver system, decarboxylation is proposed to occur via a silver-bound carboxylate, with the newly formed aryl-silver species transmetalating with palladium (Figure 1-27 B).

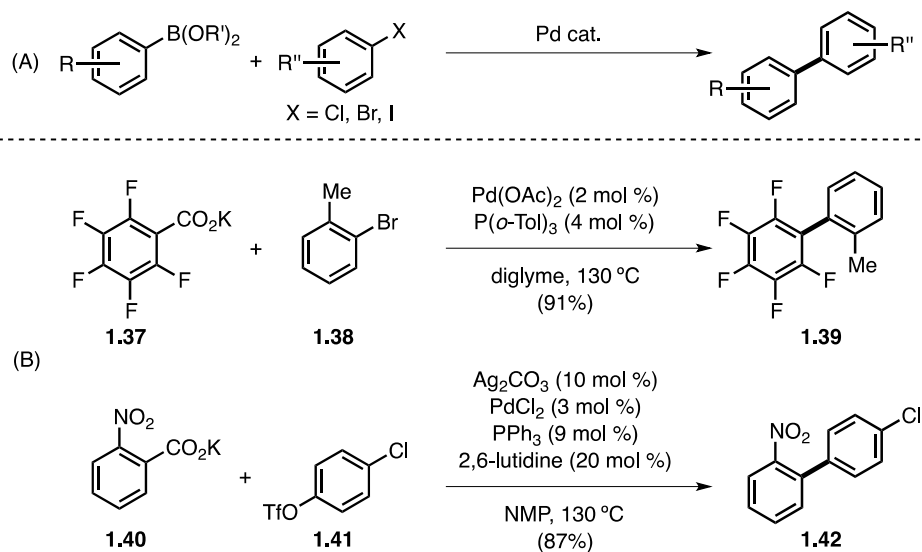


Figure 1-26 (A) Schematic palladium-catalyzed Suzuki cross-coupling reaction; (B) examples utilizing aryl-carboxylic acids as the nucleophile equivalent

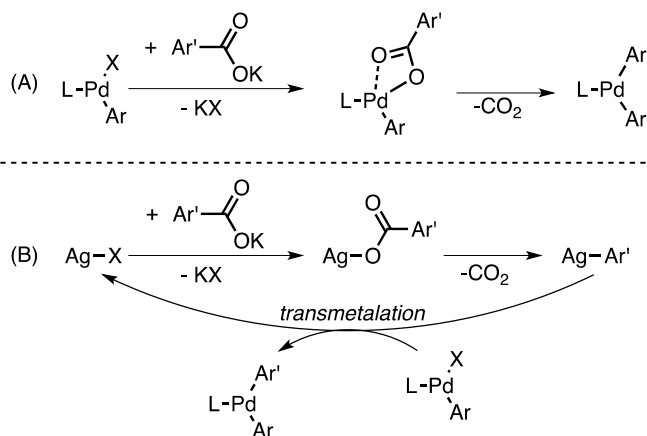


Figure 1-27 Decarboxylation and bis(aryl)palladium formation with (A) palladium or (B) silver

1.3.4 Radical Initiated Decarboxylation

Single electron oxidation of a carboxylic acid can be used to induce a decarboxylation reaction and generate a carbon-based radical. An example of this is the copper-catalyzed

decarboxylative coupling of α -amino acids (**1.43**) with aryl-alkynes (**1.44**) to generate α -alkynylated amino acids (**1.45**) (Figure 1-28 A).⁵⁷ A possible mechanism for this reaction (Figure 1-28 B) could involve two sequential single electron oxidation events, both mediated by a Cu(II). The first oxidation would generate an oxygen-based radical (**1.46**), that would decarboxylate to give the corresponding carbon-based radical (**1.47**). This species could undergo a second single electron oxidation at the nitrogen to generate an iminium species (**1.49**). The *tert*-butoxide generated in this preceding step would deprotonate the alkyne reagent, and this alkynyl carbanion (**1.51**) would neutralize the iminium to generate the product (**1.52**). This reactivity would be in line with previously observed single-electron chemistry initiated by copper.⁵⁸⁻⁵⁹

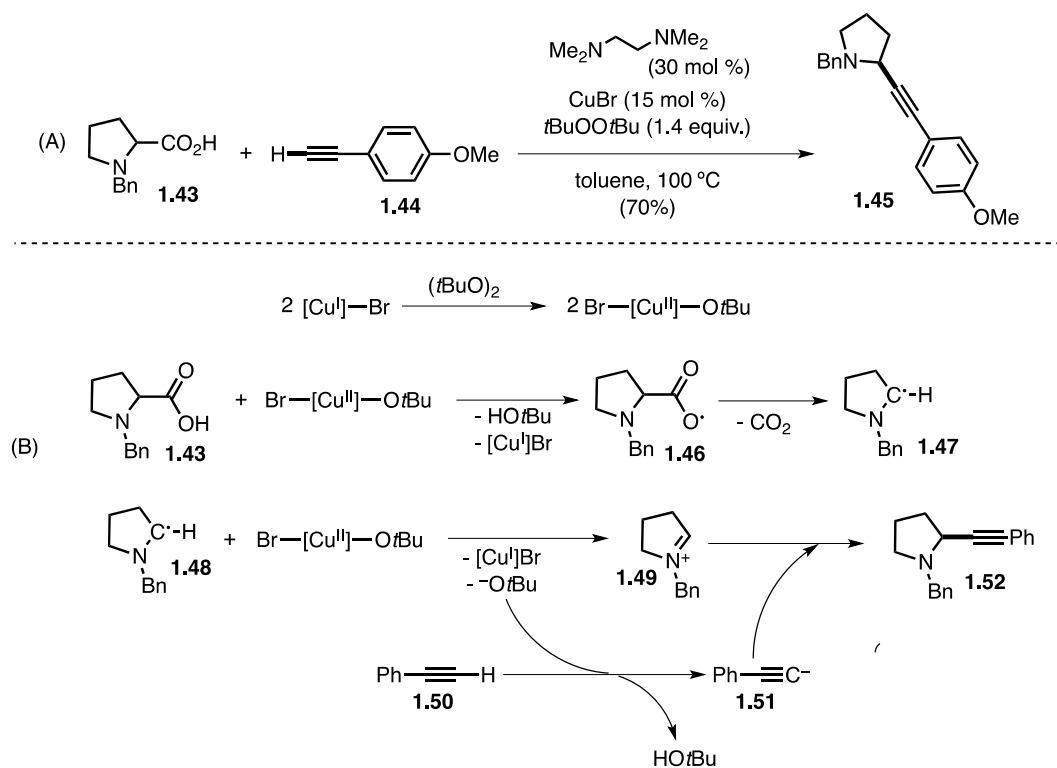


Figure 1-28 (A) Copper-catalyzed decarboxylative alkylation of α -amino acids; (B) proposed mechanism

Metal complexes that can utilize light in order to facilitate single-electron transfer events have also been utilized in decarboxylation reactions. For example, the Doyle and MacMillan groups recently disclosed an iridium-photocatalyst that promotes the decarboxylation of an α -amino acid to generate a carbon-based radical; this process was paired with a nickel-catalyzed arylation reaction (Figure 1-29).⁶⁰ Single electron oxidation of a carboxylic acid (**1.53**) by a photo-activated iridium complex (**1.54**) causes a decarboxylation to generate a carbon-based radical (**1.55**), which can then enter into a nickel-catalyzed (**1.56**) cross-coupling reaction with various aryl halides (**1.57**).

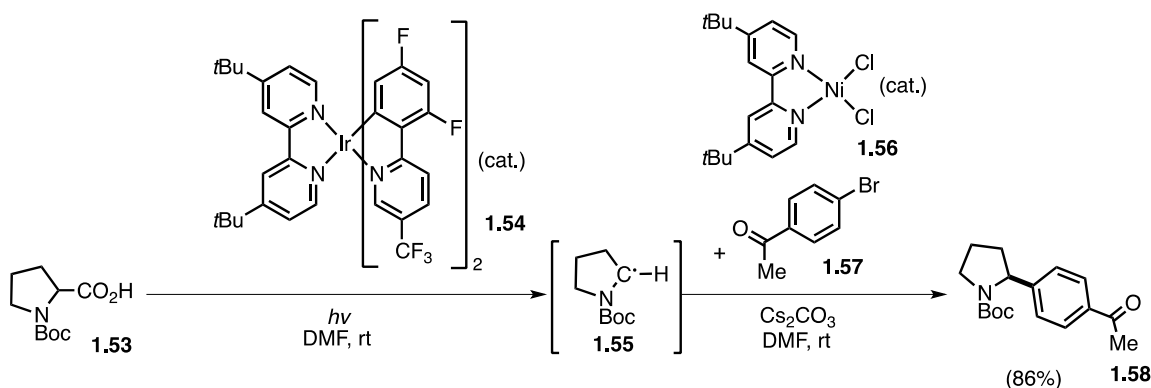


Figure 1-29 Photocatalytic SET generation of a carbon-based radical via decarboxylation coupled to a nickel-catalyzed cross-coupling reaction

We were inspired by our previous experience in oxidative cross-coupling⁴⁴ and the versatility of decarboxylative chemistry to combine these two areas to develop new organic methodologies for the mild and selective formation of carbon–carbon bonds. We recently disclosed a synthesis of aryl acetates by oxidative decarboxylative arylation of malonate half esters (**1.59**) (Figure 1-30).⁴⁴ My thesis will cover two topics related to these areas, the first being an extension of the malonate half ester arylation chemistry, utilizing monofluoro malonate half esters (**1.60**) to synthesis α -aryl- α -fluoroesters (Figure 1-31 A).⁶¹ The second topic will be my work into the scope and functionalization of a decarboxylative oxidative synthesis of diarylmethanes by copper-mediated coupling of arylboronic esters and *ortho*-nitroaryl acetates (**1.61**) (Figure 1-33 B). Our optimization and scope studies within these two areas have allowed us to develop two new organic methodologies, facilitated by a merger of the areas of decarboxylative chemistry and copper-mediated oxidative coupling reactions. These new methods provide a mild and complementary route to the synthesis of carbon–carbon bonds, providing new tools to synthetic chemists that wish to synthesize these molecular templates.

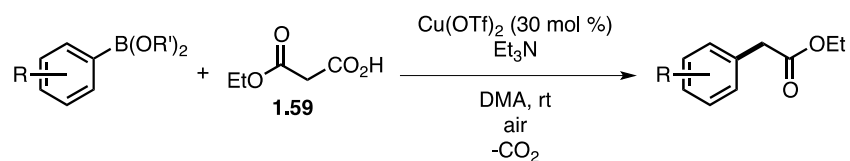


Figure 1-30 Copper-catalyzed decarboxylative arylation of malonate half-esters

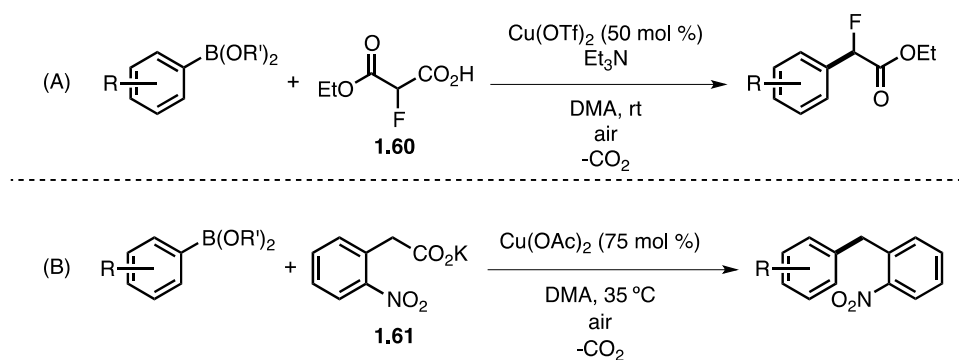


Figure 1-31 (A) Copper-mediated oxidative decarboxylative arylation of monofluoro malonate half-esters (Chapter 2); (B) copper-mediated oxidative decarboxylative arylation of *ortho*-nitroaryl acetates (Chapter 3)

CHAPTER 2 – Copper-Mediated Synthesis of Monofluoro Aryl Acetates via Decarboxylative Cross-Coupling

2.1 Introduction

2.1.1 Molecules Containing Carbon-Fluorine Bonds

Fluorine-containing organic molecules are of great importance in medicinal chemistry, as evidenced by the number of commercially available and in-the-pipeline pharmaceuticals that contain at least one fluorine atom.⁶²⁻⁶⁴ There has been considerable effort put towards developing synthetic methods to produce increasingly complex molecules containing fluorine atoms.⁶⁵⁻⁶⁷ Inspired by our previous work on the synthesis of aryl acetates by oxidative decarboxylative cross-coupling,⁶⁸ we wished to expand this reactivity in order to synthesize monofluoro aryl acetates by using monofluoro malonate half esters as the acetate substrate (Figure 2-1).

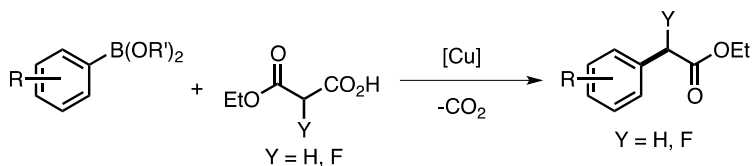


Figure 2-1 Synthesis of monoaryl acetates by decarboxylative oxidative cross-coupling, utilizing either a malonate or monofluoro malonate half-ester

The inclusion of fluorine into a molecule can have potentially confounding effects on its molecular properties when compared to other halogens. Investigations published in the mid-1960s demonstrated the effect on acidity by an α -fluorine when compared to the α -chloro and α -hydrogen species (Figure 2-2 A); fluorine acts in stark contrast to the other halogens by *increasing* the pK_a of the α -hydrogen.⁶⁹ This was further demonstrated in a study relating the

sodium methoxide-catalyzed hydrogen-deuterium exchange of an acetate species, wherein the rate of exchange dropped with the inclusion of α -fluorine atoms (Figure 2-2 B).⁷⁰ An α -fluorine can also have a profound effect on the nucleophilicity of an adjacent carbanionic centre, as demonstrated by a recent study by the Mayr and Prakash groups. Against a standard electrophile, the nucleophilicity of a carbanion increased with the addition of a fluorine atom (Figure 2-2 C).⁷¹ These observations can be rationalized by the alpha effect, wherein the lone pairs on an adjacent atom will electronically congest a carbanion, destabilizing the anionic species (thus increasing the pKa) and making said anionic species more nucleophilic.⁷² These observations must be taken into account when considering how to develop a reaction involving the use of a carbanion alpha to a fluorine atom, especially when comparing to an established methodology that does not utilize fluorine (Figure 2-2 D).

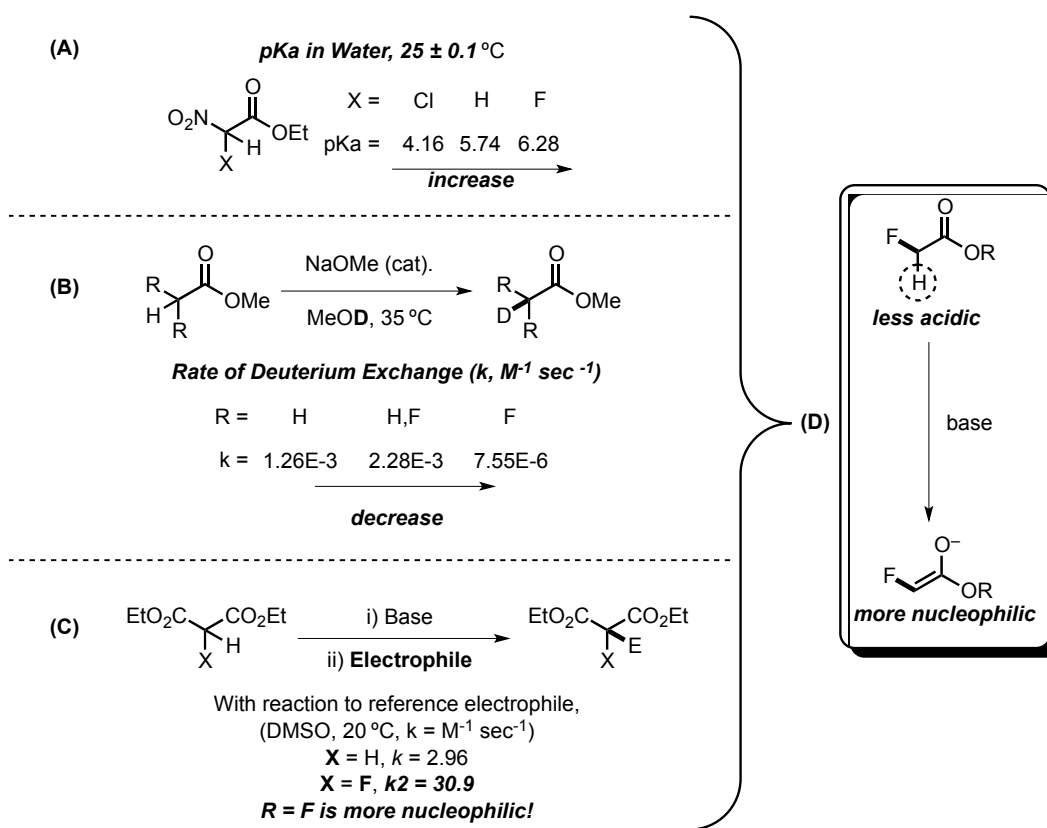


Figure 2-2 (A) effect on acidity; (B) effect on the rate of H-D exchange; (C) effect on the nucleophilicity (D) combined effects of α -hydrogen acidity and anion nucleophilicity

The synthesis of monofluoro aryl acetates by established synthetic protocols can be split into two main areas, the fluorination of aryl acetates or the arylation of fluoroacetates (Figure 2-3). For the former, formation of a new carbon-fluorine bond can be conducted by either nucleophilic or electrophilic fluorine sources.

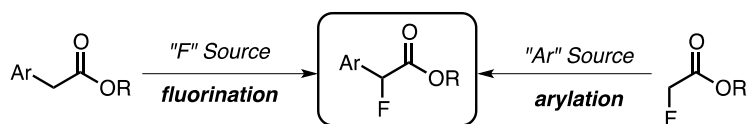


Figure 2-3 Synthetic strategies for the synthesis of monofluoro aryl acetates

2.1.2 α -Fluorination of Aryl Acetates

An early example of nucleophilic aryl acetate fluorination involved the combined use of anodic oxidation and a nucleophilic fluorine source to generate a new carbon-fluorine bond on an arylated chiral ester (**2.1** fluorinated to **2.2**) (Figure 2-4).⁷³ While simple and efficient, anodic oxidations have been reported to occur with a number of electron-rich organic functionalities,⁷⁴⁻⁷⁷ which may present chemoselectivity issues with more complicated substrates.

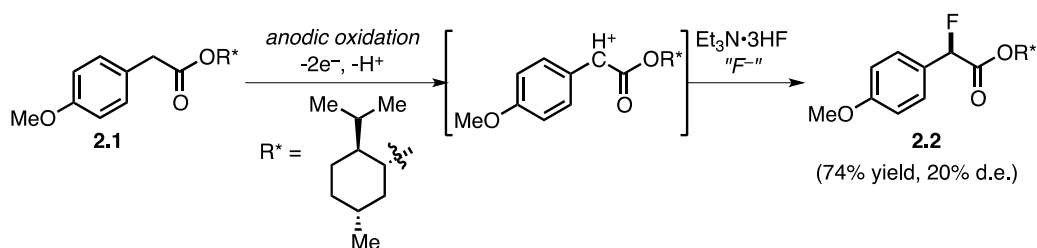


Figure 2-4 α -fluorination by anodic oxidation

The nucleophilic fluorination of α -diazo aryl acetates was demonstrated by the Doyle group (Figure 2-5).⁷⁸ The process made use of a BOX-ligated copper catalyst, with potassium fluoride as the nucleophilic fluorine source in order to α -fluorinate an α -diazo ester (**2.3** fluorinated to **2.4**). Though a mechanism is not proposed, the requirement for 1,1,1,3,3,3-hexafluoroisopropanol (HFIP) as an additive and the known reactivity modes and polarity of copper-carbenes⁷⁹ could result in the following mechanism (Figure 2-5); the formation of the copper carbene generates an electropositive carbon that can be trapped by potassium fluoride, with protonolysis by HFIP generating the product and regenerating the copper(I) catalyst. The two major advantages to this system were that the precursor diazo compounds could be generated from terminal acetates (though the yields tend to be lower for these non-aryl species),

and the direct use of KF as the fluoride source allow $K^{18}F$ to be utilized to tag biologically relevant molecules in a direct fashion for use in radiopharmaceuticals.⁸⁰⁻⁸¹ The most significant issue with this methodology is the use of diazo-esters, as these reagents present several hazards in terms of their explosiveness and toxicity.⁸²⁻⁸⁴

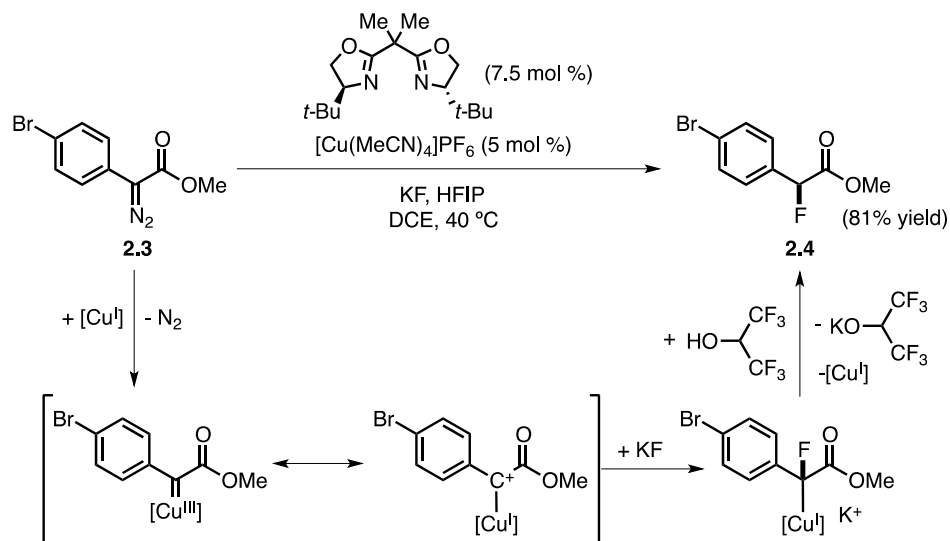


Figure 2-5 Copper-catalyzed fluorination of aryl diazoesters using potassium fluoride

Deoxyfluorination, where either an alkyl or aryl alcohol is replaced with a fluorine atom, also makes use of nucleophilic fluorine source in the preparation of α -fluoro aryl acetates. A number of reagents based on an N-heterocycle template have been developed within this area, including *PhenoFluor*TM, *PhenoFluor*TMMix, and *AlkylFluor* (Figure 2-6 A).⁸⁵⁻⁸⁸ The proposed mechanism for this transformation (Figure 2-6 B), starting from the substrate hydroxyl species (2.5), involves the generation of an O-bound N-heterocycle (2.6) by attack of the hydroxyl onto the electrophilic carbon of the fluorinated N-heterocycle with loss of HF. Subsequent heating of the reaction with excess nucleophilic fluoride (in this case, potassium fluoride) causes a

substitution to yield the fluorinated species (**2.7**). Though chemoselective, the low atom economy of this process by stoichiometric use of a large N-heterocycle and the need for superstoichiometric amounts of fluorine could inhibit its widespread adoption, especially on larger scales.

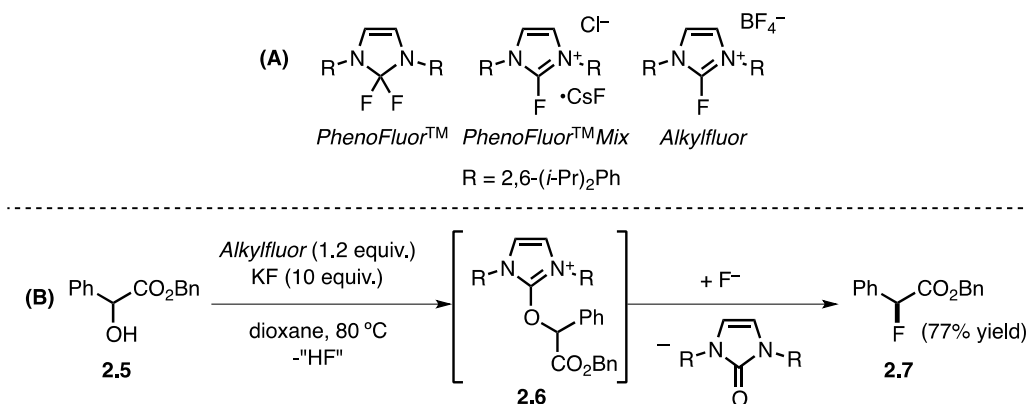


Figure 2-6 (A) Deoxyfluorination reagents utilizing N-heterocyclic scaffolds; (B) nucleophilic deoxyfluorination utilizing *Alkylfluor*, with proposed O-bound N-heterocycle intermediate

For electrophilic fluorination, the major route is by enolate trapping; the Lectka group has published work in this area involving the generation and manipulation of a metal-ketene-enolate (Figure 2-7).⁸⁹ Starting from an arylated acyl chloride (**2.8**), the metal-ketene-enolate (**2.10**) is generated via base abstraction and coordination to both a metal center and a chiral amine (**2.9**). This intermediate is trapped by N-fluorobenzenesulfonamide (NFSi), performing first a fluorination (**2.13**) and then a formation of an amide (**2.14**) that undergoes a substitution reaction with a protic nucleophile to generate the desired fluorinated aryl-ester (**2.12**). They further demonstrated the utility of this methodology by using more complex molecules, such as natural products and biologically active molecules, as their nucleophile source, again with excellent

enantioselectivity.⁹⁰ The main disadvantages of this methodology is the utilization of acyl chlorides, specifically the potential lack of selectivity that would occur if there are multiple nucleophilic sites on a target molecule.

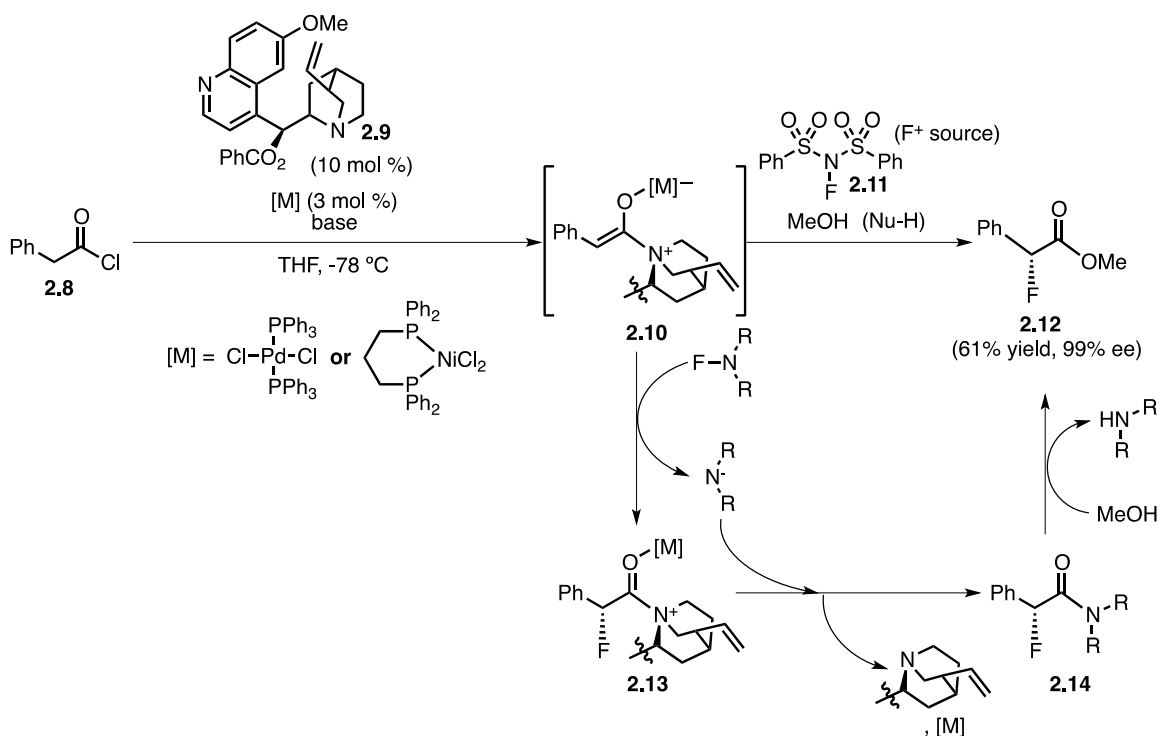


Figure 2-7 Electrophilic fluorination and substitution of a metal-ketene-enolate

2.1.3 α -Arylation of Monofluoro Acetates

The second general method for synthesizing monofluoro aryl acetates is by the arylation of fluoroacetates. This method does not make a new carbon-fluorine bond, but instead adds complexity to molecules that already contain the desired carbon-fluorine bond. A stoichiometric example of this was developed by the Sandford group in an effort to generate *ortho*-nitroaryl monofluoro malonate derivatives via S_NAr (Figure 2-8).⁹¹ This reaction occurs in two stages, the first stage being the sodium hydride S_NAr substitution of an *ortho*-nitro fluorobenzene (**2.15**) with diethyl monofluoro malonate (**2.16**) to generate an aryl monofluoro malonate (**2.17**), with hydrolysis by potassium hydroxide followed by decarboxylation of the resulting species *in situ* to generate the monofluoro aryl acetic acid (**2.18**). Due to the harsh conditions required for the reaction, the scope is limited to non-acidic functionalities and molecules with no other functionalities that can be hydrolyzed by potassium hydroxide. The aryl bromide remained intact in this reaction, which may be useful for cases where substitution of an aryl fluoride bond over that of another aryl halide bond within the same molecule is desired.

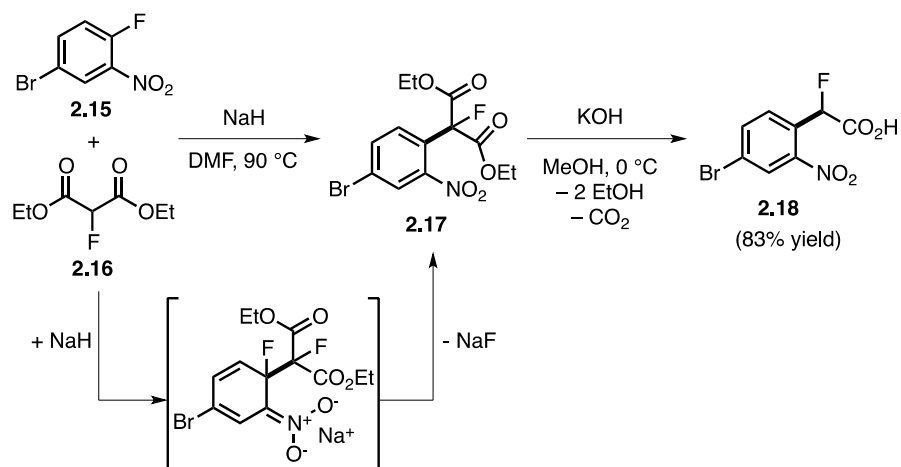


Figure 2-8 S_NAr reaction to generate monofluoro aryl acetic acids

Milder methods for fluoroacetate arylation have been developed utilizing metal-catalyzed cross-coupling reactions, centered on the use of fluorobromoacetate (**2.20**) as the fluorine-containing building block. Suzuki couplings of various arylboronic acids (**2.19**) and fluorobromoacetates have been reported, utilizing both palladium and nickel metal catalysts (Figure 2-9 A).⁹²⁻⁹³ The nickel-catalyzed process demonstrates a tolerance of a broader range of functional groups; a representative example of this is the difference in yield between the two methodologies for the *para*-bromophenyl example (**2.21**). A Hiyama cross-coupling protocol, utilizing trialkoxysilanes (**2.22**), was also developed (Figure 2-9 B). The substrate scope for this reaction included potentially problematic functional groups, including *para*-bromophenyl (**2.21**) and *para*-benzaldehydes (not depicted, 80% yield). Though a robust reaction, limitations with this methodology include the incompatibility of aryl iodides, as well as the necessity of super-stoichiometric amounts of fluoride as an activating agent.

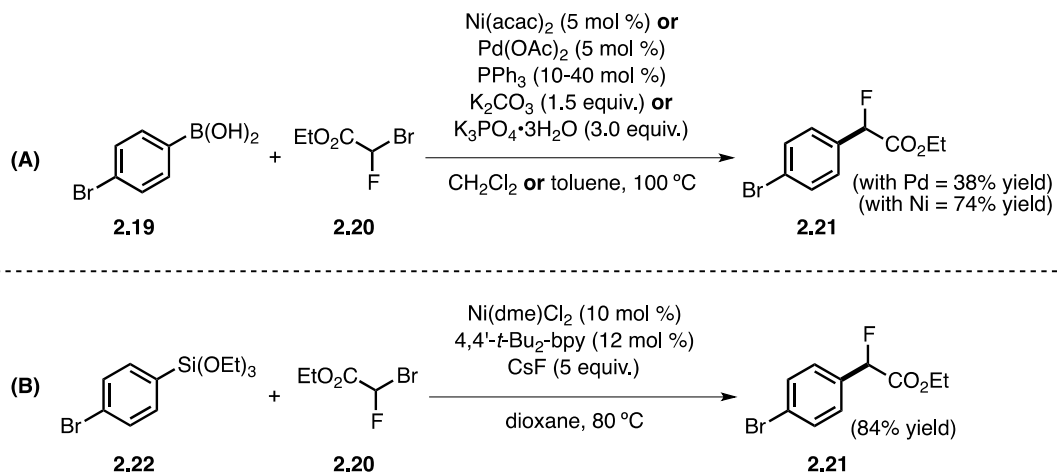


Figure 2-9 (A) Palladium-catalyzed and nickel-catalyzed Suzuki cross-coupling to generate aryl fluoro acetates; (B) nickel-catalyzed Hiyama coupling to generate aryl fluoro acetates

It can be speculated that the mechanism of the above transformations would closely mirror that of a palladium-catalyzed α -arylation⁹⁴; that is to say, by a 2-electron process. However, as palladium is known to perform radical chemistry under specific circumstances, the possibility of a single electron pathway cannot be ignored.⁹⁵ The nickel-catalyzed Suzuki and Hiyama coupling reactions are linked by the proposed generation of carbon-based radicals (Figure 2-10). A general proposed mechanism for this process begins with the generation of a nickel(I)-aryl species (**10-I**), resulting from transmetalation of either the aryl-boronic acid or aryl-trialkoxo silane onto a Ni(I) precursor (**10-II**). This undergoes a single-electron oxidative addition to generate a nickel(II) species (**10-III**) and a carbon-based radical. This radical can rebound back and trap the nickel(II), oxidizing it to a nickel(III) species (**10-IV**) that is prime for reductive elimination to generate the arylated product and regenerate the nickel(I) catalyst.

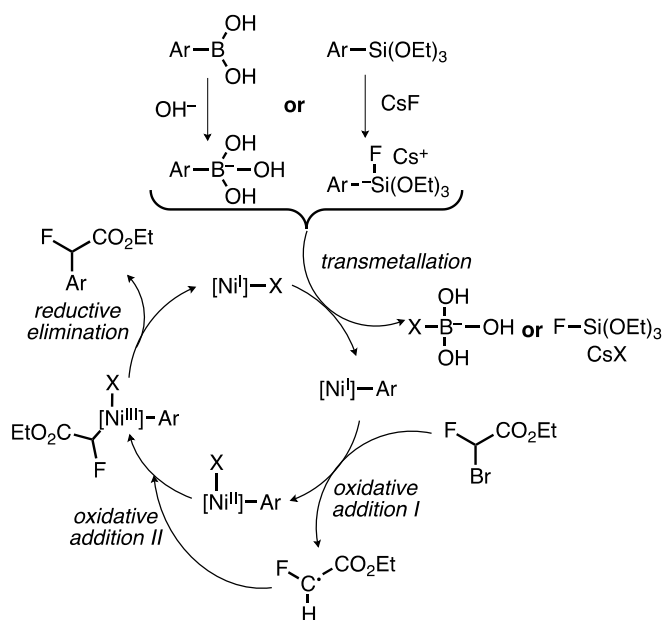


Figure 2-10 Proposed radical mechanism for nickel-catalyzed Suzuki and Hiyama cross-coupling reactions to generate aryl fluoro acetates

An iridium-photocatalytic C-H functionalization methodology has also been developed, utilizing benzofurans and benzothiophenes (such as **2.23**) (Figure 2-11 A).⁹⁶ The proposed mechanism (Figure 2-11 B) relies on homolytic cleavage of the carbon-bromine bond in the bromofluoroacetate substrate (**2.20**) via a photoexcited Ir(III) species, which can then react with the benzoheterocycle species to generate a resonance-stabilized benzyl radical (**2.25**). This intermediate is quenched by the now oxidized iridium, regenerating both the unsaturation in the heterocycle and the iridium(III) species. This methodology is only demonstrated with benzoheterocycles, implying the need for these types of scaffoldings for this reaction to occur. (refer to **2.25**, Figure 2-11 B).

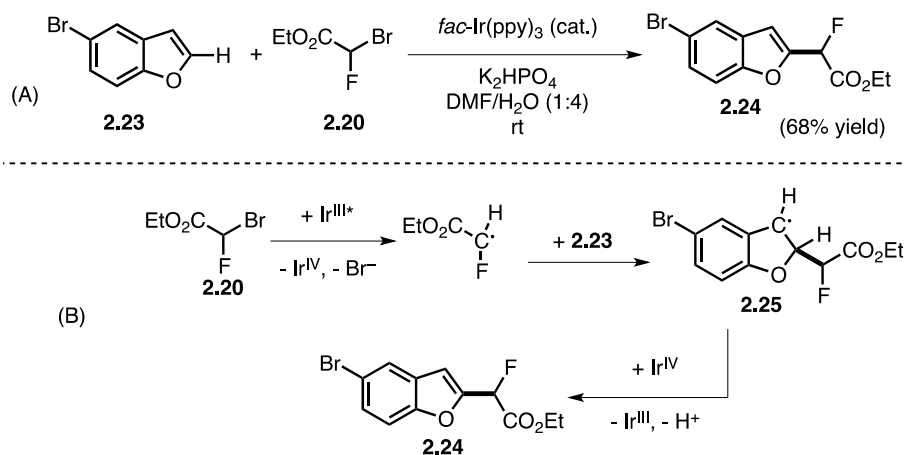


Figure 2-11 (A) C-H functionalization by iridium photocatalyst for the generation of fluoroacetate substituted benzoheterocycles ($\text{Ir}^{\text{III}*}$ = photoexcited Ir^{III}); (B) proposed mechanistic pathway

We hoped to utilize our knowledge of oxidative and decarboxylative chemistry to expand the current set of tools available for generating aryl fluoroacetates. This was accomplished by expanding on our previous work on the synthesis of arylated acetates to include monofluoro malonate half esters (**2.26**) as substrates. The following sections highlight the development and scope of this reaction (Figure 2-12).

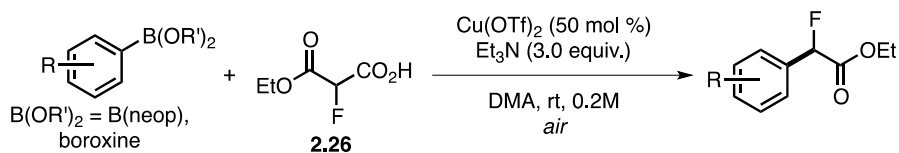


Figure 2-12 Copper-mediated decarboxylative oxidative methodology to synthesize monofluoro aryl acetates

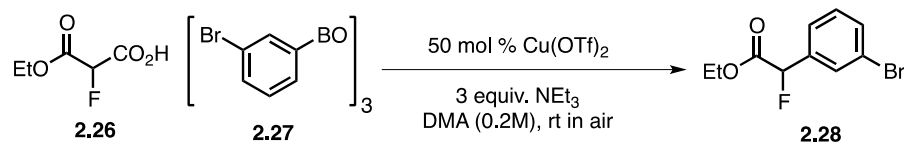
2.2 Reaction Optimization

Our optimized conditions for the copper-mediated synthesis of α -fluoro- α -aryl acetates are presented below (Figure 2-13). This specific reaction utilizes a monofluoro ethyl malonate half ester (**2.26**) and 3-bromophenylboroxine (**2.27**) to yield the desired arylated product (**2.28**). The development of this reaction was inspired by Patrick Moon's previous work into the decarboxylative oxidative arylation of unsubstituted malonate half-esters.⁶⁸ We chose to optimize this reaction utilizing 3-bromophenyl as our aryl group in order to optimize for conditions that would not react with the electrophilic carbon-bromine bond. The initial employment of Patrick Moon's conditions (Table 2-1, entry 1) gave a poor yield of product and a substantial amount of unproductive monofluoro malonate half ester consumption. Ultimately, it was discovered that by utilizing a more active arylboron source (boroxine), increasing the copper loading, and lowering the loading of triethylamine, we were able to develop a reaction that gave an excellent yield of product with complete conversion of the starting material (Table 2-1, entry 2).



Figure 2-13 Optimized conditions for the copper-mediated decarboxylative oxidative cross-coupling of arylboroxines and monofluoro malonate half esters to synthesize α -fluoro- α -aryl acetates

Table 2-1 Effect on reaction performance of the optimized reaction when compared to the previously employed reaction conditions for the ethyl malonate half ester

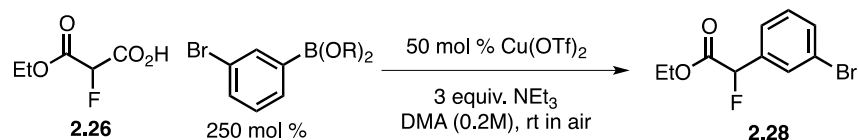


Entry	variation from standard conditions	2.26 conversion (%)	2.28 yield (%)
1	Patrick Moon's conditions ^a	68	34
2	none	>95	78

^aStandard conditions¹: 250 mol % arylboron as boroxine, 0.5 dram vial with 20 gauge needle. Conversion and yields determined by calibrated ¹H NMR. ^a2.0 equiv. ArB(neop), 6 equiv. Et₃N, 30 mol % Cu(OTf)₂, DMA (0.3M), rt in air; utilized 0.5 dram with 22 gauge needle.

The nature of the boronic acid or ester species was observed to have a profound effect on the reaction outcome (Table 2-2). The employment of arylboroxines (entry 1) gave the highest product yield. The use of neopentyl boronic esters (entry 2) provided yields close to the optimized conditions, though still lower than the arylboroxine. In contrast, the pinacol boronic ester (entry 3) provided very low yields of product with a high level of half ester conversion. The free boronic acid (entry 4) gave no discernable yield by NMR, with a very low conversion of the starting material.

Table 2-2 Effect of the boronic acid/ester on the decarboxylative oxidative arylation of a monofluoro malonate half ester

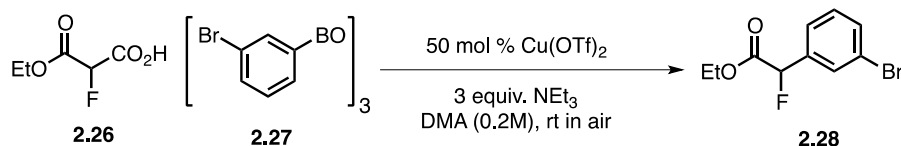


Entry	Arylboron Source	2.26 conversion (%)	2.28 yield (%)
1	(Ar-BO) ₃ (boroxine)	>95	78
2	Ar-B(neop)	88	64
3	Ar-B(pin)	70	14
4	Ar-B(OH) ₂	20	<5

Utilized 0.5 dram with 20 gauge needle. Conversion and yields determined by calibrated ¹H NMR.

The use of a weakly-coordinating counteranion on the copper species was discovered to be vital to the proficiency of the reaction (Table 2-3). The standard reaction was conducted utilizing either Cu(OTf)₂ (entry 1), a Cu(II) source with weakly coordinating triflate counterions, or [(MeCN)₄Cu]PF₆ (entry 2), a Cu(I) source with a non-coordinating hexafluorophosphate anion. Both reactions provided near identical conversion of arylboroxine and yield of product. Cu(OAc)₂ (entry 3), a Cu(II) source with strongly coordinating acetate anions, was also utilized under the standard conditions, providing very little conversion of starting material to the desired product. This not only demonstrates the necessity for weakly or non-coordinating anions in this reaction, but also demonstrates that the initial oxidation state of the copper species has little effect on the reaction outcome. This is most likely due to the expedient oxidation of the copper center by atmospheric oxygen under the employed conditions.

Table 2-3 Effect of the copper species on the decarboxylative oxidative arylation of a fluoromalonate half ester



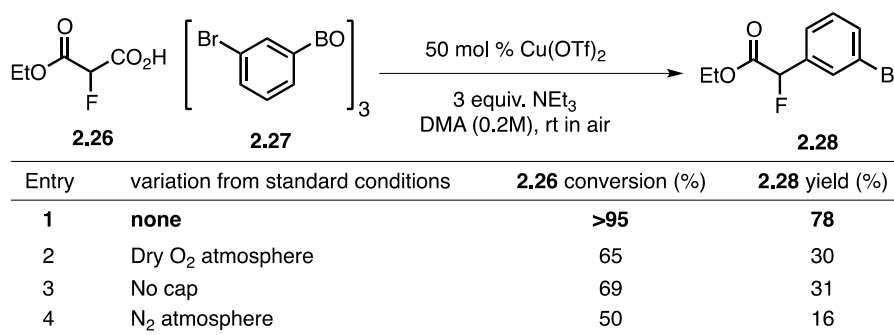
Entry	variation from standard conditions	2.26 conversion (%)	2.28 yield (%)
1	none	>95	78
2	Cu(MeCN) ₄ PF ₆ instead of Cu(OTf) ₂	94	74
3	Cu(OAc) ₂ instead of Cu(OTf) ₂	50	<5

"Standard conditions": 250 mol % arylboron as boroxine, 0.5 dram vial with 20 gauge needle. Conversion and yields determined by calibrated ¹H NMR.

The composition of the reaction headspace has a profound effect on the reaction outcome (Table 2-4). The standard conditions (entry 1) utilize a 20-gauge needle that pierces the septum cap of the reaction vial, exposing the solution to atmosphere. This allows oxygen to diffuse into the reaction mixture. If oxygen is allowed to diffuse at a greater rate, such as when an oxygen atmosphere is employed (entry 2) or the cap is entirely removed from the reaction vial (entry 3), formation of the product is impeded dramatically. This may be due to some form of oxidative degradation of the copper, which is accelerated when more oxygen is present. If oxygen is fully excluded (entry 4), the formation of product is further lowered. This reaction ceases before even one turnover of the copper is achieved (as two equivalents of copper are required for one catalytic turnover, under the assumption that this reaction proceeds in a similar fashion to the CEL system²⁸). As such, oxygen may have a role in not only turning over the copper catalytically, but also promoting the reaction. The preceding experiments demonstrate that the oxygen content in the reaction headspace and the rate of diffusion into the solution must be carefully controlled in order to have an efficient reaction. This will be important if this reaction

is scaled up, as these will change with changing reaction volume, reaction surface area, and headspace volume.

Table 2-4 Effect on the atmosphere on the decarboxylative oxidative arylation of a monofluoro malonate half ester

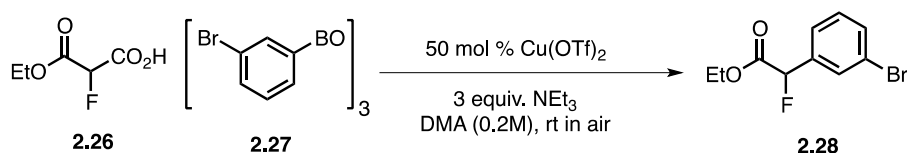


"Standard conditions": 250 mol % arylboron as boroxine, 0.5 dram vial with 20 gauge needle. Conversion and yields determined by calibrated ¹H NMR.

A number of other parameters and reaction modifications were also explored (Table 2-5). If the use of a valuable arylboroxine is required, the equivalents of arylboroxine can be lowered (entry 2) or the reaction stoichiometry can be reversed (entry 3) with moderate effects on the terminal yield of the product. The same effect can be seen if the use of the potassium salt of the carboxylate (as opposed to the free acid) is desired, as the reaction is still productive albeit with a decrease in yield (entry 4). Though the yield decreases quite dramatically, the use of a non-polar solvent such as 1,2-dichloroethane (entry 5) still provides product. This is an important parameter if the product of the reaction is water-soluble, and a loss in yield will occur if the subsequent reaction work-up involves aqueous washes; using DCE as the solvent allows direct *in vacuo* concentration of the crude reaction mixture, which can then be directly purified via flash column chromatography. Entry 6 demonstrates that this reaction can be performed without the

use of an inert-atmosphere glovebox. It is inadvisable to utilize overtly wet materials, as boronic acids (which result from the hydrolysis of boroxines) have been demonstrated to be ineffective in this chemistry (Table 2-2, entry 3). The use of dry reagents (especially copper source and arylboroxine) and dry solvents is still recommended, though these materials can be readily manipulated in atmosphere without detrimental effects to the reaction.

Table 2-5 Effect of various parameters on the decarboxylative oxidative arylation of a monofluoro malonate half ester



Entry	variation from standard conditions	2.26 conversion (%)	2.28 yield (%)
1	none	>95	78
2	1.2 equiv. arylboron as boroxine	82	58
3	Inverse stoichiometry conditions ^a	72	60
4	Potassium salt of acid	95	62
5	DCE as Solvent	94	45
6	Reaction set-up outside glovebox ^b	95	77

"Standard conditions": 250 mol % arylboron as boroxine, 0.5 dram vial with 20 gauge needle. Conversion and yields determined by calibrated ¹H NMR. ^a 1:2 arylboron as boroxine:half ester, 100 mol % Cu(OTf)₂, 6 equiv. Et₃N. ^b All reagents brought out of glovebox, exposed to atmosphere for 10 minutes, then manipulated as per the standard reaction.

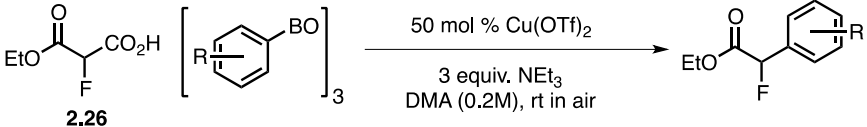
2.3 Reaction Scope

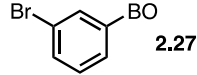
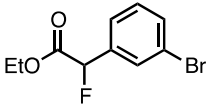
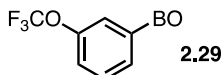
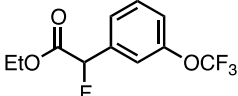
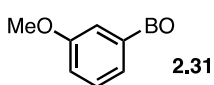
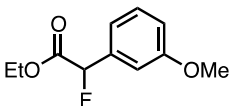
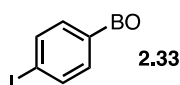
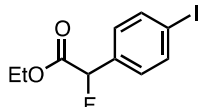
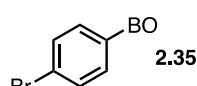
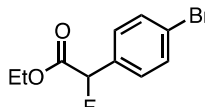
A range of substituted arylboroxines and arylboronic esters, as well as ester modifications of the monofluoro malonate half esters, were utilized in the oxidative arylation chemistry, all with moderate to good yields. Optimal yields were found for aryl groups with either moderately electron-poor or moderately electron-rich substituents.

2.3.1 Scope of Mono-Substituted Arylboroxines

A range of mono-substituted arylboroxines with varying electronic properties were utilized in this chemistry (Table 2-6, Table 2-7). Of note are the compatibility of aryl iodides (**2.33**), aryl bromides (**2.27** and **2.35**), and aryl chlorides (**2.36** and **2.38**). All of these are potentially reactive electrophilic functionalities under comparable palladium-catalyzed reactions.⁹²

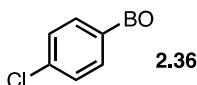
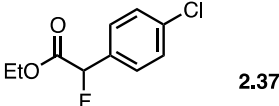
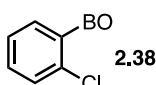
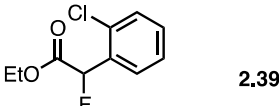
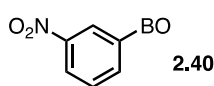
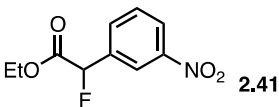
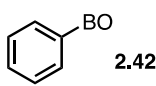
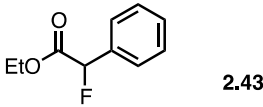
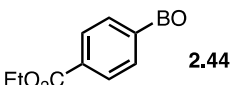
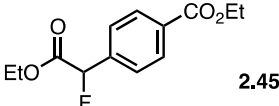
Table 2-6 Copper-mediated oxidative decarboxylative arylation of monofluoro malonate half esters using mono-substituted arylboroxines, Part 1



Entry	Substrate	Product	Yield (%)
1	 2.27	 2.28	73
2	 2.29	 2.30	70
3	 2.31	 2.32	55
4	 2.33	 2.34	59
5	 2.35	 2.21	65

250 mol % aryl-boron as boroxine. Yields are of isolated material.

Table 2-7 Copper-mediated oxidative decarboxylative arylation of monofluoro malonate half esters using mono-substituted arylboroxines, Part 2

Entry	Substrate	Product	Yield (%)
1	 2.36	 2.37	69
2	 2.38	 2.39	58
3	 2.40	 2.41	56
4	 2.42	 2.43	59 ^a
5	 2.44	 2.45	50 ^a

250 mol % aryl-boron as boroxine. Yields are of isolated material. ^aValue determined by calibrated ¹H NMR.

2.3.2 Scope of Poly-Substituted and Heteroaromatic Arylboroxines and Arylboronic Neopentyl Glycol Esters

A variety of polysubstituted aryl groups were found to give satisfactory to good yields under the employed reaction conditions (Table 2-8). The use of the less reactive (when compared to the boroxine) arylboronic neopentyl glycol ester was found to give better yields with a number of highly activated aryl groups (**2.48** and **2.50**). The boronic ester was also key to the use of heteroaryl substrates (**2.54** and **2.56**) in order to tame their reactivity, as significantly reduced

product yields were observed when using the equivalent arylboroxine. This was primarily a result of increased unproductive arylboron consumption under the reaction conditions. A Michael acceptor-substituted aryl partner (**2.58**), a potential nucleophile trap, was found to be tolerated under the reaction conditions, providing a satisfactory yield of product.

Table 2-8 Copper-mediated oxidative decarboxylative arylation of monofluoro malonate half esters using polysubstituted and heteroaromatic arylboroxines and arylboronic esters

Table 2-7
Poly-substituted aryl and heteroaryl

50 mol % Cu(OTf)₂
3 equiv. NEt₃
DMA (0.2M), rt in air

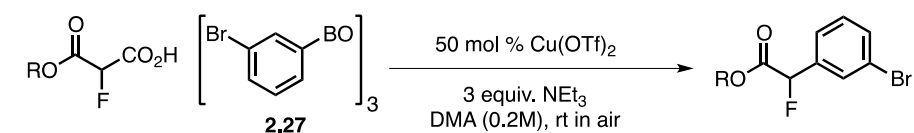
Entry	Substrate	Product	Yield (%)
1	2.46	2.47	59
2	2.48	2.49	49
3	2.50	2.51	76
4	2.52	2.53	67 ^a
5	2.54	2.55	51
6	2.56	2.57	43 ^b
7	2.58	2.59	50

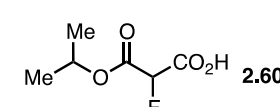
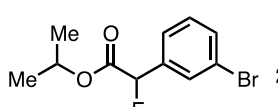
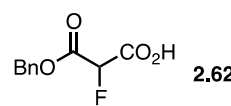
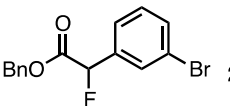
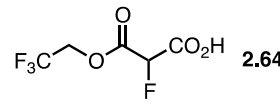
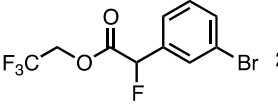
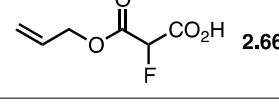
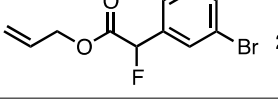
250 mol % arylboron as boroxine or neopentyl glycol boronic ester. Yields are of isolated material.
^a200 mol % arylboron as boroxine. ^b1,2-dichloroethane as solvent.

2.3.3 Scope of Ester Substitutions of the Monofluoro Malonate Half Ester

Modifications of the monofluoro malonate half ester coupling partner were also investigated, providing good to excellent yields in all cases (Table 2-9). These included the sterically hindered substituents *iso*-propyl (**2.60**) and benzyl (**2.62**), as well as the electron-deficient 2,2,2-trifluoroethyl (**2.64**). An unactivated alkene (**2.66**) was also found to be compatible under our reaction conditions.

Table 2-9 Copper-mediated oxidative decarboxylative arylation of monofluoro malonate half esters with variations on the ester



Entry	Substrate	Product	Yield (%)
1	 2.60	 2.61	69
2	 2.62	 2.63	59
3	 2.64	 2.65	59
4	 2.66	 2.67	74

250 mol % aryl-boron as boroxine. Yields are of isolated material.

2.3.4 Unsuccessful Substrates

A number of aryl and monofluoro carbonyl substrates were found to be incompatible with our established coupling conditions. Incompatible aryl partners (Table 2-10) included the

extremes of electron-poor and electron-rich aryl partners. Issues with electron-rich substrates (**2.68** and **2.70**) were likely due to the low conversion of the arylboron coupling partner, potentially resulting from a decreased rate of transmetalation. We have experienced these issues before when dealing with electron-rich arylboron reagents under oxidative conditions.^{44, 68} Alternatively, electron-poor reagents (**2.72**) suffer from two major issues. One issue is that these arylboroxines exhibit a very high reactivity profile, resulting in the unproductive consumption of the arylboron reagent. The second is that the benzylic position of the product (**2.73**) becomes sufficiently acidic, facilitating further arylation. This is exhibited by the presence of 25% α,α -diaryl product in the reaction mixture.

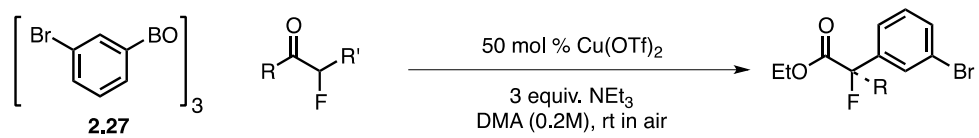
Table 2-10 Unsuccessful aryl examples in the copper-mediated oxidative decarboxylative arylation of monofluoro malonate half esters

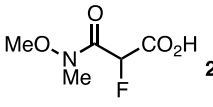
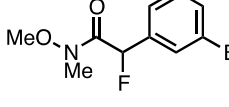
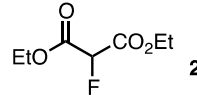
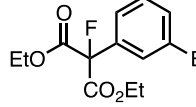
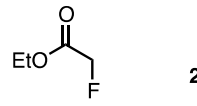
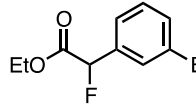
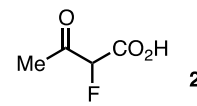
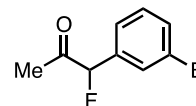
Entry	Substrate	Product	2.26 conversion (%)	Yield (%)
1	 2.68	 2.69	n.d.	37
2	 2.70	 2.71	87	23
3	 2.72	 2.73	n.d.	26 ^a

250 mol % arylboron as boroxine. Yields and conversions determined by calibrated ¹H NMR. ^aArylation of product also observed, amounting to 25%. ^bn.d. = not determined.

A number of other α -fluoro carbonyl compounds were also investigated, in the event that the scope of this reaction may be expanded beyond ester containing coupling partners (Table 2-11). The Weinreb amide (**2.74**) was synthesized and tested under the reaction conditions; as the reactivity profile of this substituent is actually closer to that of an ester than an amide⁹⁷, we had hoped that this reaction would be successful. Unfortunately, high conversion of the starting material is accompanied by only a small amount of product (**2.75**). Diethyl monofluoro malonate (**2.76**) was tested in hopes of synthesizing arylated malonate molecules similar to our previous work.⁴⁴ However, this reaction gave low yield of product (**2.77**) and only a modest conversion of starting material (**2.76**). Ethyl fluoroacetate (**2.78**) appeared to be completely unreactive, as indicated by the lack of starting material conversion. This is not surprising, as α -arylation reaction utilizing similar acetates under palladium-catalyzed conditions usually require much stronger bases.⁹⁴ Finally, the α -fluoro- β -ketoacid (**2.80**) was tested in hopes of generating α -fluoro- α -arylated ketones (**2.81**). This substrate was unsuccessful, as very little product was produced.

Table 2-11 Attempted copper-mediated oxidative arylation of α -fluoro carbonyls



Entry	Substrate	Product	fluoro conversion (%)	Yield (%)
1	 2.74	 2.75	>95	8
2	 2.76	 2.77	45	5
3	 2.78	 2.28	<5	<5
4	 2.80	 2.81	n.d.	<5

250 mol % aryl-boron as boroxine. Yields and conversions determined by calibrated ^1H NMR. ^an.d. = not determined.

The *ortho*-tolylboroxine reagent (**2.82**) was utilized in order to test sterically hindered aryl groups (Figure 2-14). The desired product (**2.83**) was not observed. Instead, the products that were isolated consisted of an *O*-arylated ester (**2.84**) and the α -arylation of this molecule (**2.85**). This result provides clues for one of the copper intermediates in this reaction. These are discussed below.

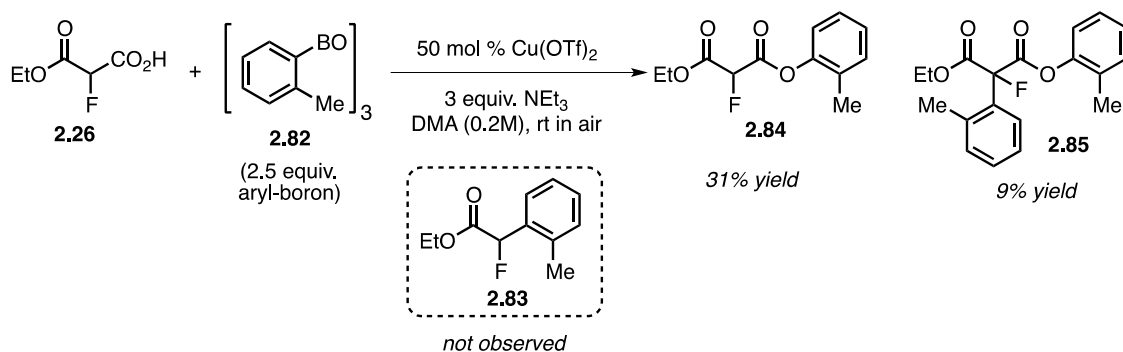


Figure 2-14 Attempted oxidative decarboxylative synthesis utilizing *ortho*-tolylboroxine (**2.82**), instead yielding an *O*-arylated ester (**2.84**) and further α -arylated product (**2.85**)

2.4 Mechanistic Considerations

An understanding of the mechanism of this reaction is currently lacking. As this reaction has similarities to the CEL reaction, whose mechanism has been extensively investigated,^{27-29, 42} we wish to use this as inspiration to propose a mechanism for this reaction (Figure 2-15). The initial Cu(II) (**15-I**) undergoes base-mediated substitution with the carboxylate (**15-II**), followed by transmetalation with the arylboron reagent to generate a Cu(II)-aryl-carboxylate species (**15-III**). This species can then undergo disproportionation with another Cu(II) to generate a Cu(III) (**15-IV**), which can reductively eliminate to give a carboxylated intermediate (**15-V**). This intermediate can decarboxylate to generate our desired monofluoro aryl acetate (**15-VI**). The Cu(I) that was generated in the reductive elimination (**15-VII**) can be reoxidized back to the Cu(II) starting point.

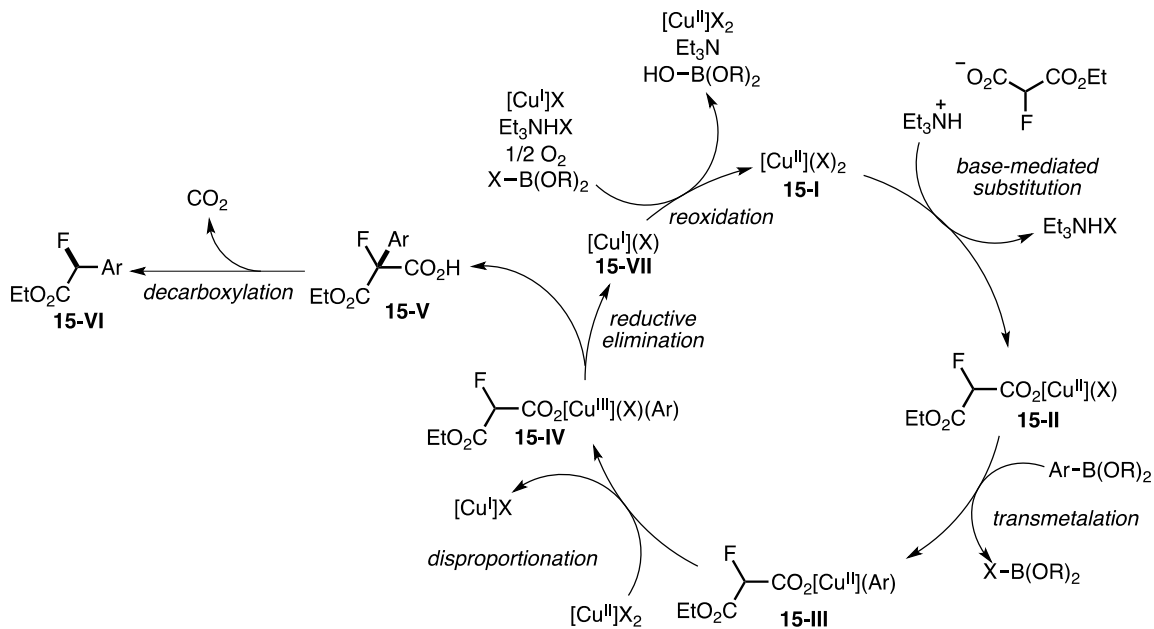


Figure 2-15 Proposed mechanistic pathways for monofluoro aryl acetate synthesis by oxidative cross-coupling

Providing evidence for the above mechanism, our previous work into malonate half esters has shown that the carbon-carbon bond formation *precedes* decarboxylation with the non-fluorine substrate, and that decarboxylation occurs rapidly *in situ* under our reaction conditions (Figure 2-16).⁹⁸ Rapid decarboxylation of the α -carboxylic acid product occurs in DMA with or without $\text{Cu}(\text{OTf})_2$, while no discernable conversion is evident when the same process is conducted in DCE (Figure 2-16 A). Additionally, the α -carboxylic acid product is detectable by NMR when the reaction is conducted in DCE as the solvent (Figure 2-16 B), providing strong evidence for arylation occurring before decarboxylation. As our fluorinated substrate of interest is not identical, this pathway is not necessarily operational. However, due to the similarities in half ester structure, this is still a viable mechanistic route.

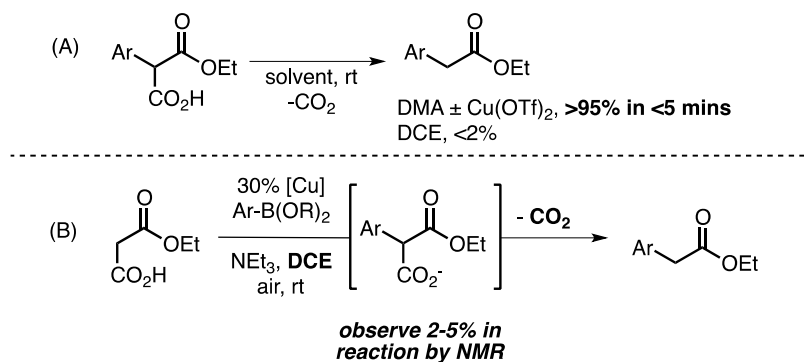


Figure 2-16 (A) Effect on the decarboxylation of the α -carboxy product in the presence of DMA (\pm Cu(OTf)₂) or DCE solvent; (B) NMR evidence for the *in situ* generation of the α -carboxy intermediate

In the above mechanistic cycle (see Figure 2-15), the carbon-carbon bond forming event occurs via an intramolecular process, where both coupling partners are bound to the copper. Omitted from the above scheme is migration in copper-binding (Figure 2-17 A) from the carboxylate (**17-I**) to the α -carbon (**17-II**), preceding reductive elimination. Alternatively, a bimolecular process involving two copper centers could be active (Figure 2-17 B). A nucleophilic Cu(II) enolate (**17-V**) could form by proton abstraction from a copper-bound carboxylate (**17-IV**). We have previously shown that the α -deprotonation of similar malonate scaffoldings can occur with triethylamine.⁴⁴ This generated enolate could perform a nucleophilic attack on an aryl-Cu(III) (**17-VI**), performing a net α -arylation (**17-VII**). This intermediate could then be hydrolyzed by the base used in the first step, yielding the desired α -arylated product prior to decarboxylation (**17-VIII**).

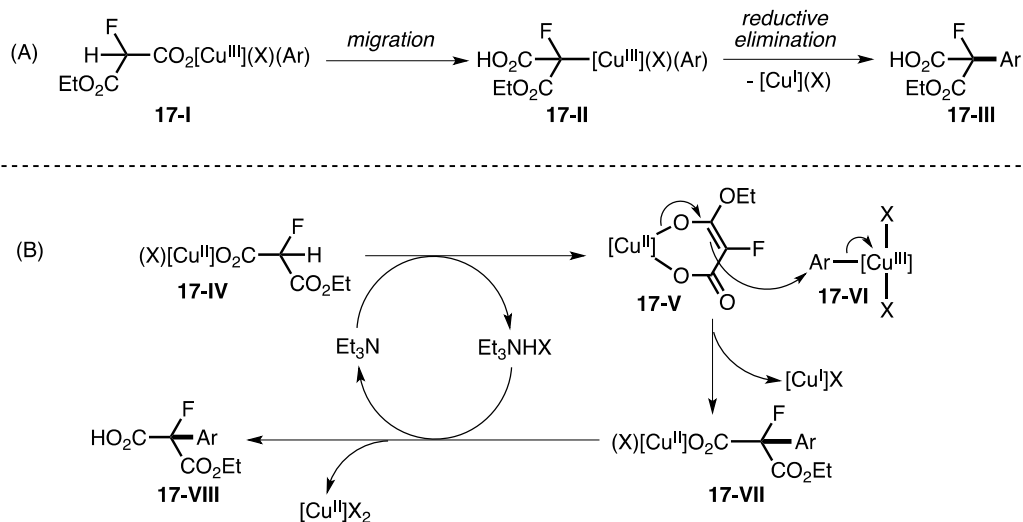


Figure 2-17 (A) Migration from carboxylate (**17-I**) to α -carbon (**17-II**) binding to copper centre, followed by reductive elimination to yield the α -arylated product prior to decarboxylation; (B) alternative bimolecular mechanism relying on the formation of a copper-bound enolate (**17-V**)

Evidence for a discrete copper-aryl species bound to a carboxylate stems from the results of the *ortho*-tolyl reaction (see Figure 2-14). The *ortho*-methyl substituent most likely prevents migration to the α -carbon-bound intermediate due to steric hindrance (Figure 2-18 A). Oxidation of the metal centre still occurs to generate a Cu(III), which reductively eliminates to give the *O*-arylated product (**2.84**). This product could be deprotonated by triethylamine, followed by binding to an aryl-Cu(II) (Figure 2-18 B). We have previously demonstrated that triethylamine can deprotonate similar malonate scaffoldings.⁴⁴ Subsequent oxidation of the metal center by disproportionation followed by reductive elimination would generate the α -arylated product (**2.85**).

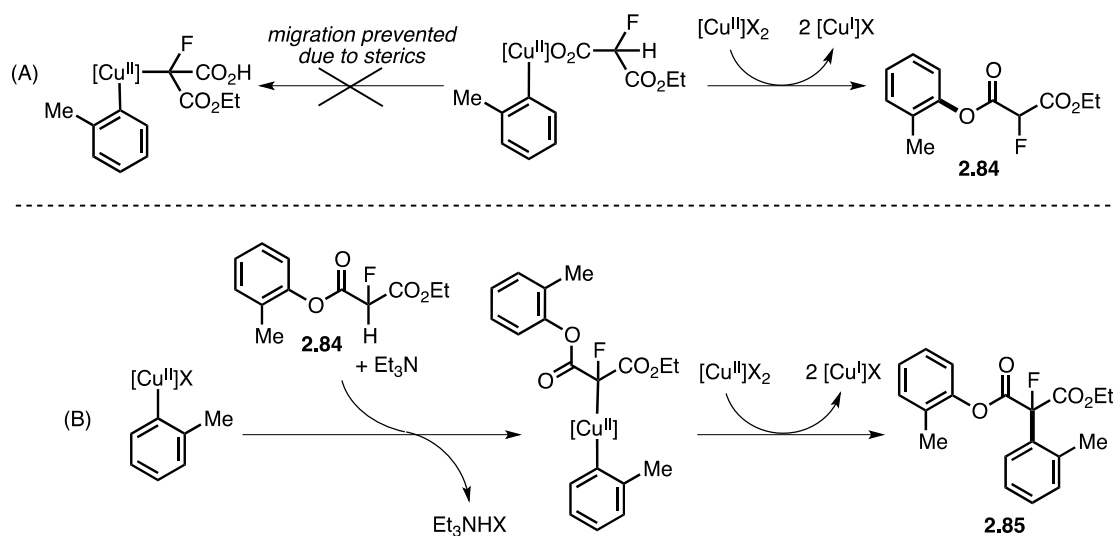


Figure 2-18 (A) Proposed reaction for generating the *O*-arylated product (**2.84**); (B) proposed reaction to form the α -arylated product (**2.85**)

Competition studies were conducted to further probe the reaction. Under the unsubstituted half ester conditions⁶⁸ (Figure 2-19), little to no conversion of the monofluoro half ester (**2.86**) was observed, while the unsubstituted half ester (**2.86**) yielded over 45% product (**2.87**). Under the monofluoro optimized conditions (Figure 2-20), the unsubstituted half ester (**2.86**) produced product (**2.87**) at a slower rate and appeared to decompose once peak product was reached. The monofluoro half ester (**2.26**) produced product (**2.28**) in an almost zero-order fashion, lagging behind its unsubstituted counterpart. These results would suggest a significant difference in binding affinity of the carboxylate intermediate to the metal center. The inductive effects of the fluorine would make the carboxylate more acidic. As increased acidity corresponds to a reduced nucleophilicity due to the increased stabilization of the anion, this increased acidity would directly affect the efficacy of the carboxylate binding onto the copper centre.

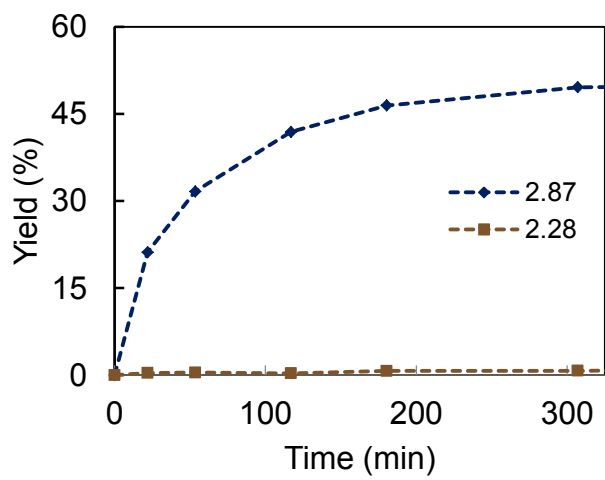
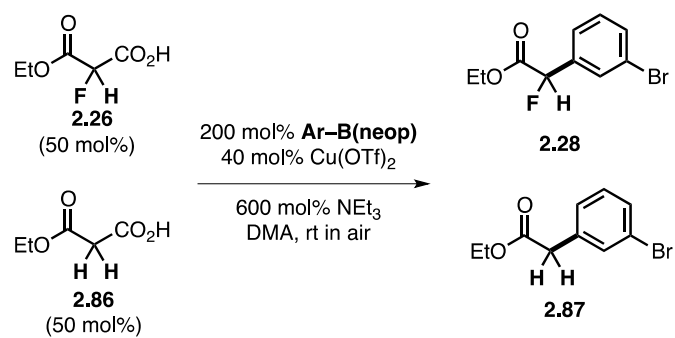


Figure 2-19 Competition study under malonate half ester optimized conditions

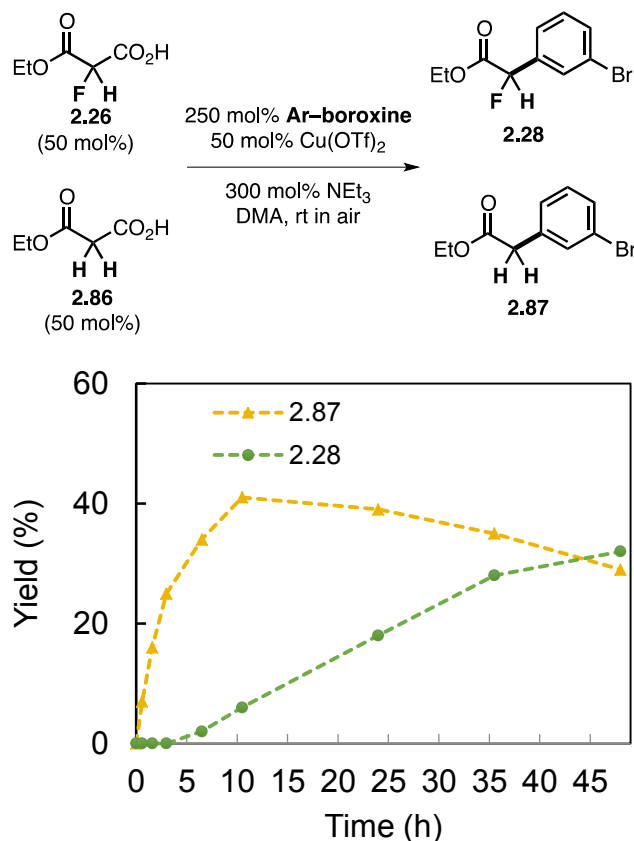


Figure 2-20 Competition study under monofluoro malonate half ester optimized conditions

To test this idea, we utilized the trifluoroethyl ester (**2.64**) and competed it against the monofluoro malonate half ester (**2.26**) under the optimized conditions (Figure 2-21). The trifluoroethyl-malonate half ester (**2.64**) generated product (**2.65**) at only a slightly faster rate than the monofluoro malonate half ester (**2.26**), with this product (**2.28**) beginning to degrade after about 15 hours. The similarity in product formation kinetics implies that the effect of the α -fluoro is due to an inductive withdrawal of electron density, as the increasing acidity of the carboxylate hinders carboxylate binding to the metal center and/or reduces the efficiency of the decarboxylation event.

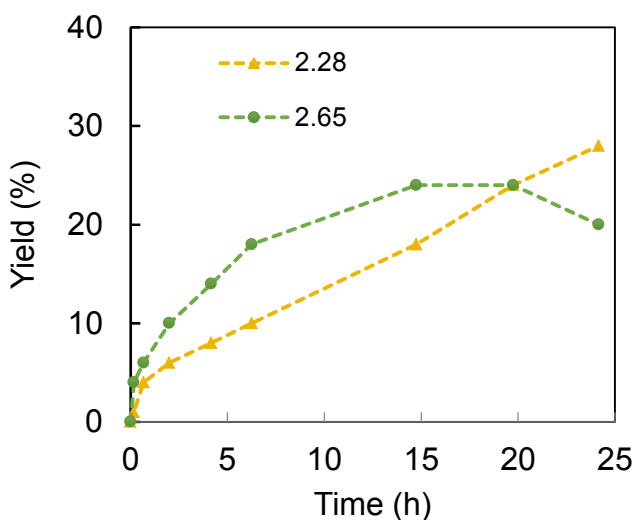
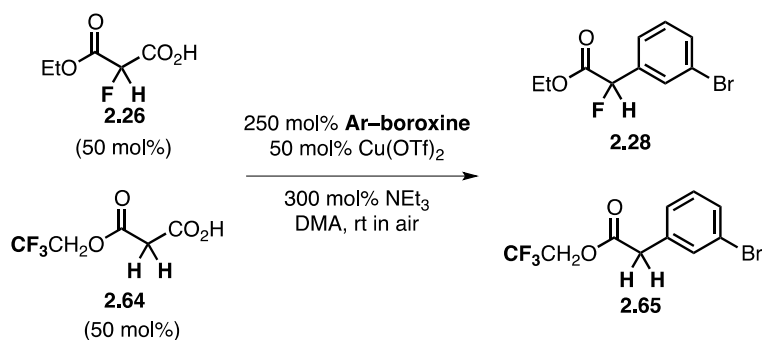


Figure 2-21 Competition study utilizing trifluoroethyl-ester (**2.64**) and α -fluoro malonate half ester (**2.26**)

2.5 Summary

A new oxidative copper-mediated method for the synthesis of α -aryl- α -fluoro acetates has been developed. This reaction couples together an arylboroxine or arylboronic ester and a monofluoro malonate half ester in a copper-mediated oxidative decarboxylative cross-coupling reaction to generate a new carbon–carbon bond. This reaction proceeds under exceptionally mild, aerobic conditions, and utilizes a relatively cheap and abundant copper-based mediator.

A range of aryl reaction partners were tested and found to be compatible under this chemistry. Potentially problematic electrophilic functionalities remained intact under our

conditions; these included aryl chlorides, aryl bromides, aryl iodides, Michael acceptors, and nitrogen-containing heterocycles. Exceptionally electron-poor or electron-rich aryl groups, as well as protic heteroatoms, did not appear to be well tolerated. A number of other α -fluoro-carbonyls, including a Weinreb amide and a methyl ketone, were tested under the reaction conditions, with none producing appreciable yields of their respective arylated products.

The unexpected results in the attempt to generate the *ortho*-tolyl product gave insights into the structure of one of the copper intermediates in the reaction mechanism, implying the presence of a carboxylate-bound copper-aryl species. Competition studies suggest a strong acidity dependence on the rate of the reaction, with this acidity dependence impacting the carboxylate binding to the metal center or the rate of decarboxylation, or both.

2.6 Procedures and Characterization

2.6.1 General Considerations

Unless noted, all reactions were setup under inert atmosphere employing standard schlenk technique or by the use of an N₂-filled glovebox. All glassware was oven-dried prior to use. Flash chromatography was performed as described by Still and co-workers⁹⁹ (SiliaFlash P60, 40-63 μ m, 60A silica gel, Silicycle) or by automated flash chromatography (Isolera, HP-SIL or Ultra SNAP silica cartridges, Biotage). Analytical thin-layer chromatography was performed using glass plates pre-coated with silica (SiliaPlate G TLC - Glass-Backed, 250 μ m, Silicycle). TLC plates were visualized by UV light and/or staining with aqueous basic potassium permanganate. Unless otherwise noted, all reagents were obtained from commercial vendors and used as supplied. Mono ethyl fluoro malonate (**2.26**) was synthesized according to literature procedure from diethyl monofluoro malonate.¹⁰⁰ Other fluoro malonate half esters were prepared according to literature procedure.¹⁰¹ Arylboroxines were prepared by dehydration of the corresponding boronic acid according to established methods.⁴⁴ Arylboronic esters were synthesized according to literature procedures.¹⁰²⁻¹⁰³ Certain compounds were not isolated and fully characterized. These include **2.43**, **2.45**, **2.59**, **2.69**, **2.71**, **2.73**, **2.75**, and **2.77**. The ¹H NMR yields reported for these compounds were by comparison to an internal standard. The diagnostic product signal that was utilized was a doublet that would appear between δ 6.0-5.5 ppm, indicative of a hydrogen coupled to a geminal fluorine, with both atoms bonded to the α -carbon of a monofluoro aryl acetate.

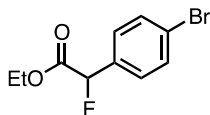
2.6.2 General Procedures for the Copper Catalyzed Synthesis of Mono-Fluoro Aryl Acetates via Decarboxylative Cross-Coupling

Procedure A (0.5 mmol scale) In an atmosphere controlled glovebox $\text{Cu}(\text{OTf})_2$ (90.4 mg, 0.250 mmol, 0.50 equiv.) and arylboronic ester (1.25 mmol, 2.5 equiv.) or arylboroxine (0.42 mmol, 2.5 equiv. Ar-B) were added sequentially to a 1 dram screw-top vial charged with a stir bar. The fluoro malonic half ester (0.50 mmol, 1.0 equiv.) was added as a solution in anhydrous DMA (1.0 mL). Additional DMA (2 x 0.6 mL) was used to quantitatively transfer the solution to the reaction mixture. The solution was stirred until the majority of the solid had dissolved, followed by the addition of NEt_3 (0.2 mL, 1.5 mmol, 3.0 equiv.). The vial was sealed with a PTFE-lined cap, removed from the glovebox, and the PTFE septum pierced with an 18 gauge needle. The reaction mixture was gently stirred at room temperature. Upon reaction completion (24 to 72 h), the reaction mixture was diluted with EtOAc (60 mL), and washed sequentially with NH_4Cl (60 mL), 0.5 M NaOH (2 x 60 mL), and brine (60 mL). The organic layer was dried with Na_2SO_4 , concentrated *in vacuo*, and purified by silica gel chromatography. Note, the needle gauge and vial size can influence the reaction rates and overall efficiency. Reactions conducted without the use of a glovebox gave similar results. $\text{Cu}(\text{OTf})_2$ and arylboroxines are hydroscopic and should be stored under inert gas.

Procedure B (0.2 mmol scale): In an atmosphere controlled glovebox $\text{Cu}(\text{OTf})_2$ (36.2 mg, 0.10 mmol, 0.50 equiv.) and arylboronic ester (0.5 mmol, 2.5 equiv.) or arylboroxine (0.17 mmol, 2.5 equiv. Ar-B) were added sequentially to a 0.5 dram screw-top vial charged with a stir bar. The fluoro malonic half ester (0.20 mmol, 1.0 equiv.) was added as a solution in anhydrous DMA (0.5 mL). Additional DMA (2 x 0.2 mL) was used to quantitatively transfer the solution to the reaction mixture. The solution was stirred until the majority of the solid had dissolved,

followed by the addition of NEt₃ (0.09 mL, 0.6 mmol, 3.0 equiv.). The vial was sealed with a PTFE-lined cap, removed from the glovebox, and the PTFE septum pierced with an 20 gauge needle. The reaction mixture was gently stirred at room temperature and worked up after completion according the procedure described above.

Procedure C (2.0 mmol scale, no glove box): To a 4 dram with a stirbar was added Cu(OTf)₂ (362 mg, 1.0 mmol, 0.50 equiv.) and 3-bromophenylboroxine (914 mg, 1.67 mmol, 2.5 equiv. Ar-B). DMA (8.9 mL) was used to quantitatively transfer (with rinsing) the fluoro malonic half ester (300 mg, 2.0 mmol, 1.0 equiv.) into the vial. The solution was stirred until the majority of the solid had dissolved, followed by the addition of NEt₃ (0.84 mL, 6.0 mmol, 3.0 equiv.). The vial was sealed with a PTFE-lined cap, and the PTFE septum was pierced with two 18 gauge needles. The reaction mixture was gently stirred at room temperature (72% yield based on calibrated ¹H NMR).



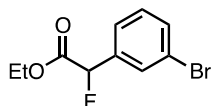
Product 2.21 Prepared according to Procedure A from the corresponding arylboroxine (229 mg, 0.42 mmol, 2.5 equiv. Ar-B) and fluoro malonic half ester (75 mg, 0.50 mmol, 1.0 equiv.), 53 h. Isolated in 65% yield after purification by column chromatography (Hex/EtOAc gradient, 98:2 to 80:20) as a light yellow oil.

¹H NMR (CDCl₃, 700 MHz) δ 7.54 – 7.52 (m, 2H), 7.35 – 7.32 (m, 2H), 5.72 (d, *J* = 47.6 Hz, 1H), 4.28 – 4.18 (m, 2H), 1.25 (t, *J* = 7.1 Hz, 3H);

¹³C NMR (CDCl₃, 126 MHz) δ 168.0 (d, *J* = 27.5 Hz), 133.3 (d, *J* = 20.9 Hz), 132.0, 128.2 (d, *J* = 6.3 Hz), 123.8 (d, *J* = 2.6 Hz), 88.7 (d, *J* = 186.6 Hz), 62.0, 14.0;

^{19}F NMR (CDCl_3 , 377 MHz) δ -181.5 (d, J = 47.6 Hz);

HRMS (EI): calcd for $\text{C}_{10}\text{H}_{10}\text{BrFO}_2$ $[\text{M}]^+$: 259.9848. Found 259.9850.



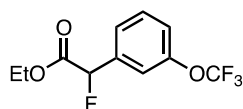
Product 2.28 Prepared according to Procedure A from the corresponding arylboroxine (229 mg, 0.42 mmol, 2.5 equiv. Ar-B) and fluoro malonic half ester (75 mg, 0.50 mmol, 1.0 equiv.), 49 h. Isolated in 73% yield after purification by column chromatography (10:1 Hex/EtOAc) as a light yellow oil.

^1H NMR (CDCl_3 , 700 MHz) δ 7.63 – 7.61 (m, 1H), 7.54 – 7.51 (m, 1H), 7.41 – 7.38 (m, 1H), 7.29 – 7.26 (m, 1H), 5.72 (d, J = 47.4 Hz, 1H), 4.30 – 4.20 (m, 2H), 1.26 (t, J = 7.2 Hz, 3H);

^{13}C NMR (CDCl_3 , 176 MHz) δ 167.9 (d, J = 27.1 Hz), 136.3 (d, J = 21.3 Hz), 132.6 (d, J = 1.9 Hz), 130.3, 129.5 (d, J = 7.0 Hz), 125.0 (d, J = 6.4 Hz), 122.8, 88.4 (d, J = 187.6 Hz), 62.1, 14.0;

^{19}F NMR (CDCl_3 , 377 MHz) δ -182.3 (d, J = 47.8 Hz);

HRMS (EI): calcd for $\text{C}_{10}\text{H}_{10}\text{BrFO}_4$ $[\text{M}]^+$: 259.9848. Found 259.9846.



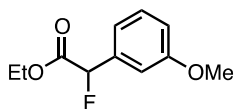
Product 2.30 Prepared according to Procedure A from the corresponding arylboroxine (235 mg, 0.42 mmol, 2.5 equiv. Ar-B) and fluoro malonic half ester (75 mg, 0.50 mmol, 1.0 equiv.), 49 h. Isolated in 70% yield after purification by column chromatography (gradient, 100% to 90% Hex/EtOAc) as a light yellow oil.

¹H NMR (CDCl₃, 700 MHz) δ 7.45 – 7.40 (m, 2H), 7.35 – 7.33 (m, 1H), 7.26 – 7.23 (m, 1H), 5.78 (d, *J* = 47.6 Hz, 1H), 4.30 – 4.21 (m, 2H), 1.26 (t, *J* = 7.17 Hz);

¹³C NMR (CDCl₃, 126 MHz) δ 167.8 (d, *J* = 26.9 Hz), 149.4 (d, *J* = 1.8 Hz), 136.4 (d, *J* = 21.3 Hz), 130.3, 124.6 (d, *J* = 6.7 Hz), 121.9, 120.4 (q, *J* = 258.9 Hz), 119.0 (d, *J* = 7.02 Hz), 88.4 (d, *J* = 187.7 Hz), 62.1, 14.0;

¹⁹F NMR (CDCl₃, 377 MHz) δ –58.0 (s, 3F), –183.2 (d, *J* = 47.5 Hz, 1F);

HRMS (EI): calcd for C₁₁H₁₀F₄O₃ [M]⁺: 266.0566. Found 266.0569.



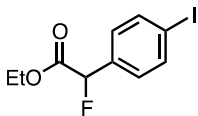
Product 2.32 Prepared according to Procedure A from the corresponding arylboroxine (167 mg, 0.42 mmol, 2.5 equiv. Ar–B) and fluoro malonic half ester (75 mg, 0.50 mmol, 1.0 equiv.), 48 h. Isolated in 55% yield after purification by column chromatography (20:1 Hex/EtOAc) as a light yellow oil.

¹H NMR (CDCl₃, 700 MHz) δ 7.32 – 7.29 (m, 1H), 7.05 – 7.02 (m, 1H), 7.00 – 6.99 (m, 1H), 6.94 – 6.91 (m, 1H), 5.73 (d, *J* = 48.0 Hz, 1H), 4.29 – 4.18 (m, 2H), 3.81 (s, 3H), 1.26 (t, *J* = 7.18 Hz, 3H);

¹³C NMR (CDCl₃, 176 MHz) δ 168.4 (d, *J* = 27.5 Hz), 159.8, 135.6 (d, *J* = 20.1 Hz), 129.8, 118.9 (d, *J* = 6.6 Hz), 115.4 (d, *J* = 2.1 Hz), 111.8 (d, *J* = 6.72 Hz), 89.2 (d, *J* = 185.7 Hz), 61.8, 55.3, 14.0;

¹⁹F NMR (CDCl₃, 377 MHz) δ –180.4 (d, *J* = 48.0 Hz);

HRMS (EI): calcd for C₁₁H₁₃FO₃ [M]⁺: 212.0849. Found 212.0849.



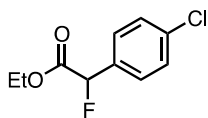
Product 2.34 Prepared according to Procedure A from the corresponding arylboroxine (287 mg, 0.42 mmol, 2.5 equiv. Ar–B) and fluoro malonic half ester (75 mg, 0.50 mmol, 1.0 equiv.), 49 h. Isolated in 59% yield after purification by column chromatography (Hex/EtOAc gradient, 98:2 to 80:20) as a clear, light-yellow oil.

¹H NMR (CDCl₃, 700 MHz) δ 7.75 – 7.72 (m, 2H), 7.21 – 7.18 (m, 2H), 5.70 (d, *J* = 47.5 Hz, 1H), 4.28 – 4.18 (m, 2H), 1.25 (t, *J* = 7.1 Hz);

¹³C NMR (CDCl₃, 126 MHz) δ 168.0 (d, *J* = 27.3 Hz), 137.9, 134.0 (d, *J* = 20.9 Hz), 128.3 (d, *J* = 6.3 Hz), 95.7 (d, *J* = 2.8 Hz), 88.8 (d, *J* = 186.7 Hz), 62.0, 14.0;

¹⁹F NMR (CDCl₃, 377 MHz) δ –181.9 (d, *J* = 47.6 Hz);

HRMS (EI): calcd for C₁₀H₁₀FIO₂ [M]⁺: 307.9710. Found 307.9710.



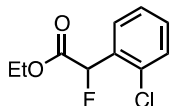
Product 2.37 Prepared according to Procedure A from the corresponding arylboroxine (173 mg, 0.42 mmol, 2.5 equiv. Ar–B) and fluoro malonic half ester (75 mg, 0.50 mmol, 1.0 equiv.), 48 h. Isolated in 69% yield after purification by column chromatography (20:1 Hex/EtOAc) as a light yellow oil.

¹H NMR (CDCl₃, 700 MHz) δ 7.42 – 7.38 (m, 4H), 5.73 (d, *J* = 47.6 Hz, 1H), 4.29 – 4.19 (m, 2H), 1.25 (t, *J* = 7.15 Hz, 3H);

¹³C NMR (CDCl₃, 176 MHz) δ 168.1 (d, *J* = 27.5 Hz), 135.6 (d, *J* = 2.4 Hz), 132.8 (d, *J* = 21.1 Hz), 129.1, 127.9 (d, *J* = 6.3 Hz), 88.6 (d, *J* = 186.6 Hz), 62.0, 14.0;

^{19}F NMR (CDCl_3 , 377 MHz) δ -181.0 (d, J = 47.5 Hz);

HRMS (EI): calcd for $\text{C}_{10}\text{H}_{10}\text{ClFO}_2$ $[\text{M}]^+$: 216.0353. Found 216.0356.



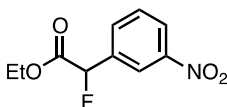
Product 2.39 Prepared according to Procedure A from the corresponding arylboroxine (173 mg, 0.42 mmol, 2.5 equiv. Ar-B) and fluoro malonic half ester (75 mg, 0.50 mmol, 1.0 equiv.), 43 h. Isolated in 58% yield after purification by column chromatography (20:1 Hex:EtOAc) as a light yellow oil.

^1H NMR (CDCl_3 , 700 MHz) δ 7.51 – 7.48 (m, 1H), 7.43 – 7.41 (m, 1H), 7.39 – 7.30 (m, 2H), 6.19 (d, J = 46.5 Hz, 1H), 4.31 – 4.22 (m, 2H), 1.26 (t, J = 7.2 Hz, 3H);

^{13}C NMR (CDCl_3 , 176 MHz) δ 168.0 (d, J = 27.5 Hz), 133.6 (d, J = 4.4 Hz), 132.4 (d, J = 20.8 Hz), 130.9 (d, J = 2.4 Hz), 129.9, 128.6 (d, J = 6.3 Hz), 127.3, 86.2 (d, J = 184.6 Hz), 62.0, 14.0;

^{19}F NMR (CDCl_3 , 377 MHz) δ -180.9 (d, J = 46.7 Hz);

HRMS (EI): calcd for $\text{C}_{10}\text{H}_{10}\text{ClFO}_2$ $[\text{M}]^+$: 216.0353. Found 216.0355.



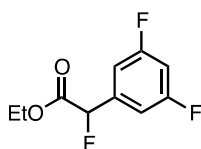
Product 2.41 Prepared according to Procedure A from the corresponding arylboroxine (186 mg, 0.42 mmol, 2.5 equiv. Ar-B) and fluoro malonic half ester (75 mg, 0.50 mmol, 1.0 equiv.), 47 h. 66% yield based on calibrated ^1H NMR, isolated in 56% yield (17:1 product:diarylation at the α position) yield after purification by column chromatography (2:1 Tol/Hex to 100% Tol) as a light yellow oil.

¹H NMR (CDCl₃, 700 MHz) δ 8.36 – 8.35 (m, 1H), 8.27 – 8.25 (m, 1H), 7.83 – 7.81 (m, 1H), 7.63 – 7.60 (m, 1H), 5.88 (d, *J* = 47.2 Hz, 1H), 4.32 – 4.22 (m, 2H), 1.28 (t, *J* = 7.2 Hz, 3H);

¹³C NMR (CDCl₃, 176 MHz) δ 167.3 (d, *J* = 26.6 Hz), 148.4, 136.4 (d, *J* = 21.6), 132.0 (d, *J* = 6.5 Hz), 129.9, 124.3 (d, *J* = 1.1 Hz), 121.5 (d, *J* = 7.5 Hz), 88.0 (d, *J* = 189.0 Hz), 62.4, 14.0;

¹⁹F NMR (CDCl₃, 377 MHz) δ -184.4 (d, *J* = 47.1 Hz);

HRMS (ESI): calcd for C₁₀H₁₀FNO₄ [M+Na]⁺: 250.0486. Found 250.0483.



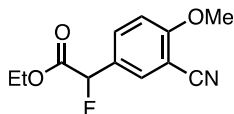
Product 2.47 Prepared according to Procedure A from the corresponding aryl neopentyl boronic ester (283 mg, 1.25 mmol, 2.5 equiv. Ar–B) and fluoro malonic half ester (75 mg, 0.5 mmol, 1.0 equiv.), 48 h. Isolated in 59% yield after purification by column chromatography (20:1 Hex/EtOAc) as a light yellow oil.

¹H NMR (CDCl₃, 700 MHz) δ 7.06 – 7.02 (m, 2H), 6.89 – 6.83 (m, 1H), 5.76 (d, *J* = 47.5 Hz, 1H), 4.35 – 4.24 (m, 2H), 1.31 (t, *J* = 7.14 Hz, 3H);

¹³C NMR (CDCl₃, 176 MHz) δ 167.4 (d, *J* = 26.6 Hz), 163.0 (dd, *J* = 250.1, 12.6 Hz), 137.7 (d, *J* = 21.8 Hz), 109.4 (ddd, *J* = 21.8, 7.5, 7.3 Hz), 104.9 (td, *J* = 25.2, 1.0 Hz), 88.0 (dt, *J* = 188.8, 2.2), 62.3, 14.0;

¹⁹F NMR (CDCl₃, 377 MHz) δ -108.2 (m, 2F), -184.4 (d, *J* = 47.5 Hz, 1F);

HRMS (EI): calcd for C₁₀H₉F₃O₂ [M]⁺: 218.0555. Found 218.0558.



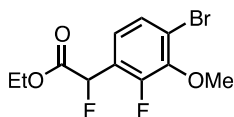
Product 2.49 Prepared according to Procedure B from the corresponding aryl neopentyl boronic ester (123 mg, 0.50 mmol, 2.5 equiv. Ar-B) and fluoro malonic half ester (30 mg, 0.20 mmol, 1.0 equiv.), 48 h. Isolated in 49% yield after purification by column chromatography (Hex/EtOAc gradient, 90:10 to 50:50) as a yellow oil.

$^1\text{H NMR}$ (CDCl_3 , 700 MHz) δ 7.66 – 7.63 (m, 2H), 7.01 – 7.00 (m, 1H), 5.70 (d, $J = 47.2$ Hz, 1H), 4.30 – 4.19 (m, 2H), 3.95 (s, 3H), 1.26 (t, $J = 7.1$ Hz, 3H);

$^{13}\text{C NMR}$ (CDCl_3 , 126 MHz) δ 167.8 (d, $J = 27.7$ Hz), 162.0 (d, $J = 1.5$ Hz), 132.7 (d, $J = 5.8$ Hz), 132.2 (d, $J = 6.3$ Hz), 127.1 (d, $J = 22.0$ Hz), 115.6, 111.7, 102.4, 87.9 (d, $J = 187.3$ Hz), 62.2, 56.3, 14.1;

$^{19}\text{F NMR}$ (CDCl_3 , 377 MHz) δ -179.7 (d, $J = 47.3$ Hz);

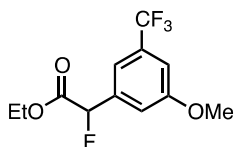
HRMS (EI): calcd for $\text{C}_{12}\text{H}_{12}\text{FNO}_3$ $[\text{M}]^+$: 237.0801. Found 237.0805.



Product 2.51 Prepared according to Procedure A from the corresponding aryl neopentyl boronic ester (396 mg, 1.25 mmol, 2.5 equiv. Ar-B) and fluoro malonic half ester (75 mg, 0.50 mmol, 1.0 equiv.), 49 h. Isolated in 76% yield after purification by column chromatography (Hex/EtOAc gradient, 100:0 to 90:10) as a light yellow oil.

$^1\text{H NMR}$ (CDCl_3 , 700 MHz) δ 7.38 – 7.36 (m, 1H), 7.06 – 7.03 (m, 1H), 5.98 (d, $J = 46.9$ Hz, 1H), 4.32 – 4.22 (m, 2H), 3.97 (d, $J = 1.5$ Hz, 3H), 1.27 (t, $J = 7.1$ Hz, 3H);

^{13}C NMR (CDCl_3 , 126 MHz) δ 167.4 (dd, $J = 27.4$, 1.3 Hz), 153.8 (dd, $J = 255.0$, 4.3 Hz), 145.6 (d, $J = 12.6$ Hz), 128.5 Hz (dd, $J = 4.0$, 0.9 Hz), 123.3 (dd, $J = 5.5$, 3.1 Hz), 123.0 (dd, $J = 21.2$, 12.9 Hz), 119.5 (t, $J = 3.0$ Hz), 83.1 (dd, $J = 186.1$, 4.3 Hz), 62.2, 61.6 (d, $J = 5.0$ Hz), 14.0;
 ^{19}F NMR (CDCl_3 , 377 MHz) δ -131.4 (dp, $J = 6.5$, 1.6 Hz, 1F), -181.5 (d, $J = 47.0$ Hz, 1F);
HRMS (EI): calcd for $\text{C}_{11}\text{H}_{11}\text{BrF}_2\text{O}_3$ $[\text{M}]^+$: 307.9860. Found 307.9861.



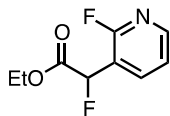
Product 2.53 Prepared according to Procedure B from the corresponding arylboroxine (81 mg, 0.13 mmol, 2.0 equiv. Ar-B) and fluoro malonic half ester (30 mg, 0.20 mmol, 1.0 equiv.), 48 h. Isolated in 67% yield after purification by column chromatography (Hex/EtOAc gradient, 98:2 to 82:18) as a colorless oil.

^1H NMR (CDCl_3 , 700 MHz) δ 7.31 – 7.29 (m, 1H), 7.18 – 7.17 (m, 1H), 7.15 – 7.14 (m, 1H), 5.78 (d, $J = 47.4$ Hz, 1H), 4.25 (m, 2H), 3.85 (s, 3H), 1.26 (t, $J = 7.3$ Hz, 3H);

^{13}C NMR (CDCl_3 , 126 MHz) δ 167.7 (d, $J = 26.9$ Hz), 161.1 Hz, 136.7 (d, $J = 21.2$ Hz), 132.4 (q, $J = 32.9$ Hz), 123.4 (q, $J = 271.9$ Hz), 115.4 – 115.2 (m), 115.1 – 115.0 (m), 112.1 – 112.0 (m), 88.5 (d, $J = 187.7$ Hz), 62.2, 55.7, 14.0;

^{19}F NMR (CDCl_3 , 377 MHz) δ -63.0 (s, 3F), -183.4 (d, $J = 47.7$ Hz, 1F);

HRMS (EI): calcd for $\text{C}_{12}\text{H}_{12}\text{F}_4\text{O}_3$ $[\text{M}]^+$: 280.0723. Found 280.0722.



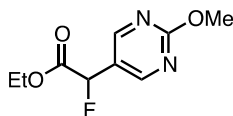
Product 2.55 Prepared according to Procedure A from the corresponding aryl neopentyl boronic ester (261 mg, 1.25 mmol, 2.5 equiv. Ar–B) and fluoro malonic half ester (75 mg, 0.50 mmol, 1.0 equiv.), 50 h. Isolated in 51% yield after purification by column chromatography (Hex/EtOAc gradient, 94:6 to 50:50) as a light yellow oil.

¹H NMR (CDCl₃, 700 MHz) δ 8.29 – 8.26 (m, 1H), 7.93 – 7.89 (m, 1H), 7.28 – 7.26 (m, 1H), 5.99 (d, *J* = 46.7 Hz, 1H), 4.32 – 4.22 (m, 2H), 1.27 (t, *J* = 7.2 Hz, 3H);

¹³C NMR (CDCl₃, 126 MHz) δ 167.1 (d, *J* = 27.5 Hz), 160.6 (dd, *J* = 241.5, 4.6 Hz), 149.1 (dd, *J* = 15.0, 2.4 Hz), 139.4 (dd, *J* = 5.8, 3.8 Hz), 121.8 (d, *J* = 4.5 Hz), 117.2 (dd, *J* = 22.3, 29.4 Hz), 83.3 (dd, *J* = 186.2, 2.4 Hz), 62.4, 14.0;

¹⁹F NMR (CDCl₃, 377 MHz) δ –70.9 (d, *J* = 9.1 Hz, 1F), –184.4 (d, *J* = 46.8 Hz, 1F);

HRMS (EI): calcd for C₉H₉FNO₂ [M]⁺: 201.0601. Found. 201.0596.



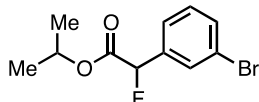
Product 2.57 Prepared according to Procedure B, with the modification of using 1,2-dichloroethane as the solvent, from the corresponding aryl neopentyl boronic ester (95 mg, 0.430 mmol, 2.15 equiv. Ar–B) and fluoro malonic half ester (30 mg, 0.20 mmol, 1.0 equiv.), 48 h. The solvent was removed *in vacuo* and the resulting oil was purified by column chromatography (Hex/EtOAc gradient, 20:80 to 0:100); the product was isolated in 43% yield as a yellow oil.

¹H NMR (CDCl₃, 700 MHz) δ 8.60 – 8.59 (m, 2H), 5.75 (d, *J* = 47.1 Hz, 1H), 4.32 – 4.23 (m, 2H), 4.03 (s, 3H), 1.27 (td, *J* = 7.3, 0.4 Hz, 3H);

^{13}C NMR (CDCl_3 , 126 MHz) δ 167.4 (d, $J = 27.5$ Hz), 166.3 (d, $J = 1.5$ Hz), 158.2 (d, $J = 5.3$ Hz), 121.8 (d, $J = 22.1$ Hz), 85.5 (d, $J = 187.0$ Hz), 62.5, 55.3, 14.0;

^{19}F NMR (CDCl_3 , 377 MHz) δ -181.5 (d, $J = 47.5$ Hz);

HRMS (EI): calcd for $\text{C}_9\text{H}_{11}\text{FN}_2\text{O}_3$ $[\text{M}]^+$: 214.0754. Found 214.0759.



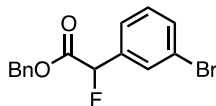
Product 2.61 Prepared according to Procedure B from the corresponding arylboroxine (92 mg, 0.167 mmol, 2.5 equiv. Ar-B) and fluoro malonic half ester (32.8 mg, 0.20 mmol, 1.0 equiv.), 48 h. Isolated in 69% yield after purification by column chromatography (Hex/EtOAc gradient, 99:1 to 88:12) as a pale yellow oil.

^1H NMR (CDCl_3 , 400 MHz) δ 7.65 – 7.64 (m, 1H), 7.56 – 7.52 (m, 1H), 7.43 – 7.40 (m, 1H), 7.32 – 7.27 (m, 1H), 5.71 (d, $J = 47.8$ Hz, 1H), 5.13 (hept, $J = 6.3$ Hz, 1H), 1.30 (d, $J = 6.3$ Hz, 3H), 1.22 (d, $J = 6.3$ Hz, 3H);

^{13}C NMR (CDCl_3 , 126 MHz) δ 167.4 (d, $J = 27.0$ Hz), 136.5 (d, $J = 20.5$ Hz), 132.5 (d, $J = 1.9$ Hz), 130.3, 129.5 (d, $J = 6.9$ Hz), 125.0 (d, $J = 6.4$ Hz), 122.7, 88.5 (d, $J = 187.8$ Hz), 70.1, 21.7, 21.5;

^{19}F NMR (CDCl_3 , 377 MHz) δ -182.2 (d, $J = 47.7$ Hz);

HRMS (EI): calcd for $\text{C}_{11}\text{H}_{12}\text{BrFO}_2$ $[\text{M}]^+$: 274.0005. Found 274.0001.



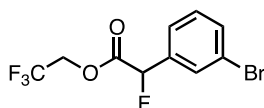
Product 2.63 Prepared according to Procedure A from the corresponding arylboroxine (229 mg, 0.417 mmol, 2.5 equiv. Ar–B) and fluoro malonic half ester (106 mg, 0.50 mmol, 1.0 equiv.), 44 h. Isolated in 59% yield after purification by column chromatography (Hex/EtOAc gradient, 98:2 to 82:18) as a yellow oil.

¹H NMR (CDCl₃, 700 MHz) δ 7.61 – 7.60 (m, 1H), 7.53 – 7.51 (m, 1H), 7.38 – 7.36 (m, 1H), 7.36 – 7.31 (m, 3H), 7.28 – 7.24 (m, 3H), 5.77 (d, *J* = 47.4 Hz, 1H), 5.21 (dd, *J* = 39.7, 12.3 Hz, 2H);

¹³C NMR (CDCl₃, 126 MHz) δ 167.6 (d, *J* = 27.5 Hz), 136.1 (d, *J* = 20.7 Hz), 134.7, 132.7 (d, *J* = 1.8 Hz), 130.3, 129.6 (d, *J* = 6.9 Hz), 128.7, 128.7, 128.3, 125.1 (d, *J* = 6.3 Hz), 122.8, 88.4 (d, *J* = 188.3 Hz), 67.6;

¹⁹F NMR (CDCl₃, 377 MHz) δ –182.1 (d, *J* = 47.8 Hz);

HRMS (EI): calcd for C₁₅H₁₂BrFO₂ [M]⁺: 322.0005. Found 322.0005.



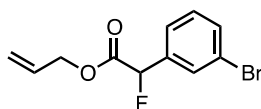
Product 2.65 Prepared according to Procedure B from the corresponding arylboroxine (92 mg, 0.167 mmol, 2.5 equiv. Ar–B) and fluoro malonic half ester (41 mg, 0.20 mmol, 1.0 equiv.), 20 h. Isolated in 56% yield after purification by column chromatography (Hex/EtOAc gradient, 98:2 to 80:20) as a yellow oil.

¹H NMR (CDCl₃, 500 MHz) δ 7.66 – 7.64 (m, 1H), 7.59 – 7.54 (m, 1H), 7.43 – 7.40 (m, 1H), 7.34 – 7.30 (m, 1H), 5.87 (d, *J* = 49.6 Hz, 1H), 4.65 – 4.50 (m, 2H);

^{13}C NMR (CDCl_3 , 126 MHz) δ 166.5 (d, $J = 28.7$ Hz), 135.1 (d, $J = 21.4$ Hz), 133.2 (d, $J = 2.0$ Hz), 130.5, 129.5 (d, $J = 5.9$ Hz), 125.0 (d, $J = 6.0$ Hz), 123.0, 122.4 (q, $J = 278.8$ Hz), 88.0 (d, $J = 188.7$ Hz), 61.1 (d, $J = 36.8$ Hz);

^{19}F NMR (CDCl_3 , 498 MHz) δ -73.7 (t, $J = 8.2$ Hz, 3F), -182.7 (d, $J = 47.1$ Hz, 1F);

HRMS (EI): calcd for $\text{C}_{10}\text{H}_7\text{BrF}_4\text{O}_2$ $[\text{M}]^+$: 313.9566. Found 313.9568.



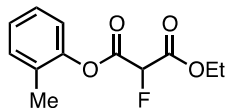
Product 2.67 Prepared according to Procedure A from the corresponding arylboroxine (147.4 mg, 0.417 mmol, 2.5 equiv. Ar-B) and fluoro malonic half ester (75.1 mg, 0.50 mmol, 1.0 equiv.), 49 h. Isolated in 74% yield after purification by column chromatography (Hex/EtOAc, 99:1 to 90:10) as a yellow oil.

^1H NMR (CDCl_3 , 700 MHz) δ 7.64 – 7.62 (m, 1H), 7.54 – 7.51 (m, 1H), 7.41 – 7.38 (m, 1H), 7.29 – 7.26 (m, 1H), 5.89 – 5.83 (m, 1H), 5.76 (d, $J = 47.1$ Hz, 1H), 5.28 – 5.23 (m, 2H), 4.71 – 4.64 (m, 2H);

^{13}C NMR (CDCl_3 , 126 MHz) δ 167.7 (d, $J = 27.7$ Hz), 136.2 (d, $J = 21.2$ Hz), 132.7 (d, $J = 1.7$ Hz), 130.9, 130.3, 129.6 (d, $J = 6.8$ Hz), 125.1 (d, $J = 6.3$ Hz), 122.8, 119.4, 88.4 (d, $J = 188.2$ Hz), 66.4;

^{19}F NMR (CDCl_3 , 498 MHz) δ -182.2 (d, $J = 48.6$ Hz)

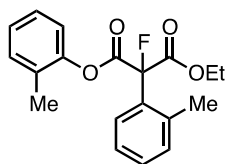
HRMS (EI): calcd for $\text{C}_{11}\text{H}_{10}\text{BrFO}_2$ $[\text{M}]^+$: 271.9848. Found 271.9848.



Product 2.84 Prepared according to Procedure B from the corresponding arylboroxine (92 mg, 0.167 mmol, 2.5 equiv. Ar-B) and fluoro malonic half ester (32 mg, 0.20 mmol, 1.0 equiv.), 45 h. Isolated in 31% yield after purification by column chromatography (10:1 Hex/EtOAc).

$^1\text{H NMR}$ (CDCl_3 , 700 MHz) δ 7.26 – 7.24 (m, 1H); 7.24 – 7.21 (m, 1H); 7.20 – 7.17 (m, 1H); 7.06 – 7.05 (m, 1H); 5.53 (d, $J = 48.1$ Hz, 1H); 4.39 (q, $J = 7.3$ Hz, 2H); 2.19 (s, 3H); 1.37 (t, $J = 7.2$ Hz, 3H);

HRMS (EI): calcd for $\text{C}_{12}\text{H}_{13}\text{FO}_4$ $[\text{M}]^+$: 240.0798. Found 140.0798.



Product 2.85 Isolated from the same reaction mixture as **2.84**. Isolated in 9% yield after purification by column chromatography (10:1 Hex/EtOAc).

$^1\text{H NMR}$ (CDCl_3 , 700 MHz) δ 7.36 – 7.33 (m, 1H), 7.30 – 7.20 (m, 5H), 7.17 – 7.14 (m, 1H), 7.11 – 7.09 (m, 1H), 4.49 – 4.12 (m, 2H), 2.45 (d, $J = 3.34$ Hz, 3H), 2.13 (s, 3H), 1.38 (t, $J = 7.1$ Hz, 3H);

HRMS (EI): calcd for $\text{C}_{19}\text{H}_{19}\text{FO}_4$ $[\text{M}]^+$: 330.1267. Found 330.1265.

CHAPTER 3 – Synthesis of Diarylmethanes *via* Decarboxylative Benzylation of sp^2 -Organoboron Reagents: Scope and Functionalization

3.1 Introduction

3.1.1 The Diarylmethane Unit

The diarylmethane unit is found in many pharmacologically relevant compounds. A number of diarylmethane-containing molecules that have potential uses in the treatment of HIV,¹⁰⁴ opportunistic infections,¹⁰⁵ Cushing's syndrome,¹⁰⁶ insomnia,¹⁰⁷ and hypertension¹⁰⁸ are presented below (Figure 3-1). As their utility has been increasingly explored, so too have the synthetic methodologies related to their production. Four general categories will be discussed, these being Friedel-Crafts alkylations, nucleophile-electrophile cross-coupling reactions, radical benzylation reactions, and palladium-catalyzed decarboxylative coupling of sp^2 -electrophiles and nitroaryl acetates (Figure 3-2).

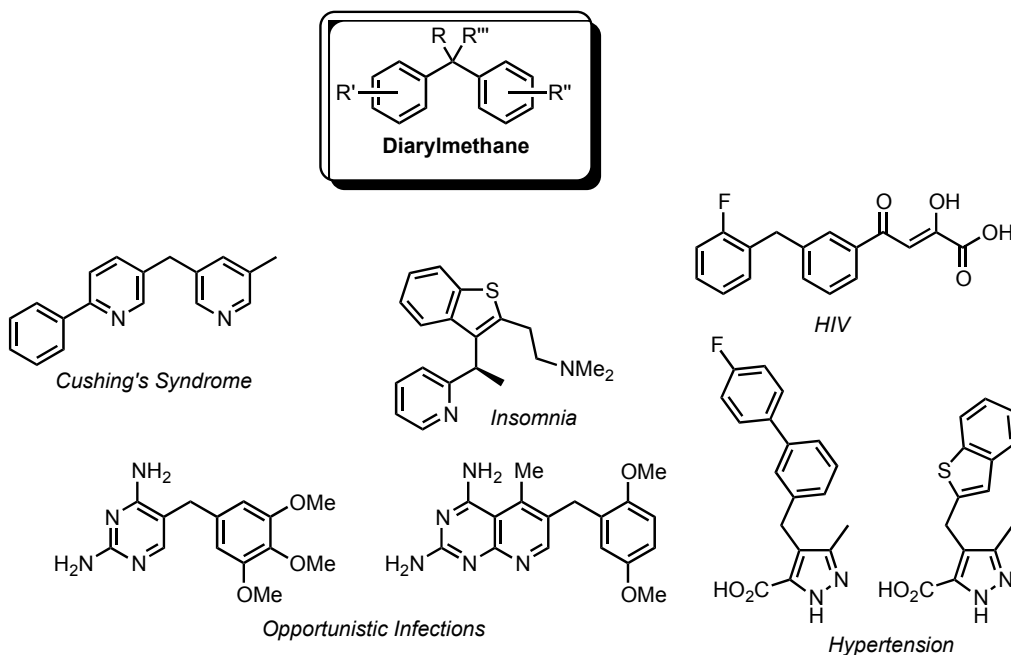


Figure 3-1 Diarylmethane containing molecule with potential uses in treating various conditions

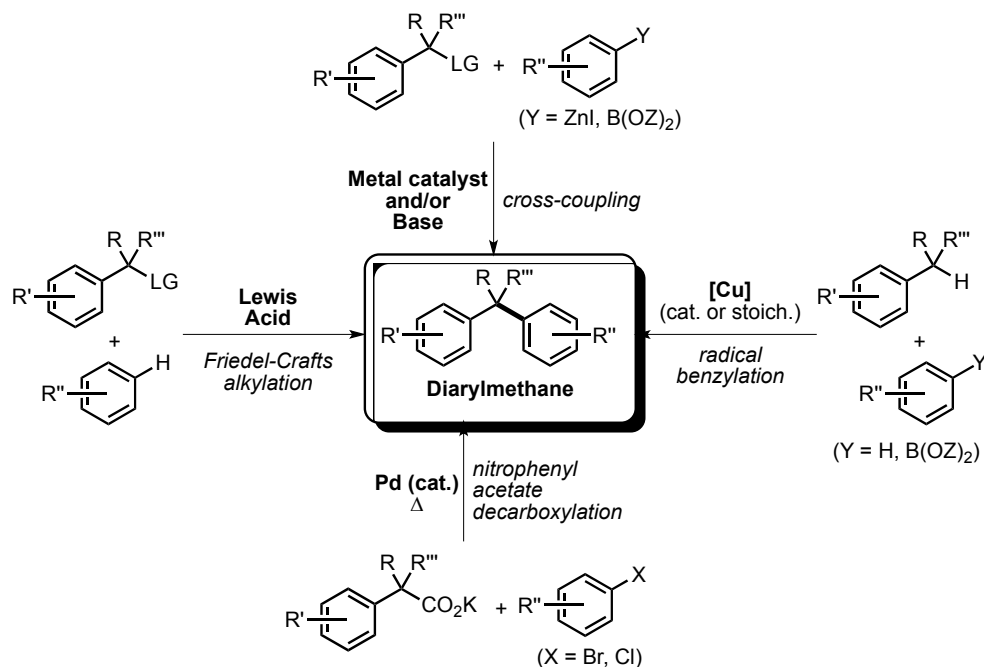


Figure 3-2: Methodologies for the synthesis of diarylalkanes

3.1.2 Diarylmethane Synthesis by Friedel-Crafts Alkylation

The Friedel-Crafts (FC) alkylation reaction utilizes an electrophilic aromatic substitution of an aromatic ring with an alkyl halide by use of a strong Lewis acid (such as AlCl_3) as an activator (Figure 3-3). For the presented example, the reaction begins with a chloride abstraction from benzyl chloride (**3.1**) to generate a benzylic carbocation (**3.2**), which can undergo electrophilic aromatic substitution with another aryl ring (**3.3**) to generate an arylated cationic intermediate (**3.4**). Neutralization by proton abstraction enables the reestablishment of aromaticity, generating the product (**3.5**).

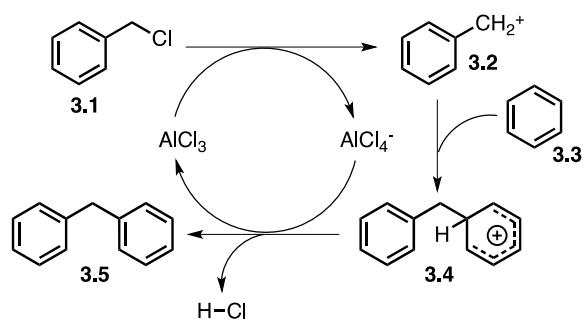


Figure 3-3 Schematic Friedel-Crafts alkylation

The Friedel-Crafts reaction was established almost a century and a half ago, and has undergone many innovations since its inception.¹⁰⁹⁻¹¹⁰ Modern investigations have aimed to increase the substrate scope afforded in FC alkylations. For example, the Hall group recently demonstrated the use of a unique ferroceniumboronic acid hexafluoroantimonate salt (**3.6**) as the catalyst in the FC reaction of deactivated benzyl alcohols and substituted arenes (Figure 3-4 A)¹¹¹ Their conditions were demonstrated to be tolerable to aryl chloride and aryl bromide functionalities (**3.7**), which may be problematic under palladium-catalyzed conditions. The use

of electron-deficient benzyl partners (**3.8**) were also demonstrated, as well as the synthesis of a pharmaceutical compound (**3.9**). The boronic acid catalyst was purported to provide a stabilizing factor to the generated carbocationic species via zwitterion formation (**3.10**) coupled with solvation of the charged carbocation by the solvent (Figure 3-4 B). These mechanistic attributes (zwitterion formation and carbocation solvation) are implicated towards their mild reaction conditions and expanded substrate scope when compared to other FC alkylation reactions.

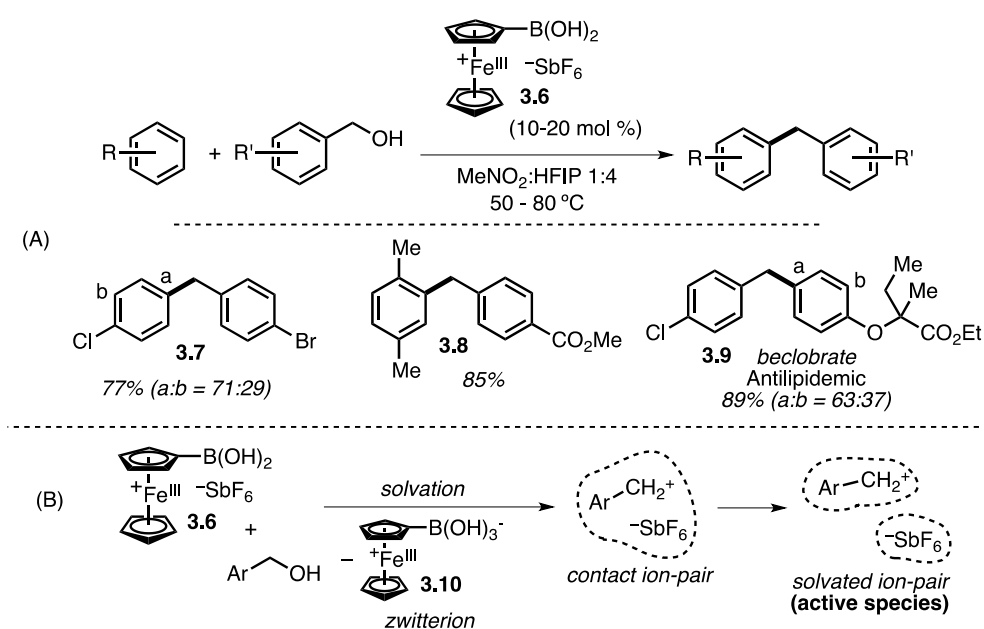


Figure 3-4 (A) Ferrocenium boronic acid catalyzed FC reaction; (B) proposed formation of carbocation stabilized by solvation interactions and zwitterion formation

A related study by Moran and coworkers utilizing catalytic Brønsted acids in HFIP was able to further expand the scope of FC benzylations to include other deactivated benzyl alcohols. The inclusion of deactivating *para*-nitro (**3.11**), *para*-cyano, and (**3.12**), 3,5-di(trifluoromethyl)-benzyl groups (**3.13**), not compatible under the boronic-acid catalyzed chemistry, where

benzylated in good yield (Figure 3-5).¹¹² Potential issues with FC alkylations include potential problems with regioselectivity with substituted aryl groups, decreased yields with electron-deficient benzyl substrates, and undesired reactivity by nucleophilic functionalities interacting with the intermediate benzyl-cation.

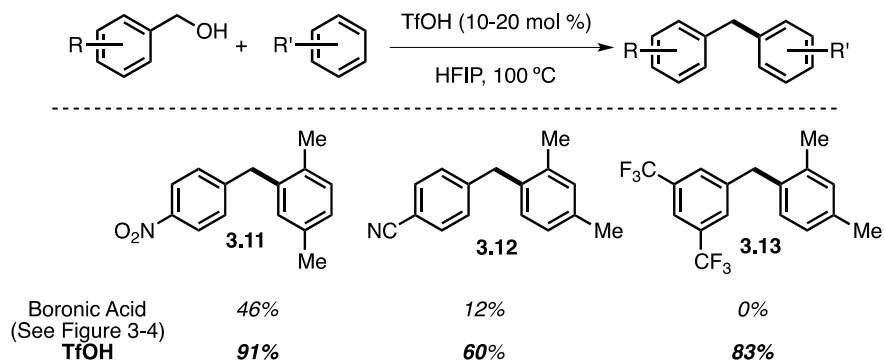


Figure 3-5 Triflic acid catalyzed FC reaction

3.1.3 Nucleophile-Electrophile Cross-Coupling to Synthesize Diarylmethanes

Nucleophile-electrophile coupling, both with and without the aid of metal-catalysts, has also been utilized in the synthesis of diarylmethanes. In the realm of metal-free reactions, base-mediated couplings of aryl-boronic acids and benzyl halides has been reported (Figure 3-6 A).¹¹³⁻¹¹⁴ Additionally, benzyl mesylates have been used in place of the benzyl halides, with this allowing the use of potassium fluoride as the activating reagent (Figure 3-6 B).¹¹⁴ The mechanism of this reaction (Figure 3-7) was proposed to consist of a base-mediated formation of a negatively-charged aryl-borate complex (**7-I** and **7-II**), which enables a nucleophilic displacement of the benzyl leaving group by the aryl (**7-III** and **7-IV**) to generate a new carbon-carbon bond. Aryl halides (including aryl iodides) are typically tolerated under these conditions.

For satisfactory yields, electron-rich boronic acids are required, as they destabilize the borate and make the substitution more favourable. The use of stoichiometric strong base (such as lithium *tert*-butoxide) limits this reactions chemoselectivity towards base sensitive functionalities. Issues may also arise with other nucleophilic functionalities interacting with the benzyl substrate due to the inclusion of a leaving group in the benzylic position.

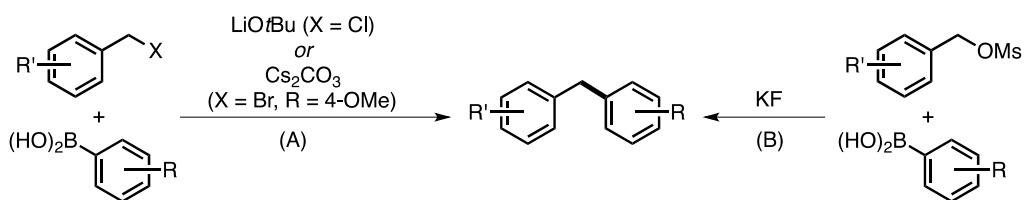


Figure 3-6 (A) Base-mediated coupling of arylboronic acids and benzyl halides; (B) fluoride-mediated coupling of arylboronic acids and benzyl mesylates

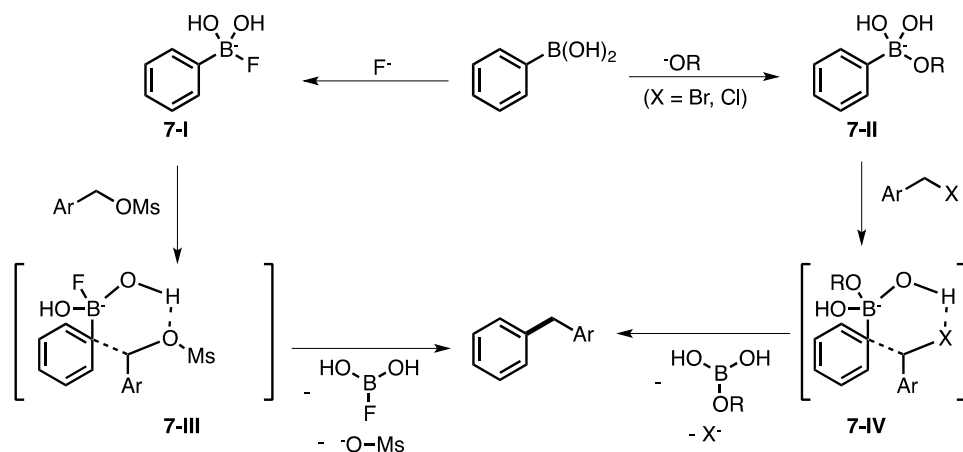


Figure 3-7 Mechanistic steps of arylboronic acid coupling to benzyl halides/mesylates under metal-free conditions

The use of metal catalysts in the synthesis of diarylmethanes enables the generation of substitute diarylalkanes by way of substituted benzyl starting materials (Figure 3-8). The Fu group has reported a Negishi arylation reaction between benzyl mesylates (the mesylate is generated *in situ* from the corresponding benzyl alcohol) and aryl zinc reagents to generate enantioenriched diarylalkanes (Figure 3-9).¹¹⁵ A wide substrate scope is demonstrated, ranging from electron-rich to electron-poor aryl substituents, as well as aryl-iodides, all of which give good yields and good enantiometric excesses. Issues with this methodology could stem from the necessity for -45 °C temperatures (with this being an issue for larger scale reactions), and well as the potential reactivity of the aryl-zinc reagent with electrophilic functionalities such as alkyl-halides or protic heteroatoms.

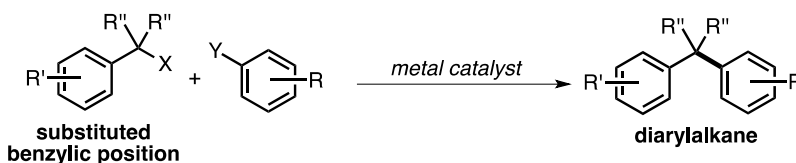


Figure 3-8 Schematic synthesis of diarylalkanes (benzylic-substituted diarymethanes)

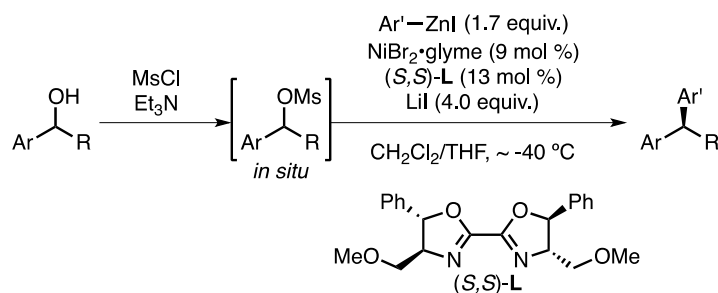


Figure 3-9 Nickel-catalyzed Negishi-arylation to generate diarylalkanes

The Watson group devised a nickel-catalyzed stereospecific reaction to generate quaternary carbon-centers (**3.16**) based around the diarylmethane scaffold (Figure 3-10), utilizing chiral tertiary acetate building blocks (**3.14**) and arylboronic esters (**3.15**).¹¹⁶ A catalytic cycle for this reaction was proposed (Figure 3-11). A bridged nickel-acetate transition state (**11-II**) is implicated in the oxidative addition step, generating an η^3 -nickel intermediate (**11-III**). This can undergo transmetalation with the arylboronic ester to generate an arylated nickel intermediate (**11-IV**), which enables a reductive elimination to generate the product and close the catalytic cycle. Limitations include the use of a methoxide base (as this may scramble with esters and other functionalities that are prone to hydrolysis), as well as the incompatibility of aryl bromides and aryl iodides. Additionally, the naphthyl substituent (**3.14**), or other aryl-groups with extended conjugation, appears necessary for above satisfactory yields under their reaction conditions.

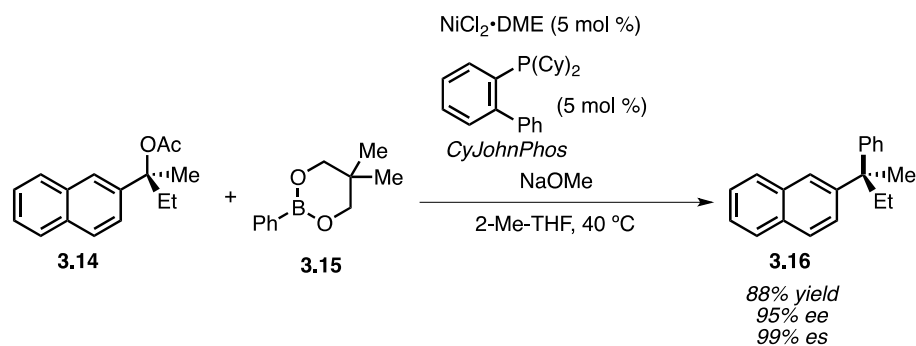


Figure 3-10 Quaternary stereocenters synthesis by nickel-catalyzed cross-coupling

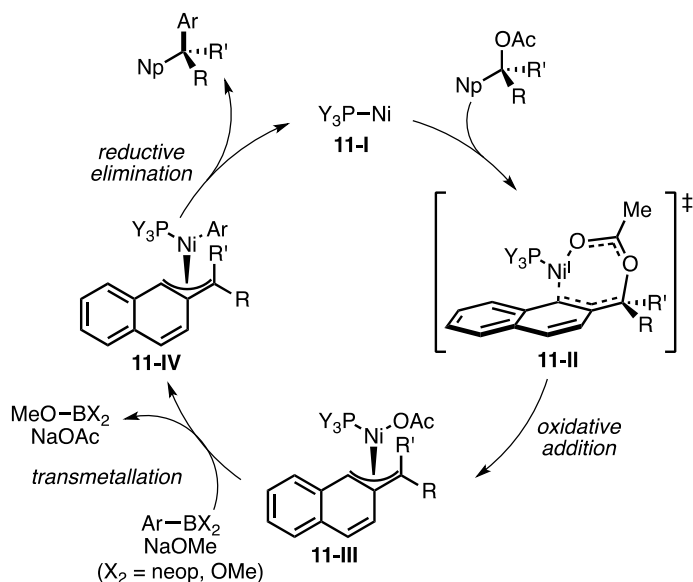


Figure 3-11 Catalytic cycle for nickel-catalyzed quaternary-center synthesis ($PY_3 = CyJohnPhos$)

3.1.4 Diarylmethane Synthesis via Radical Chemistry

Radical chemistry, both metal-mediated and metal-catalyzed, has also been utilized in synthesizing diarylmethanes. A cross-dehydrogenative-coupling reaction of electron-rich arenes (**3.17**) and toluenes (**3.18**) mediated by copper has been reported (Figure 3-12), with an additional dehydrobromination in the product (**3.19**). This methodology is plagued by low yields and the need for a vast excess of the toluene reagent (25 equivalents).¹¹⁷ Copper-catalyzed diarylmethane syntheses involving radicals have also been reported. A representative pair of examples are the Stahl and Liu systems that were recently disclosed in back-to-back publications (Figure 3-13).¹¹⁸⁻¹¹⁹ Both of these reactions are oxidative in nature, as they utilize nucleophilic arylboron reagents in the functionalization of C–H bonds. Both systems also utilize a Cu(I) based catalyst. Yields in these reactions appear moderate to good, with both systems exhibiting

satisfactory yields when using aryl-bromides. The Stahl system also showed additional tolerance towards aryl iodides.

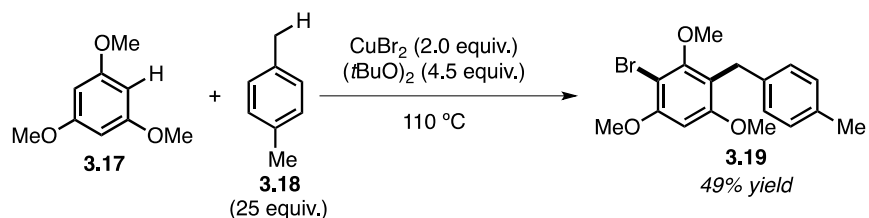


Figure 3-12 Copper-mediate cross-dehydrogenative-coupling of electron-rich arenes with toluenes

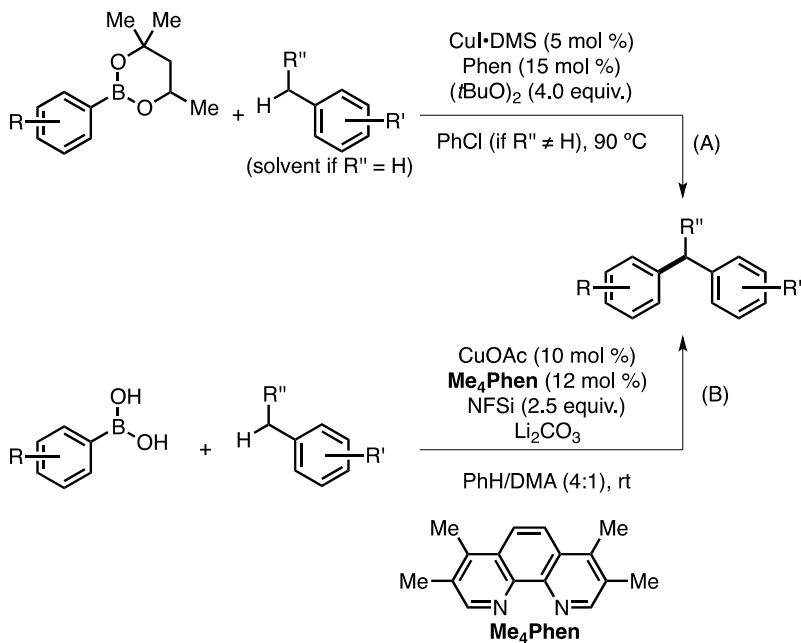


Figure 3-13 Stahl (A) and Liu (B) systems for copper-catalyzed radical synthesis of diarylalkanes

Both reactions follow a similar mechanistic pathway (Figure 3-14), in that an initiator (either di-*tert*-butyl peroxide or N-fluorobenzenesulfonimide) performs a single electron oxidation to generate a Cu(II) centre (**14-II**) and a radical. This radical can perform a hydrogen atom abstraction at the benzyl position, generating a benzylic radical that can trap the copper centre to generate a Cu(III)-benzyl (**14-III**). Subsequent transmetalation to generate a Cu(III)-aryl (**14-IV**) and reductive elimination yields the desired diarylalkane product and closes the catalytic cycle. For the Stahl system, limitations stem from the need of an excess of the benzyl partner (10 equivalent or as the solvent). The Liu system is more forgiving, with equal stoichiometry for both reaction partners as well as having the reactions conducted at room temperature; however, issues with this system may manifest in a lack of regioselectivity if multiple benzylic positions are present, and at least one example was reported to undergo diarylation (**3.23**) (Figure 3-15), indicating potential issues with sterically uncongested benzylic position (**3.20**) when coupled with exceedingly electron-deficient arylboron reagents (**3.21**).

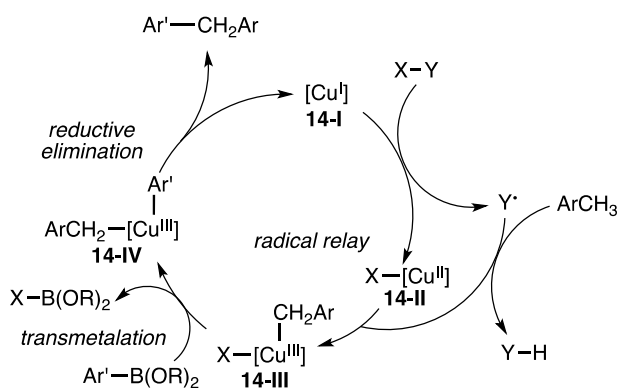


Figure 3-14 Catalytic cycle for copper-catalyzed radical synthesis of diarylalkanes (X, Y = *t*BuO or X = F, Y = N(S(O)₂Ph)₂)

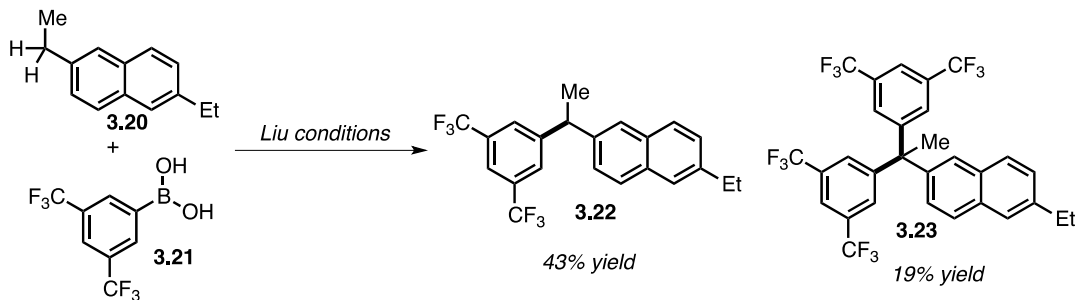


Figure 3-15 Example of diarylation of unhindered benzyl positions with electron-deficient arylboronic acids

3.1.5 Synthesis of Diarylmethanes by Palladium-Catalyzed Decarboxylative Electrophile Trapping of Nitroaryl Acetates

The generation of benzyl anions via decarboxylative chemistry has also been utilized in the synthesis of diarylmethanes, more specifically with the decarboxylation of nitro-substituted aryl acetates (**3.24**) to generate nitro-stabilized carbanions (**3.25**) (Figure 3-16). The anion stabilization afforded by the inclusion of the nitro substituent allows both *ortho* and *para*-substituted nitroarenes to be utilized as reagents in nucleophilic substitution reactions¹²⁰ and to be incorporated into cross-coupling methodologies. Of particular interest are the palladium-catalyzed intermolecular cross-coupling reactions that pair nitrophenyl acetates with either alkenyl triflates¹²¹, or aryl bromides and aryl chlorides¹²² (Figure 3-17).

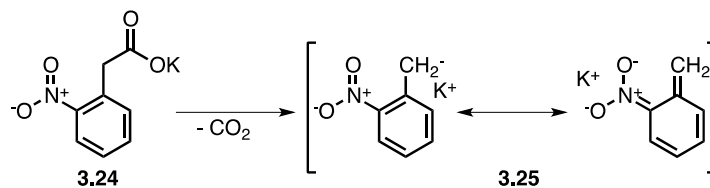


Figure 3-16 Nitroaryl acetate decarboxylation and anion resonance

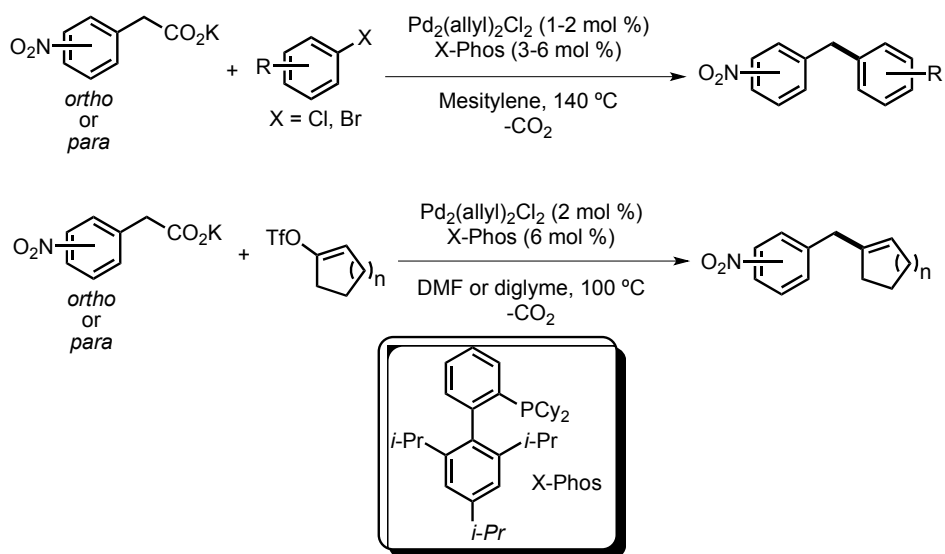


Figure 3-17 Palladium-catalyzed decarboxylative cross-coupling of nitrophenyl acetates with activated electrophiles

The alkenyl triflate scope was limited towards relatively unfunctionalized organic molecules (**3.26** and **3.27**). This was warranted as the authors hoped to utilize this methodology in the synthesis of a specific natural product with a known set of functional group. As such, the demonstration of an expanded functional-group tolerance was not necessary for their purposes. The aryl halide system demonstrated a broader scope, including heterocyclic compounds with good yields, and the synthesis of diarylalkanes by utilizing substituted benzyl carboxylates.

However, the conditions are quite forcing (140 °C), which may prove detrimental towards thermally unstable functionalities; in addition, aryl bromides and aryl iodides, as well as protic heteroatoms and alkyl halides, are not demonstrated in their substrate scope, implying their incompatibility. The authors propose a mechanism (Figure 3-18) where oxidative addition of the alkenyl triflate to generate a palladium-alkenyl (**19-II**) is followed by transmetalation of the carboxylate to generate a carboxylate-bound palladium (**19-III**). Decarboxylation is proposed to occur from this species, generating a palladium-benzyl intermediate (**19-IV**). Reductive elimination from this intermediate generates the desired diarylalkane products, and closes the catalytic cycle.

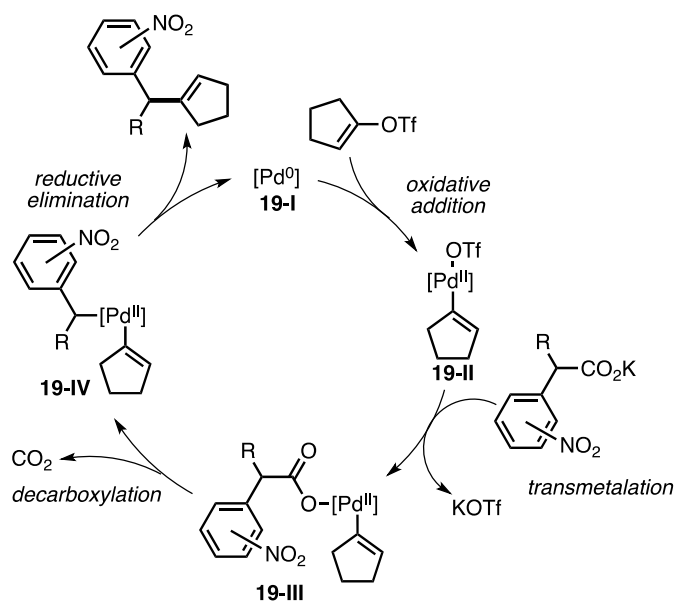


Figure 3-18 Catalytic cycle for palladium-catalyzed decarboxylative cross-coupling of nitrophenyl acetates with alkenyl-triflates

By combining oxidative copper-mediated or catalyzed cross-coupling chemistry^{44, 61, 68} and the decarboxylation of nitroaryl acetates (**3.24**) to generate nucleophilic benzyl species, we envisioned that we could develop a methodology to synthesize diarylmethane product under much milder conditions than afforded by palladium-catalyzed cross-coupling reactions, as well as with an expanded functional group tolerance when compared to other established methods for the synthesis of diarylmethanes. Such a reaction has been developed in our group (Figure 3-19). Patrick Moon was responsible for the optimization of this reaction. My contribution to this work was in exploring the substrate scope of the *ortho*-nitro phenyl acetate and the functionalization of the reaction products. It is this work that will be detailed in the following sections.

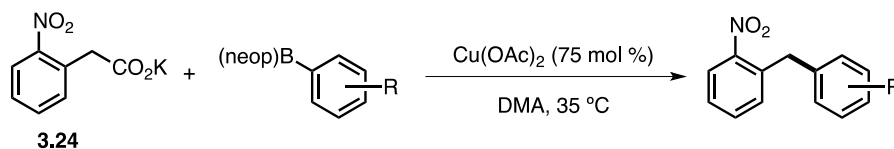


Figure 3-19 Copper-mediated oxidative decarboxylative coupling of arylboronic esters and nitrophenyl acetates

3.2 Reaction Optimization

The conditions for the optimized reaction are presented below (Figure 3-20). The vast majority of the optimization work for this reaction was conducted by P. J. Moon. My contributing work to the optimization consisted of assessing the water and oxygen effects in this chemistry.

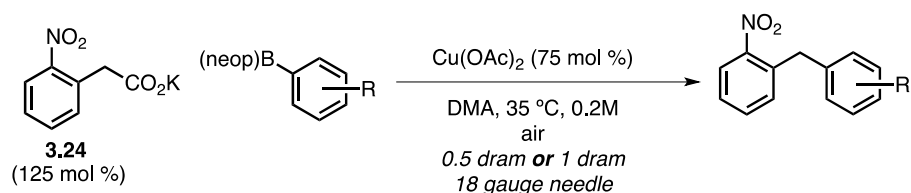


Figure 3-20 Optimized reaction conditions for the oxidative decarboxylative copper-mediated synthesis of diarylmethanes by coupling of arylboronic esters and *ortho*-nitroaryl acetates

Water has a detrimental effect on the selectivity of this reaction (Table 3-1). Potassium carboxylate that was left overnight exposed to atmosphere (entry 1) produced a lower yield of product (**3.26**) and more proto-decarboxylation byproduct (**3.27**) than the dried material (entry 2), demonstrating the detrimental effect of water on this reaction. The control of oxygen diffusion into the reaction, and thus the oxygen content of the headspace above the reaction, is imperative for reaction success (Table 3-2). Optimized conditions utilize an 18 gauge needle (entry 1) to expose the reaction to atmosphere. As the total area of exposure to atmosphere was increased by increasing the number of needles utilized or by using 16 gauge needles (inner diameter is inversely proportional to gauge number), the terminal yield of the reaction drops. This will have ramifications for any attempts at scaling up this reaction, as our current system is

based on empirical needle gauge screening. We currently do not have a quantitative method for assigning optimal atmosphere exposure in relation to reaction volume and surface area.

Table 3-1 Effect of water on the copper-mediated oxidative decarboxylative benzylation of arylboronic esters

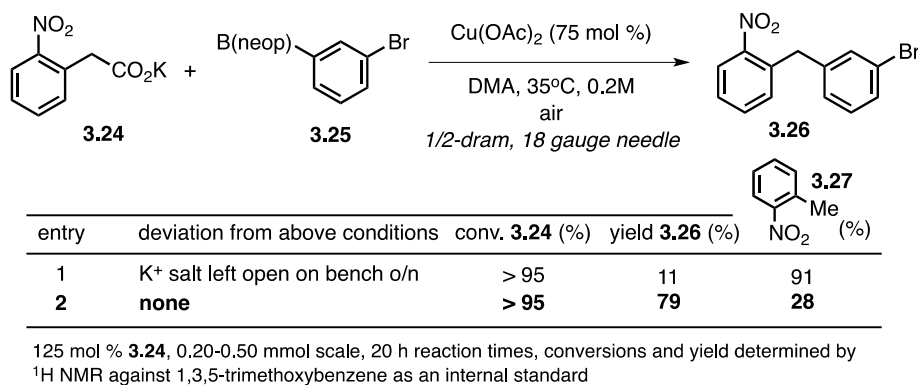
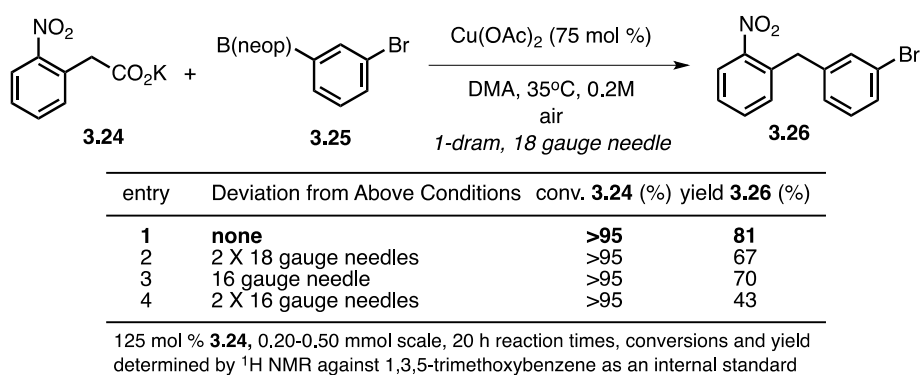


Table 3-2 Effect of modulating the area of atmosphere exposure on the copper-mediated oxidative decarboxylative benzylation of arylboronic esters



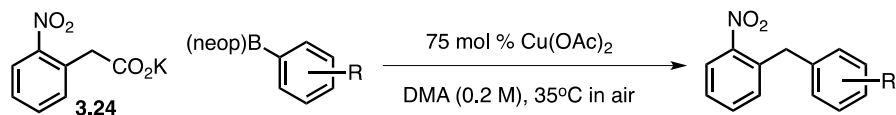
3.3 Reaction Scope

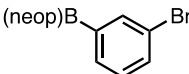
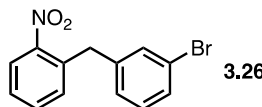
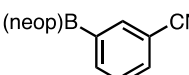
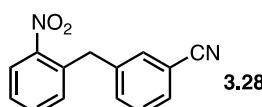
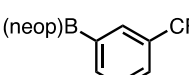
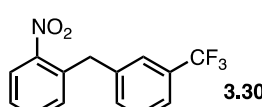
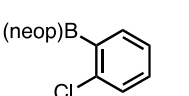
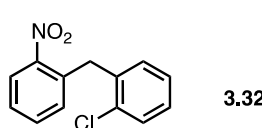
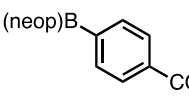
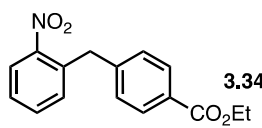
A variety of mono and poly-substituted arylboronic acid neopentyl glycol esters were utilized in the copper-mediated decarboxylative oxidative coupling regime with (except for one example) the potassium salt of *ortho*-nitrophenyl acetic acid. Successful examples, as well a number of less successful ones, will be highlighted in the upcoming sections.

3.3.1 Scope of Mono-Substituted Arylboronic Esters

Table 3-3 and Table 3-4 demonstrate the scope of the reaction in terms of electron-deficient aryl substitutions. Aryl halides, including bromide (**3.25**), chloride (**3.31**), and iodide (**3.35**) were all well tolerated under the optimized conditions. Electrophilic functionalities that could intercept nucleophiles, such as aldehydes (**3.37**) and Michael acceptors (**3.41**), were also well tolerated. Secondary amides (**3.43**) did not appear to have an adverse effect on the chemistry and the cyclopropane ring remained intact, generating a satisfactory yield of this product.

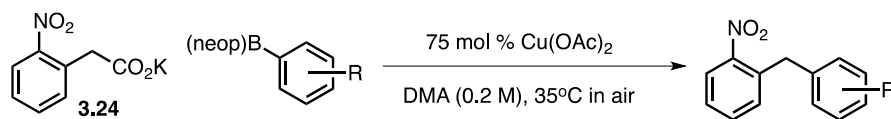
Table 3-3 Copper-mediated oxidative decarboxylative benzylation of mono-substituted arylboronic esters with electron-withdrawing groups, Part 1



Entry	Substrate	Product	Yield (%)
1	 3.25	 3.26	73
2	 3.27	 3.28	66
3	 3.29	 3.30	69
4	 3.31	 3.32	58
5	 3.33	 3.34	63

125 mol % of K-salt. Yields are of isolated material.

Table 3-4 Copper-mediated oxidative decarboxylative benzylation of mono-substituted arylboronic esters with electron-withdrawing groups, Part 2

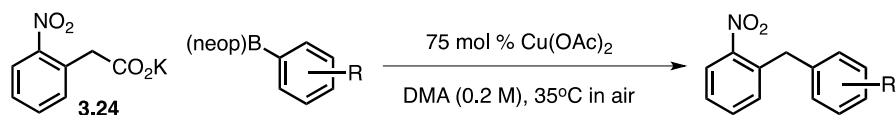


Entry	Substrate	Product	Yield (%)
1	3.35	3.36	55
2	3.37	3.38	52
3	3.39	3.40	50
4	3.41	3.42	61
5	3.43	3.44	52

125 mol % of K-salt. Yields are of isolated material.

A range of electron-donating substituents on the arylboronic ester were also well tolerated (Table 3-5). These included methoxy, (**3.45**, **3.47**), thiomethyl (**3.51**) and trimethylsilyl (**3.53**) substitutions. A sterically hindered *ortho*-tolylboronic ester (**3.55**) was compatible with this chemistry, providing a good yield. Excessively electron-rich substitutions, such as a Boc-protected amine (**3.57**) were not well tolerated.

Table 3-5 Copper-mediated oxidative decarboxylative benzylation of mono-substituted arylboronic esters with electron-donating groups



Entry	Substrate	Product	Yield (%)
1			64
2			71
3			71
4			49
5			62 ^a
6			65 ^a
7			34 ^{a,b}

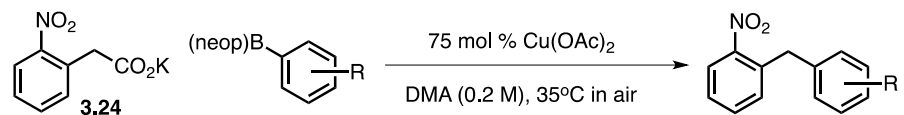
125 mol % of K-salt. Yields are of isolated material. ^aValue determined by calibrated ¹H NMR. ^b110 mol % K-salt.

3.3.2 Scope of Poly-substituted and Complex Arylboronic Esters

Multiple, relatively simple substitutions on a single arylboronic ester unit appeared to be compatible with this chemistry (Table 3-6). These spanned the range from electron-withdrawing

(**3.61**, **3.63**) to electron-donating (**3.65**). We noticed a drop in yield for *ortho*-fluorine substituted phenylboronic esters (**3.67**, **3.69**). Electronically, it is puzzling as to why these substrates appear to be less productive than other phenyl groups with similar electronic environments. We believe this may have to do with the *ortho*-fluorine changing the reactivity of the boron center. A number of more complicated aryl-substituents were also demonstrated to be compatible with this chemistry (Table 3-7). These included another example of a secondary amide (**3.71**), a tertiary amide (**3.73**), and a tertiary sulfonamide (**3.75**). An indomethacin scaffolding (**3.77**) also provided an acceptable yield of the desired product. By using an alternative set of conditions (Figure 3-21) that utilized a copper carboxylate (**3.79**) as the copper source, we also demonstrated the tolerance of this reaction to an unprotected, primary alcohol (**3.80**).

Table 3-6 Copper-mediated oxidative decarboxylative benzylation of poly-substituted arylboronic esters



Entry	Substrate	Product	Yield (%)
1	 3.59	 3.60	72
2	 3.61	 3.62	61
3	 3.63	 3.64	57 ^a
4	 3.65	 3.66	67 ^a
5	 3.67	 3.68	44 ^{a,b}
6	 3.69	 3.70	40 ^a

125 mol % of K-salt. Yields are of isolated material. ^aValue determined by calibrated ¹H NMR. ^bReaction conducted at 40°C.

Table 3-7 Copper-mediated oxidative decarboxylative benzylation of complex arylboronic esters with electron-withdrawing groups

Entry	Substrate	Product	Yield (%)
1	 3.71	 3.72	55
2	 3.73	 3.74	55
3	 3.75	 3.76	66
4	 3.77	 3.78	48

125 mol % of K-salt. Yields are of isolated material.

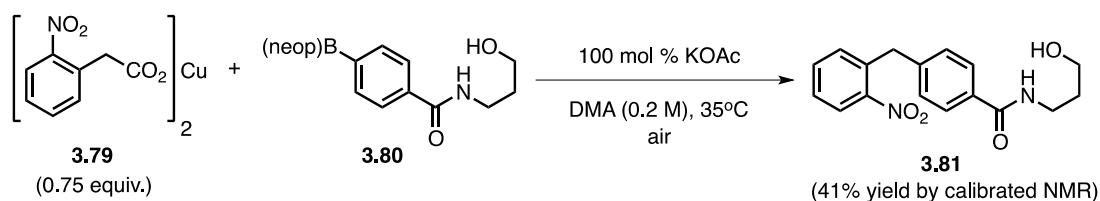


Figure 3-21 Cu-carboxylate synthesis of a diarylmethane containing a terminal alcohol

3.3.3 Scope of Heteroaromatic Arylboronic Esters

A variety of heteroaromatic boronic esters were tested under our oxidative methodology, to varying degrees of success (Table 3-8). A thiophene boronic esters, substituted in the 3-position (**3.82**), provided a satisfactory yield of the desired product (**3.83**). The yields provided by nitrogen-heterocycles were dependent on substitution patterns and electronics. Relatively electron neutral heterocycles, such as a 2-chloropyridyl-5-boronic ester (**3.84**) and a quinoline-boronic ester (**3.86**), were well tolerated and resulted in satisfactory yields. Electron-poor pyrimidines (**3.88**) and pyrazoles (**3.90**) did not appear to fare well, resulting in low product yields. A bromo-fluoro-substituted pyridine (**3.92**) also gave a poor yield of product. We are unsure if this is due to the electron-deficiency of the molecules (as this increases unproductive arylboron consumption), or the effect of the *ortho*-fluorine atom, as previously discussed.

Table 3-8 Copper-mediated oxidative decarboxylative benzylation of heteroaromatic arylboronic esters

Entry	Substrate	Product	Yield (%)
1			56
2			51
3			47
4			35 ^a
5			22 ^a
6			16 ^a

125 mol % of K-salt, Yields are of isolated material. ^aValue determined by calibrated ¹H NMR.

3.4 Functionalization Studies on Benzylated *Ortho*-Nitrobenzenes

Our methodology is limited to the use of electron-deficient aryl acetates. Among a number of tested aryl acetates, *ortho*- and *para*-substituted nitroarenes performed the best.⁹⁸ This is most likely due to the resonance stabilization of the anionic intermediate formed by decarboxylation (Figure 3-22). This resonance stabilization is increased with increasing electron-deficient arenes, thus allowing for milder conditions to be employed for their decarboxylation. A

balance must be struck between stability and reactivity. If the aryl acetate is inadequately electron-deficient, harsher conditions may be required to initiate the decarboxylation. Additionally, since decreased stabilization of the generated anion would lead to a increased reactivity profile, product stability may be compromised. If excessively electron-deficient aryl acetates are used, an insufficiently reactive anion may result, in addition to the potential for further reactivity at the methylene position of the diarylmethane product (due to the increased acidity at this position).

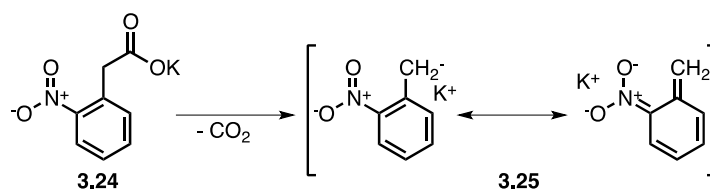


Figure 3-22 Nitroaryl acetate decarboxylation and anion resonance

The presented work focused on the use of *ortho*-nitroaryl acetates. To emphasize the utility of these diarylmethane-containing molecules that our methodology provides (despite the restriction of requiring an electron-deficient aryl acetate), we sought to perform various functionalizations on these molecules to generate a number of potentially useful analogues. The majority of these transformations focused on generating a useful functional handle out of the required nitro substituent.

We first sought to chemoselectively reduce the nitroarene to an aniline (Figure 3-23). For the reduction of the nitroarene (3.94) to generate the aniline (3.95), we utilized a stoichiometric metal reduction using zinc in an acidic methanol solution.¹²³ This compound was then further diversified, as described in the proceeding sections. We originally utilized water, as described in

literature¹²³, as the solvent (Figure 3-23 B). However we saw a significant amount of a hydroxyl-aniline (**3.97**), which we deduced was originating from a S_NAr reaction (**3.96**) prior to reduction.

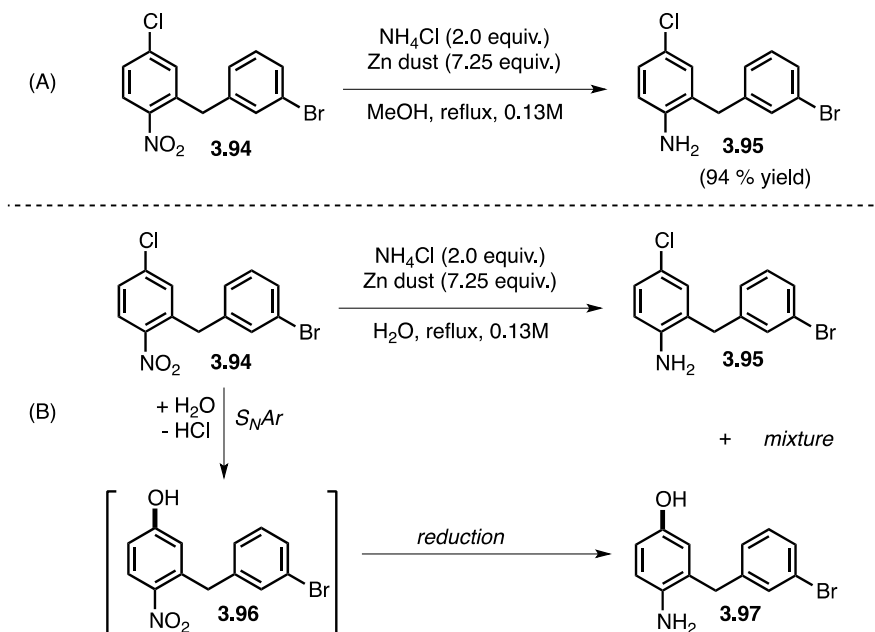


Figure 3-23 (A) Zinc metal mediated reduction of a nitroarene (**3.94**) to an aniline (**3.95**); (B) S_NAr byproduct (**3.97**) generated under aqueous conditions

Iodination of the aniline was conducted under literature conditions, utilizing an aqueous HCl/MeCN solution (Figure 3-24).¹²⁴ This reaction proceeded with *in-situ* generation of the aryl diazonium salt (**3.99**) followed by quenching with iodide to generate the desired aryl iodide (**3.98**). The deamino-borylation reaction (Figure 3-25) also relied on the *in-situ* generation of the same aryl diazonium salt (**3.99**) in an acidic methanol/acetonitrile mixture, which was then reacted with a methanol-activated B₂pin₂ to generate the aryl Bpin product (**3.100**).¹²⁵

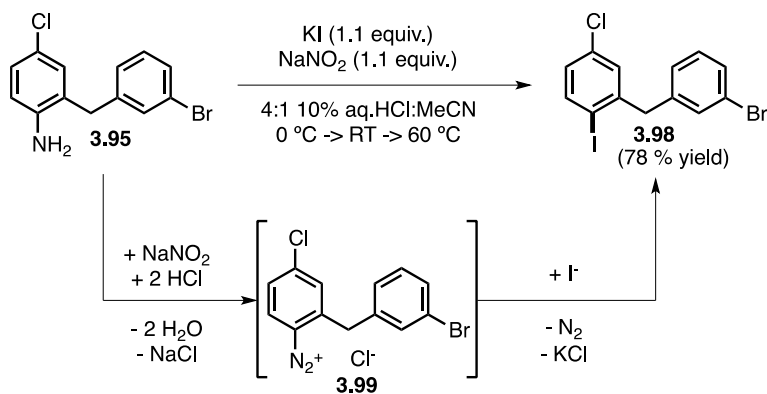


Figure 3-24 Deaminoiodination to generate an aryl iodide (**3.98**) via a diazonium salt intermediate (**3.99**)

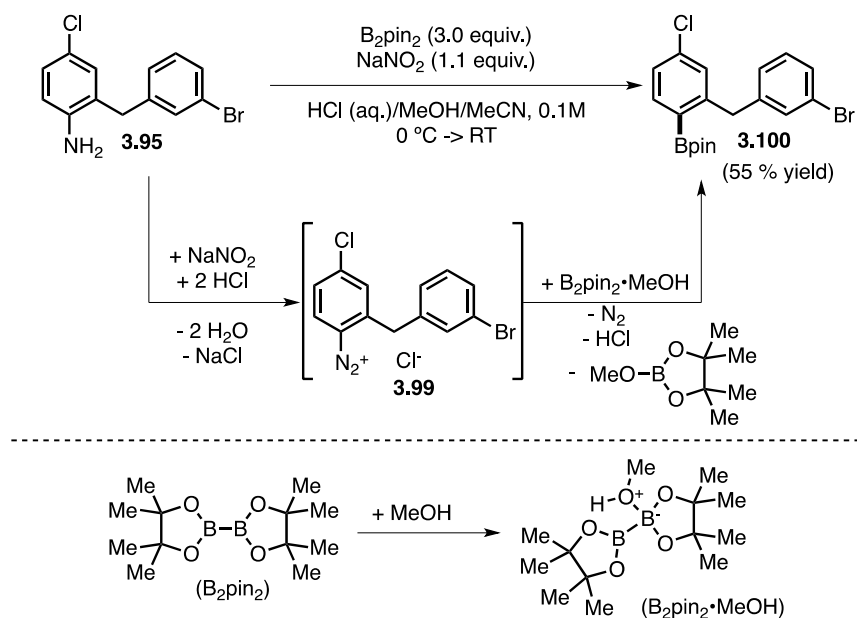


Figure 3-25 Deaminoborylation to generate an aryl-Bpin (**3.100**) via a diazonium salt intermediate

The alkenylation reaction (Figure 3-26 A) relied on the *in-situ* generation of an aryl diazonium salt in acidic media, which then participates as the electrophile in a palladium-

catalyzed Heck-Matsuda reaction to generate the product (**3.101**).¹²⁶ This reaction originally utilized lowered Pd(OAc)₂ loadings (2.2 & 4.4 mol %), which contributed to lowered yield. Increasing the loading to 6 mol % alleviated this issue, generating a good yield of product. This reaction generates the aryl diazonium salt catalytically, meaning that only sub-stoichiometric quantities of the active diazonium species are available *in-situ* at any one time (Figure 3-26 B). For the allylation of the methylene position to generate the allylated product (**3.102**), literature conditions to allylate similar diarylmethane scaffoldings were utilized (Figure 3-27).¹²² Increased allyl bromide and base loadings (when compared to literature¹²²) were required for an adequate yield.

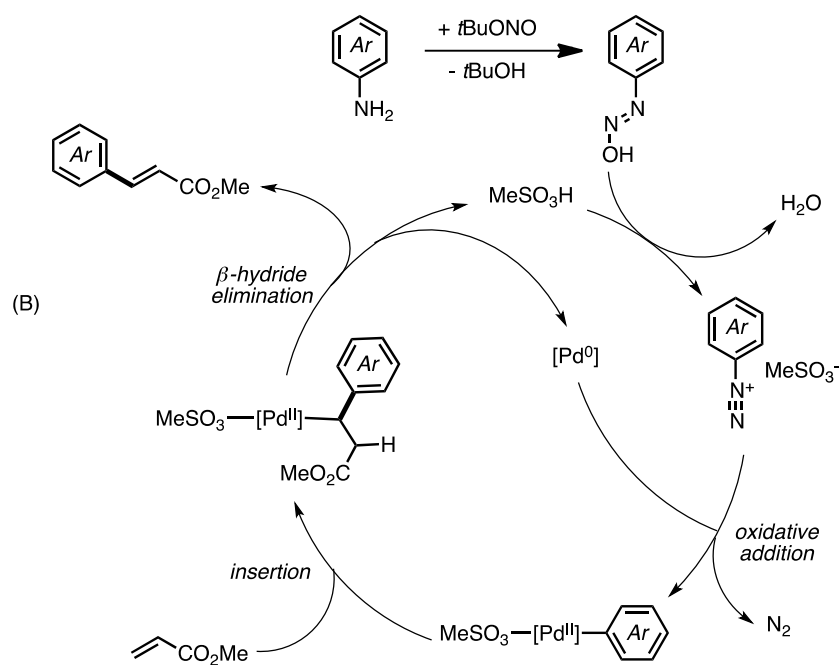
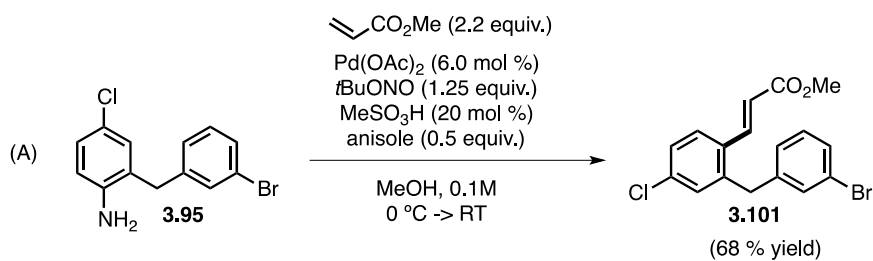


Figure 3-26 (A) Palladium-catalyzed Heck-Matsuda reaction to generate a functionalized alkene (**3.101**) via a diazonium salt intermediate; (B) proposed mechanism of dual-catalysis to generate sub-stoichiometric quantities of aryl-diazonium salt intermediate, coupled to a palladium-catalyzed Heck-Matsuda reaction

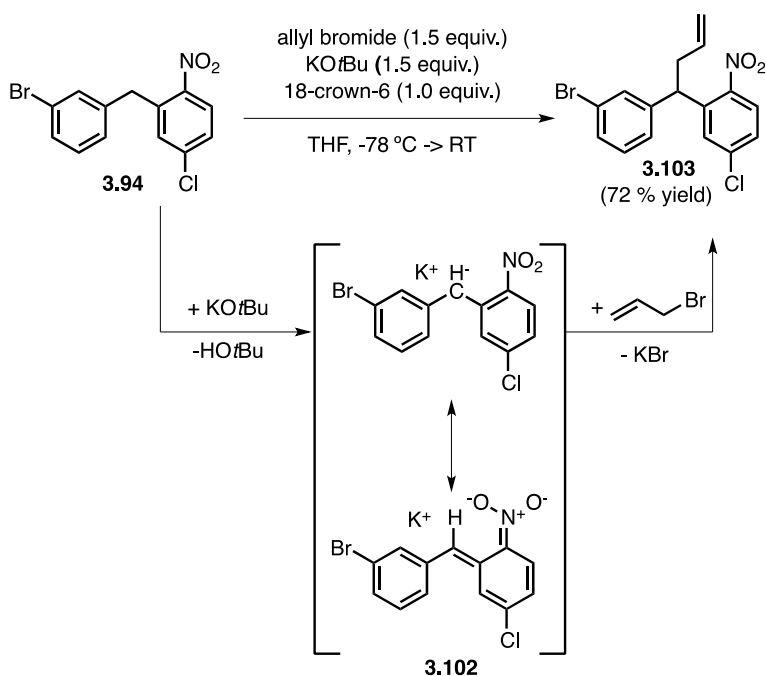


Figure 3-27 Methylene allylation to generate allylated product (**3.103**)

3.5 Proposed Mechanism

Preliminary mechanistic work in this reaction performed within our group (not included in this thesis) point towards a decarboxylation event occurring before the formation of the carbon-carbon bond.⁹⁸ Utilizing this information, we wish to propose the following potential mechanistic pathway (Figure 3-28). Starting from a Cu(II) species (**28-I**), transmetalation occurs with an arylboron to generate a Cu(II)-aryl (**28-II**). This is followed by trapping of an *in-situ* generated benzyl anion by decarboxylation, generating a new Cu(II)-aryl-benzyl species (**28-III**). This can be oxidized to Cu(III) (**28-IV**) by a disproportionation process, with a subsequent reductive elimination forming the desired product and a Cu(I) species (**28-V**). Oxidation of this metal centre by oxygen regenerates the Cu(II) (**28-I**), closing the cycle. A number of mechanistic questions remain unanswered, which require further work. In the presented mechanism, we

proposed that transmetalation of the arylboron occurs before the trapping of the benzyl anion. The inverse of this, trapping of the benzyl anion followed by transmetalation of the arylboron, is also a possibility. Another puzzling results it that this reaction performs poorly (~25% product yield) when no oxygen is present.⁹⁸ This is less than one productive turnover of catalyst. As such, oxygen may play multiple roles in this reaction, not solely as a turnover reagent (though the loading of metal is quite high, this reaction is catalytic by definition).

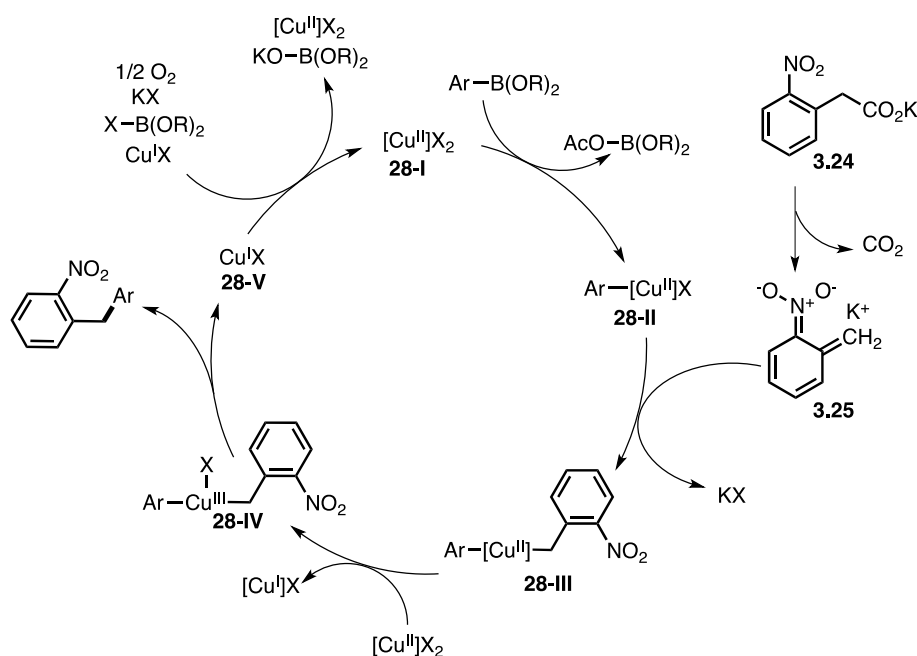


Figure 3-28 Proposed mechanisms for the copper-mediated decarboxylative oxidative synthesis of diarylmethanes by coupling of *ortho*-nitrophenyl acetates and arylboronic esters

3.6 Summary

We have developed a mild, copper-mediated synthesis of diarylmethanes by the oxidative decarboxylative coupling of *ortho*-nitroaryl acetates and arylboronic esters. The detrimental effect on water on the productive reaction, as well as the dependence on a specific rate of oxygen

diffusion into the reaction by atmospheric exposure, was demonstrated. A wide scope was explored, demonstrating the reaction's robust tolerance of a variety of functional groups. These include electrophilic functionalities such as aryl-halides and Michael acceptors, as well as protic-functionalities such as secondary amides and a primary alcohol. We saw significant limitations with arylboronic esters with *ortho*-fluorine substituents, and only a small number of heterocycles were successfully employed in this chemistry.

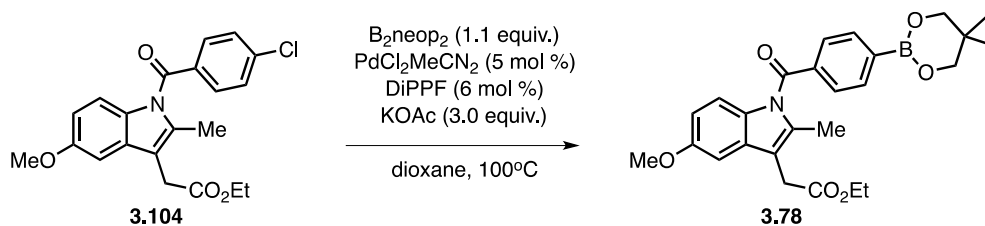
The utility of our synthesized diarylmethanes were demonstrated by a series of functionalizations. The chemoselective reduction of the nitroarene to the aniline was demonstrated in the presence of both an aryl-chloride and an aryl-bromide. This amine was transformed into a pinacol boronic ester, an iodide, and an acrylate, all proceeding through a diazonium salt intermediate that was generated *in-situ*. Allylation of the methylene position was also demonstrated. We proposed that this reaction proceeded through a Cu(I)/Cu(II)/Cu(III) catalytic cycle, with decarboxylation of the aryl acetate occurring prior to carbon-carbon bond formation.

3.7 Procedures and Characterization

3.7.1 General Considerations

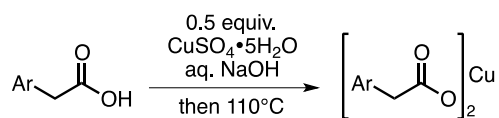
Unless noted, all reactions were conducted under inert atmosphere employing standard schlenk technique or by the use of a N₂-filled glovebox. All glassware was oven-dried prior to use. Flash chromatography was performed as described by Still and co-workers⁹⁹ (SiliaFlash P60, 40-63µm, 60A silica gel, Silicycle) or by automated flash chromatography (Isolera, HP-SIL or Ultra SNAP silica cartridges, Biotage). Analytical thin-layer chromatography was performed using glass plates pre-coated with silica (SiliaPlate G TLC - Glass-Backed, 250µm, Silicycle). TLC plates were visualized by UV light and/or staining with aqueous basic potassium permanganate. Unless otherwise noted, all reagents were obtained from commercial vendors and used as supplied. Potassium nitrophenylacetate salts were synthesized from the corresponding nitrophenylacetic acid as described by Liu and co-workers.¹²² Boronic esters were synthesized according to literature procedures from the corresponding boronic acids.¹⁰²⁻¹⁰³ Indomethacin ethyl ester (**3.104**) was prepared according to a literature procedure from Indomethacin, with a modified work-up procedure.¹²⁷ Certain compounds were not isolated and fully characterized. These include **3.58**, **3.64**, **3.66**, **3.68**, **3.70**, **3.89**, **3.91**, and **3.93**. The ¹H NMR yields reported for these compounds were by comparison to an internal standard. The diagnostic product signal that was utilized was a sharp singlet that would appear between δ 4.4-4.2 ppm, indicative of the methylene CH₂ of a diarylmethane where one of the aryl groups is an *ortho*-nitrophenyl.

3.7.2 Synthesis of Starting Materials



Starting Material 3.78 To a 1-dram vial in a nitrogen-filled glovebox was added $PdCl_2(MeCN)_2$ (14.3 mg, 0.055 mmol, 0.05 equiv.), 1,1'-bis(diisopropylphosphino)ferrocene (27.6 mg, 0.066 mmol, 0.06 equiv.), and anhydrous 1,4-dioxane (3.7 mL). Indomethacin ethyl ester (**3.104**) (424.4 mg, 1.10 mmol, 1.0 equiv.), $B_2(neop)_2$ (74.5 mg, 0.33 mmol, 1.1 equiv.), and potassium acetate (88.3 mg, 0.90 mmol, 3.0 equiv.) were sequentially added. The vial was sealed with a PTFE-lined septum cap, removed from the glovebox and heated at 100°C for 20 h. The reaction was cooled to room temperature and filtered through plug of silica, rinsing with ethyl acetate. The solution was concentrated *in vacuo* to provide a yellow solid, which was broken up. Pentane (10 mL) was added to the solid, and the suspension was sonicated for 10 minutes. The pentane was carefully removed via pipette, and this was repeated four additional times. The remaining pale yellow solid was dissolved in 10 mL of toluene, and concentrated *in vacuo* to azeotropically remove traces of water. The isolated material (**3.78**) was obtained in 66% yield (>95% pure by 1H NMR) and used without further purification.

General Procedure for the Synthesis of Copper(II) Arylacetate Salts



Starting Material 3.79 Carboxylic acid (1 equiv.) and 1M aq. NaOH (1 equiv) are combined and sonicated until mostly homogeneous (2–3 minutes). $\text{CuSO}_4 \cdot 5\text{H}_2\text{O}$ (0.5 equiv.) is added in one portion as a 1M aqueous solution. A precipitate immediately forms, and the mixture is gently stirred by agitation. The mixture is left to stand at least 30 minutes, at which point the precipitate is isolated by filtration. The obtained copper(II) arylacetate hydrate was dried under vacuum at 110°C for at least 2 hours to provide anhydrous copper(II) arylacetate in near quantitative yield (>90%).

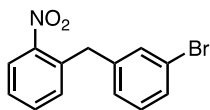
3.7.3 Oxidative Benzylolation Procedures and Characterization Data

General Procedure A (0.5 mmol scale): To a 1 dram vial was added $\text{Cu}(\text{OAc})_2$ (68.1 mg, 0.375 mmol, 0.75 equiv.), arylboronic neopentyl ester (0.50 mmol, 1.0 equiv.), and potassium nitrophenyl acetate (0.625 mmol, 1.25 equiv.), and charged with a stir-bar. Anhydrous DMA (2.5 mL) was added, and the solution was stirred 2 minutes until mostly homogeneous. The vial was sealed with a PTFE-lined cap and pierced with an 18 gauge needle, then gently stirred at 35°C . Upon reaction completion as monitored by ^1H NMR (12 to 48 h), the reaction mixture was diluted with EtOAc, and washed with saturated aqueous NH_4Cl , 0.1M aqueous KOH, and brine. The organic layer was dried with Na_2SO_4 , concentrated *in vacuo*, and purified by silica gel chromatography. For some reactions, additional KOH (0.1M, aq.) and deionized water washes were used to remove remaining arylboronic ester and diol respectively. *Select reactions were*

conducted on 0.2 mmol scale instead of 0.5 mmol scale, using a 0.5 dram vial instead of a 1 dram vial.

General Procedure B (using Cu(II) arylacetate salts): To a 0.5 dram vial was added Cu(II) arylacetate salt (0.15 mmol, 0.75 equiv.), arylboronic neopentyl ester (0.20 mmol, 1.0 equiv.), and potassium acetate (19.6 mg, 0.2 mmol, 1.0 equiv.), and charged with a stir-bar. Anhydrous DMA (1.0 mL) was added, and the solution was stirred 2 minutes. The vial was sealed with a PTFE-lined cap and pierced with an 18 gauge needle, then gently stirred at the indicated temperature (rt–40°C). Upon reaction completion as monitored by ¹H NMR (12 to 48 h), the reaction mixture was diluted with EtOAc, and washed with saturated aqueous NH₄Cl, 0.1M aqueous KOH, and brine. The organic layer with dried with Na₂SO₄, concentrated *in vacuo*, and purified by silica gel chromatography.

General Procedure C (using Cu(II) arylacetate salt as the limiting reagent): To a 0.5 dram vial was added Cu(II) arylacetate salt (0.1 mmol, 0.5 equiv.), arylboronic neopentyl ester (1.5 – 2.0 equiv.), and potassium acetate (9.8 mg, 0.1 mmol, 0.5 equiv.), and charged with a stir-bar. Anhydrous DMA (1.0 mL) was added, and the solution was stirred 2 minutes. The vial was sealed with a PTFE-lined cap and pierced with a 16 gauge needle, then gently stirred at 35°C. Upon reaction completion as monitored by ¹H NMR (12 to 48 h), the reaction mixture was diluted with EtOAc, and washed with saturated aqueous NH₄Cl, 0.1M aqueous KOH, and brine. The organic layer with dried with Na₂SO₄, concentrated *in vacuo*, and purified by silica gel chromatography.

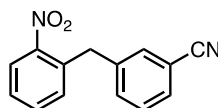


Product 3.26 Prepared according to the General Procedure A from the corresponding arylboronic neopentyl ester (135 mg, 0.50 mmol, 1.0 equiv.) and nitrophenylacetate salt (137 mg, 0.625 mmol, 1.25 equiv.), 20 h. Isolated in 71% yield after purification by silica gel chromatography (13:1 hexane:EtOAc) as a light yellow oil.

¹H NMR (CDCl₃, 498 MHz) δ 7.97 (m, 1H), 7.55 (m, 1H), 7.42 (m, 1H), 7.36 (m, 1H), 7.31 – 7.26 (m, 2H), 7.16 (m, 1H), 7.09 (m, 1H), 4.28 (s, 2H);

¹³C NMR (CDCl₃, 126 MHz) δ 149.3, 141.2, 134.9, 133.3, 132.6, 132.0, 130.3, 129.9, 127.9, 127.8, 125.2, 122.8, 38.2;

HRMS (EI): calcd for C₁₃H₁₀BrNO₂ [M]⁺: 290.9895. Found 290.9885.

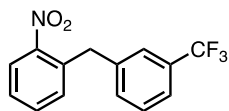


Product 3.28 Prepared according to the General Procedure A from the corresponding arylboronic neopentyl ester (108 mg, 0.50 mmol, 1.0 equiv.) and nitrophenylacetate salt (137 mg, 0.625 mmol, 1.25 equiv.), 23 h. Isolated in 66% yield after purification by silica gel chromatography (20:1 to 2:1 hexane:EtOAc) as a light yellow oil.

¹H NMR (CDCl₃, 700 MHz) δ 8.00 (dd, *J* = 8.2, 1.2 Hz, 1H), 7.59 (td, *J* = 7.6, 1.3 Hz, 1H), 7.51 (m, 1H), 7.46 (m, 1H), 7.42 – 7.37 (m, 3H), 7.30 (m, 1H), 4.34 (m, 2H);

¹³C NMR (CDCl₃, 176 MHz) δ 149.1, 140.3, 134.0, 133.5, 133.3, 132.6, 132.2, 130.4, 129.4, 128.2, 125.3, 118.7, 112.7, 38.2;

HRMS (EI): calcd for C₁₄H₉N₂O₂ [M-H]⁺: 237.0664. Found 237.0666.



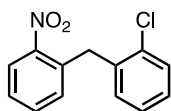
Product 3.30 Prepared according to the General Procedure A from the corresponding arylboronic neopentyl ester (129 mg, 0.50 mmol, 1.0 equiv.) and nitrophenylacetate salt (137 mg, 0.625 mmol, 1.25 equiv.), 26 h. Isolated in 69% yield after purification by silica gel column chromatography (40:1 to 10:1 Hexane:EtOAc, 5% toluene additive) as a light-yellow oil.

¹H NMR (CDCl₃, 400 MHz) δ 8.01 (dd, *J* = 8.2, 1.3 Hz, 1H), 7.59 (td, *J* = 7.5, 1.4 Hz, 1H), 7.51 (m, 1H), 7.48 – 7.41 (m, 3H), 7.36 (m, 1H), 7.31 (m, 1H), 4.39 (s, 2H);

¹³C NMR (CDCl₃, 126 MHz) δ 149.2, 139.7, 134.6, 133.2, 132.4, 132.3, 131.1 (q, *J* = 32.6 Hz), 129.0, 127.9, 125.5 (q, *J* = 3.9 Hz), 125.1, 124.0 (q, *J* = 272.5 Hz), 123.5 (q, *J* = 3.9 Hz), 38.2;

¹⁹F NMR (CDCl₃, 376 MHz) δ -62.6 (s);

HRMS (EI): calcd for C₁₄H₉F₃NO₂ [M-H]⁺: 280.0585. Found 280.0586.

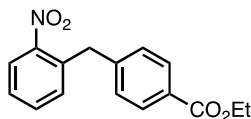


Product 3.32 Prepared according to the General Procedure A from the corresponding arylboronic neopentyl ester (112 mg, 0.50 mmol, 1.0 equiv.) and nitrophenylacetate salt (137 mg, 0.625 mmol, 1.25 equiv.), 19 h. Isolated in 58% yield after purification by silica gel chromatography (40:1 hexane:EtOAc) as a light yellow oil.

¹H NMR (CDCl₃, 498 MHz) δ 8.00 (dd, *J* = 8.1, 1.4 Hz, 1H), 7.61 (td, *J* = 7.6, 1.4 Hz, 1H), 7.44 – 7.39 (m, 2H), 7.27 – 7.19 (m, 2H), 7.13 (m, 1H), 7.08 (m, 1H), 4.45 (s, 2H);

^{13}C NMR (CDCl_3 , 126 MHz) δ 149.4, 136.5, 134.5, 134.4, 133.1, 131.7, 130.9, 129.7, 128.3, 127.5, 127.1, 124.8, 36.1;

HRMS (EI): calcd for $\text{C}_{13}\text{H}_{10}\text{ClNO}_2$ $[\text{M}]^+$: 247.0400. Found 247.0396.

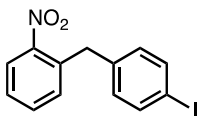


Product 3.34 Prepared according to the General Procedure A from the corresponding arylboronic neopentyl ester (131 mg, 0.50 mmol, 1.0 equiv.) and nitrophenylacetate salt (137 mg, 0.625 mmol, 1.25 equiv.), 24 h. Isolated in 63% yield after purification by silica gel chromatography (10:1 Hexane:EtOAc, 2% toluene) as a light yellow oil.

^1H NMR (CDCl_3 , 700 MHz) δ 8.00 – 7.97 (m, 3H), 7.56 (td, $J = 7.6, 1.3$ Hz, 1H), 7.43 (m, 1H), 7.31 – 7.29 (m, 1H), 7.25 – 7.22 (m, 2H), 4.39 (s, 2H), 4.38 (q, $J = 7.1$ Hz, 2H), 1.40 (t, $J = 7.2$ Hz, 3H);

^{13}C NMR (CDCl_3 , 126 MHz) δ 166.4, 149.3, 143.9, 134.8, 133.1, 132.5, 129.9, 129.0, 128.9, 127.8, 125.0, 60.9, 38.5, 14.3;

HRMS (EI): calcd for $\text{C}_{16}\text{H}_{15}\text{NO}_4$ $[\text{M}]^+$: 285.1001. Found 285.0995.

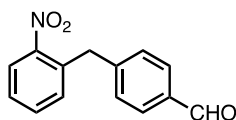


Product 3.36 Prepared according to the General Procedure A from the corresponding arylboronic neopentyl ester (158 mg, 0.50 mmol, 1.0 equiv.) and nitrophenylacetate salt (137 mg, 0.625 mmol, 1.25 equiv.), 23 h. Isolated in 55% yield after purification by silica gel chromatography (40:1 to 10:1 hex:EtOAc, 2% toluene additive) as a light yellow oil.

¹H NMR (CDCl₃, 700 MHz) δ 7.94 (dd, *J* = 8.2, 1.2 Hz, 1H), 7.61 – 7.58 (m, 2H), 7.52 (td, *J* = 7.6, 1.2 Hz, 1H), 7.40 – 7.38 (m, 1H), 7.26 – 7.24 (m, 1H), 6.90 – 6.88 (m, 2H), 4.24 (s, 2H);

¹³C NMR (CDCl₃, 176 MHz) δ 149.2, 138.4, 137.7, 135.0, 133.1, 132.4, 130.9, 127.7, 124.9, 91.9, 38.0;

HRMS (EI): calcd for C₁₃H₁₀INO₂ [M]⁺: 338.9756. Found 338.9751.

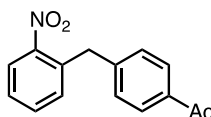


Product 3.38 Prepared according to the General Procedure A from the corresponding arylboronic neopentyl ester (109 mg, 0.50 mmol, 1.0 equiv.) and nitrophenylacetate salt (137 mg, 0.625 mmol, 1.25 equiv.), 19h. Isolated in 57% yield after purification by silica gel chromatography (19:1 to 1.5:1 Hexane:EtOAc) as a light yellow oil.

¹H NMR (CDCl₃, 400 MHz) δ 9.98 (s, 1H), 8.00 (dd, *J* = 8.2, 1.1 Hz, 1H), 7.83 – 7.79 (m, 2H), 7.57 (td, *J* = 7.6, 1.3 Hz, 1H), 7.43 (m, 1H), 7.34 – 7.29 (m, 3H), 4.40 (s, 2H);

¹³C NMR (CDCl₃, 126 MHz) δ 191.8, 149.2, 145.9, 135.0, 134.4, 133.3, 132.6, 130.1, 129.5, 128.0, 125.1, 38.8;

HRMS (EI): calcd for C₁₄H₁₀NO₄ [M-H]⁺: 240.0661. Found 240.0659.

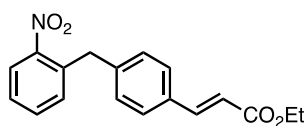


Product 3.40 Prepared according to the General Procedure A from the corresponding arylboronic neopentyl ester (116 mg, 0.5 mmol, 1.0 equiv.) and nitrophenylacetate salt (137 mg,

0.625 mmol, 1.25 equiv.), 20h. Isolated in 50% yield after purification by silica gel chromatography (4:1 to 1:1 Hexane:EtOAc) as a colorless oil.

$^1\text{H NMR}$ (CDCl_3 , 400 MHz) δ 7.98 (dd, $J = 8.1, 1.2$ Hz, 1H), 7.91 – 7.86 (m, 2H), 7.56 (td, $J = 7.5, 1.2$ Hz, 1H), 7.43 (m, 1H), 7.30 (m, 1H), 7.26 – 7.22 (m, 2H), 4.37 (s, 2H), 2.57 (s, 3H);

$^{13}\text{C NMR}$ (CDCl_3 , 126 MHz) δ 197.7, 149.2, 144.3, 135.6, 134.6, 133.2, 132.6, 129.1, 128.7, 127.9, 125.1, 38.5, 26.6;

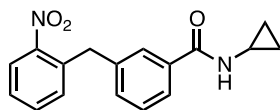


Product 3.42 Prepared according to the General Procedure A from the corresponding arylboronic neopentyl ester (57.6 mg, 0.20 mmol, 1.0 equiv.) and nitrophenylacetate salt (54.8 mg, 0.25 mmol, 1.25 equiv.), 15h. 61% by $^1\text{H NMR}$ using durene as internal standard. Isolated in 48% (>90% pure, diaryl ether side-product present) yield after purification by silica gel chromatography (50:1 to 4:1 hexane:EtOAc) as a yellow solid.

$^1\text{H NMR}$ (CDCl_3 , 498 MHz) δ 7.98 (dd, $J = 8.3, 1.4$ Hz, 1H), 7.67 (d, $J = 16.1$ Hz, 1H), 7.56 (td, $J = 7.6, 1.3$ Hz, 1H), 7.49 – 7.45 (m, 2H), 7.43 (m, 1H), 7.31 (dd, $J = 7.8, 1.1$ Hz, 1H), 7.21 – 7.11 (m, 2H), 6.42 (d, $J = 16.0$ Hz, 1H), 4.35 (s, 2H), 4.28 (q, $J = 7.1$ Hz, 2H), 1.35 (t, $J = 7.1$ Hz, 3H);

$^{13}\text{C NMR}$ (CDCl_3 , 126 MHz) δ 167.0, 149.3, 144.1, 141.1, 135.0, 133.1, 132.9, 132.5, 129.4, 128.3, 127.7, 125.0, 118.0, 60.5, 38.3, 14.3;

HRMS (EI): calcd for $\text{C}_{18}\text{H}_{17}\text{NO}_4$ $[\text{M}]^+$: 311.1158. Found 311.1155.

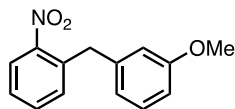


Product 3.44 Prepared according to the General Procedure A from the corresponding arylboronic neopentyl ester (54.6 mg, 0.20 mmol, 1.0 equiv.) and nitrophenylacetate salt (54.8 mg, 0.25 mmol, 1.25 equiv.), 25h. Isolated in 52% yield after purification by silica gel chromatography (1:1 hexane:EtOAc) as a yellow solid.

¹H NMR (CDCl₃, 700 MHz) δ 7.94 (dd, J = 8.2, 1.3 Hz, 1H), 7.55 – 7.53 (m, 2H), 7.52 (dd, J = 7.6, 1.4 Hz, 1H), 7.39 (m, 1H), 7.33 (t, J = 8.1 Hz, 1H), 7.28 – 7.25 (m, 2H), 6.15 (bs, 1H), 4.33 (s, 2H), 2.87 (m, 1H), 0.87 – 0.83 (m, 2H), 0.61 – 0.58 (m, 2H);

¹³C NMR (CDCl₃, 126 MHz) δ 168.8, 149.2, 139.3, 135.0, 134.9, 133.2, 132.5, 132.0, 128.8, 127.7, 127.6, 125.0, 124.9, 38.3, 23.2, 6.8;

HRMS (ESI): calcd for C₁₇H₁₆N₂O₃Na [M+Na]⁺: 319.1053. Found 319.1057.

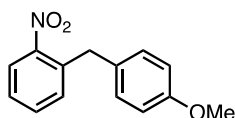


Product 3.46 Prepared according to the General Procedure A from the corresponding arylboronic neopentyl ester (110 mg, 0.50 mmol, 1.0 equiv.) and nitrophenylacetate salt (137 mg, 0.625 mmol, 1.25 equiv.), 19h. Isolated in 64% yield after purification by silica gel chromatography (30:1 to 20:1 hexane:EtOAc) as a light yellow oil.

¹H NMR (CDCl₃, 498 MHz) δ 7.95 (dd, J = 8.3, 1.4 Hz, 1H), 7.53 (td, J = 7.5, 1.4, 1H), 7.40 (m, 1H), 7.30 (m, 1H), 7.23 (t, J = 8.1 Hz, 1H), 6.79 (m, 1H), 6.76 (m, 1H), 6.72 (m, 1H), 4.31 (s, 2H), 3.79 (s, 3H);

^{13}C NMR (CDCl_3 , 126 MHz) δ 159.8, 149.3, 140.2, 135.5, 132.9, 132.3, 129.6, 127.4, 124.8, 121.4, 114.9, 111.8, 55.2, 38.3;

HRMS (EI): calcd for $\text{C}_{14}\text{H}_{13}\text{NO}_3$ $[\text{M}]^+$: 243.0895. Found 243.0889.

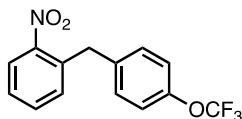


Product 3.48 Prepared according to the General Procedure A from the corresponding arylboronic neopentyl ester (110 mg, 0.50 mmol, 1.0 equiv.) and nitrophenylacetate salt (121 mg, 0.55 mmol, 1.1 equiv.), 34 h. Isolated in 71% yield after purification by silica gel chromatography (20:1 to 10:1 hexane:EtOAc) as a light yellow oil.

^1H NMR (CDCl_3 , 498 MHz) δ 7.92 (m, 1H), 7.51 (m, 1H), 7.37 (m, 1H), 7.28 (m, 1H), 7.11—7.06 (m, 2H), 6.87 – 6.82 (m, 2H), 4.26 (s, 2H), 3.80 (s, 3H);

^{13}C NMR (CDCl_3 , 126 MHz) δ 158.5, 149.5, 136.4, 133.0, 132.4, 130.8, 130.2, 127.4, 124.8, 114.2, 55.4, 37.6;

HRMS (EI): calcd for $\text{C}_{14}\text{H}_{13}\text{NO}_3$ $[\text{M}]^+$: 243.0895. Found 243.0889.



Product 3.50 Prepared according to the General Procedure A from the corresponding arylboronic neopentyl ester (137 mg, 0.50 mmol, 1.0 equiv.) and nitrophenylacetate salt (137 mg, 0.625 mmol, 1.25 equiv.), 26 h. Isolated in 71% yield after purification by silica gel chromatography (20:1 Hexane:EtOAc, 2% toluene additive) as a clear, light-yellow oil.

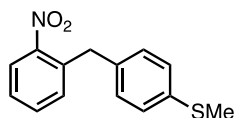
¹H NMR (CDCl₃, 498 MHz) δ 7.96 (dd, *J* = 8.1, 1.3 Hz, 1H), 7.55 (dd, *J* = 7.59, 1.3 Hz, 1H), 7.44 – 7.39 (m, 1H), 7.30 – 7.27 (m, 1H), 7.19 – 7.11 (m, 4H), 4.31 (s, 2H);

¹³C NMR (CDCl₃, 126 MHz) δ 149.2, 147.9 (d, *J* = 1.3 Hz), 137.4, 135.1, 133.2, 132.4, 130.2, 127.8, 125.0, 121.1, 120.4 (q, *J* = 257.2 Hz), 37.6;

¹⁹F NMR (CDCl₃, 376 MHz) δ –58.0 (s);

HRMS (EI): calcd for C₁₄H₉F₃NO₃ [M-H]⁺: 296.0535. Found 296.0533.

HRMS (EI): calcd for C₁₅H₁₃NO₃ [M]⁺: 285.0895. Found 285.0889.

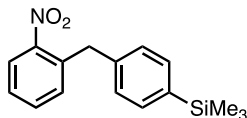


Product 3.52 Prepared according to the General Procedure A from the corresponding arylboronic neopentyl ester (118 mg, 0.50 mmol, 1.0 equiv.) and nitrophenylacetate salt (137 mg, 0.625 mmol, 1.25 equiv.), 19h. Isolated in 49% yield after purification by silica gel chromatography (99:1 to 9:1 hexane:EtOAc) as a light yellow oil.

¹H NMR (CDCl₃, 700 MHz) δ 7.92 (dd, *J* = 8.2, 1.3 Hz, 1H), 7.50 (td, *J* = 7.6, 1.3 Hz, 1H), 7.37 (m, 1H), 7.26 (m, 1H), 7.19 – 7.17 (m, 2H), 7.08 – 7.05 (m, 2H), 4.25 (s, 2H), 2.45 (s, 3H);

¹³C NMR (CDCl₃, 126 MHz) δ 149.3, 136.6, 135.63, 135.61, 133.0, 132.3, 129.5, 127.5, 127.0, 124.8, 37.8, 16.0;

HRMS (EI): calcd for C₁₄H₁₃NO₂S [M]⁺: 259.0667. Found 259.0667.

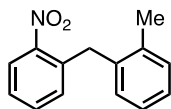


Product 3.54 Prepared according to the General Procedure A from the corresponding arylboronic neopentyl ester (131 mg, 0.50 mmol, 1.0 equiv.) and nitrophenylacetate salt (137 mg, 0.625 mmol, 1.25 equiv.), 50h. 61% yield by ^1H NMR using durene as internal standard. Isolated in 42% yield after purification by silica gel chromatography (30:1 Hexane:EtOAc) as a light yellow oil.

^1H NMR (CDCl_3 , 400 MHz) δ 7.94 (dd, $J = 8.2, 1.3$ Hz, 1H), 7.52 (td, $J = 7.6, 1.4$ Hz, 1H), 7.46 – 7.43 (m, 2H), 7.38 (m, 1H), 7.29 (m, 1H), 7.16 – 7.13 (m, 2H), 4.30 (s, 2H), 0.25 (s, 9H);

^{13}C NMR (CDCl_3 , 126 MHz) δ 149.3, 139.2, 138.5, 135.6, 133.7, 132.9, 132.5, 128.4, 127.4, 124.8, 38.3, -1.1;

HRMS (EI): calcd for $\text{C}_{16}\text{H}_{19}\text{NO}_2\text{Si}$ $[\text{M}]^+$: 285.1185. Found 285.1179.

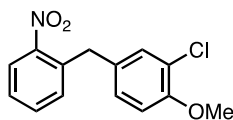


Product 3.56 Prepared according to the General Procedure A from the corresponding arylboronic neopentyl ester (102 mg, 0.50 mmol, 1.0 equiv.) and nitrophenylacetate salt (137 mg, 0.625 mmol, 1.25 equiv.), 26 h. 65% yield by ^1H NMR using durene as internal standard.

^1H NMR (CDCl_3 , 498 MHz) δ 7.99 (dd, $J = 8.1, 1.4$ Hz, 1H), 7.48 (td, $J = 7.6, 1.3$ Hz, 1H), 7.4 (m, 1H) 7.24 – 7.14 (m, 3H), 7.07 – 7.04 (m, 1H), 6.99 (m, 1H), 4.32 (s, 2H), 2.23 (s, 3H);

^{13}C NMR (CDCl_3 , 126 MHz) δ 149.5, 136.8, 136.7, 135.4, 133.0, 131.4, 130.5, 129.7, 127.2, 127.0, 126.3, 124.7, 35.9, 19.5;

HRMS (EI): calcd for $\text{C}_{14}\text{H}_{13}\text{NO}_2$ $[\text{M}]^+$: 227.0946. Found 227.0946.

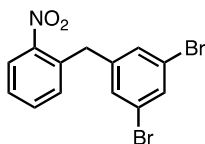


Product 3.60 Prepared according to the General Procedure A from the corresponding arylboronic neopentyl ester (50.9 mg, 0.20 mmol, 1.0 equiv.) and nitrophenylacetate salt (54.8 mg, 0.25 mmol, 1.25 equiv.), 12h. Isolated in 70% yield after purification by silica gel chromatography (50:1 to 19:1 Hexane:EtOAc) as a light yellow oil.

¹H NMR (CDCl₃, 700 MHz) δ 7.93 (dd, J = 8.2, 1.3 Hz, 1H), 7.52 (td, J = 7.6, 1.3 Hz, 1H), 7.38 (m, 1H), 7.26 (m, 1H), 7.14 (d, J = 2.2 Hz, 1H), 7.01 (dd, J = 8.5, 2.2 Hz, 1H), 6.84 (d, J = 8.4 Hz, 1H), 4.22 (s, 2H), 3.86 (s, 3H);

¹³C NMR (CDCl₃, 126 MHz) δ 153.7, 149.2, 135.4, 133.1, 132.3, 131.8, 130.6, 128.3, 127.6, 124.9, 122.5, 56.2, 37.3;

HRMS (ESI): calcd for C₁₄H₁₁ClNO₃ [M-H]⁻: 276.0433. Found 276.0429.

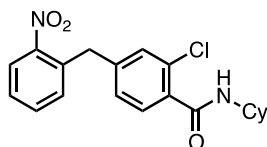


Product 3.64 Prepared according to the General Procedure A from the corresponding arylboronic neopentyl ester (174 mg, 0.50 mmol, 1.0 equiv.) and nitrophenylacetate salt (137 mg, 0.625 mmol, 1.25 equiv.), 17 h. 57% yield by ¹H NMR using durene as internal standard. Isolated in 39% yield after purification by silica gel chromatography (hexane to 16:1 hexane:EtOAc) as puffy white solid.

¹H NMR (CDCl₃, 498 MHz) δ 8.03 (dd, J = 8.3, 1.1 Hz, 1H), 7.60 (td, J = 7.6, 1.3 Hz, 1H), 7.55 (m, 1H), 7.46 (m, 1H), 7.30 (m, 1H), 7.25 – 7.23 (m, 2H), 4.27 (s, 2H);

^{13}C NMR (CDCl_3 , 126 MHz) δ 149.0, 142.7, 133.9, 133.5, 132.6, 132.4, 130.7, 128.2, 125.3, 123.1, 37.9;

HRMS (EI): calcd for $\text{C}_{13}\text{H}_9\text{Br}_2\text{NO}_2$ $[\text{M}]^+$: 368.9000. Found 368.9007.

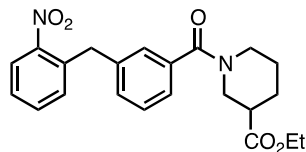


Product 3.72 Prepared according to the General Procedure A from the corresponding arylboronic neopentyl ester (69.9 mg, 0.20 mmol, 1.0 equiv.) and nitrophenylacetate salt (54.8 mg, 0.25 mmol, 1.25 equiv.), 8h. Isolated in 55% yield after purification by silica gel chromatography (2:1 Hexane:EtOAc) as a yellow solid.

^1H NMR (CDCl_3 , 700 MHz) δ 7.99 (dd, $J = 8.2, 1.4$ Hz, 1H), 7.57 (d, $J = 8.0$ Hz, 1H), 7.56 (td, $J = 7.6, 1.3$ Hz, 1H), 7.42 (m, 1H), 7.27 (dd, $J = 7.7, 1.0$ Hz, 1H), 7.15 (m, 1H), 7.09 (m, 1H), 6.02 (d, $J = 7.5$ Hz, 1H), 4.30 (s, 2H), 4.09 (m, 1H), 2.04 – 1.99 (m, 2H), 1.75 – 1.70 (m, 2H), 1.62 (m, 1H), 1.45 – 1.38 (m, 2H), 1.28 – 1.18 (m, 3H);

^{13}C NMR (CDCl_3 , 126 MHz) δ 165.3, 149.1, 142.5, 134.2, 133.8, 133.4, 132.6, 130.7, 130.4, 130.3, 128.1, 127.6, 125.2, 48.9, 38.0, 32.9, 25.6, 24.7;

HRMS (ESI): calcd for $\text{C}_{20}\text{H}_{21}\text{ClN}_2\text{O}_3\text{Na}$ $[\text{M}+\text{Na}]^+$: 395.1133. Found 395.1135.

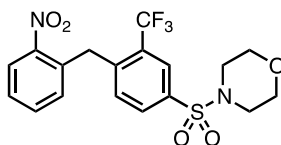


Product 3.74 Prepared according to the General Procedure A from the corresponding arylboronic neopentyl ester (93.3 mg, 0.25 mmol, 1.0 equiv.) and nitrophenylacetate salt (68.5 mg, 0.313 mmol, 1.25 equiv.), 18h. Isolated in 55% yield after purification by silica gel chromatography (2:1 to 1:1 hexane:EtOAc) as a thick light yellow oil.

¹H NMR (DMSO-*d*₆, 120 °C, 400 MHz) δ 7.87 (dd, $J = 8.2, 1.3$ Hz, 1H), 7.61 (td, $J = 7.6, 1.3$ Hz, 1H), 7.49 – 7.42 (m, 2H), 7.30 (t, $J = 7.8$ Hz, 1H), 7.19 – 7.15 (m, 2H), 7.07 (m, 1H), 4.25 (s, 2H), 4.03 (qd, $J = 7.0, 1.5$ Hz, 2H), 3.93 (m, 1H), 3.61 (m, 1H), 3.18 (dd, $J = 12.8, 9.3$ Hz, 1H), 3.03 (m, 1H), 2.46 (m, 1H), 1.94 (m, 1H), 1.65 (m, 2H), 1.40 (m, 1H), 1.13 (t, $J = 7.0$ Hz, 3H);

¹³C NMR (DMSO-*d*₆, 120 °C, 101 MHz) δ 172.7, 169.7, 150.0, 139.7, 137.1, 134.6, 133.5, 132.9, 129.9, 128.9, 128.4, 127.2, 125.2, 124.7, 60.4, 46.2, 45.3, 41.2, 37.5, 27.0, 24.1, 14.3;

HRMS (ESI): calcd for C₂₂H₂₅N₂O₅ [M+H]⁺: 397.1758. Found 397.1750.



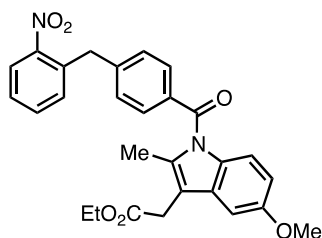
Product 3.76 Prepared according to the General Procedure A from the corresponding arylboronic neopentyl ester (81.4 mg, 0.20 mmol, 1.0 equiv.) and nitrophenylacetate salt (54.8 mg, 0.25 mmol, 1.25 equiv.), 8h. Isolated in 66% yield (95% purity, 5% protodeborylation side-product present) after purification by silica gel chromatography (10:1 to 1:4 Hexane:EtOAc) as a yellow solid.

¹H NMR (CDCl₃, 700 MHz) δ 8.11 (dd, *J* = 8.1, 1.3 Hz, 1H), 8.09 (m, 1H), 7.79 (dd, *J* = 8.2, 1.7 Hz, 1H), 7.63 (td, *J* = 7.6, 1.3 Hz, 1H), 7.53 (m, 1H), 7.19 (m, 1H), 7.15 (m, 1H), 4.61 (s, 2H), 3.79 – 3.76 (m, 4H), 3.06 – 3.03 (m, 4H);

¹³C NMR (CDCl₃, 126 MHz) δ 149.2, 143.4 (q, *J* = 1.3 Hz), 134.5, 133.7, 132.9, 132.8, 131.4, 131.1 (q, *J* = 1.1 Hz), 129.9 (q, *J* = 31.2 Hz), 128.6, 125.7 (q, *J* = 6.0 Hz), 125.4, 123.5 (q, *J* = 274.6 Hz), 66.0, 45.9, 35.3 (q, *J* = 2.6 Hz);

¹⁹F NMR (CDCl₃, 376 MHz) -60.7 (s);

HRMS (ESI): calcd for C₁₈H₁₆F₃N₂O₅S [M-H]⁻: 429.0738. Found 429.0732.

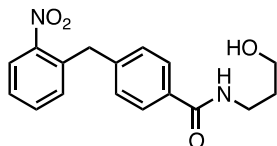


Product 3.78 Prepared according to the General Procedure A from the corresponding arylboronic neopentyl ester (96.4 mg, 0.20 mmol, 1.0 equiv.) and nitrophenylacetate salt (54.8 mg, 0.25 mmol, 1.25 equiv.), 10h. Isolated in 48% yield after purification by silica gel chromatography (16:1 to 1:1 Hexane:EtOAc) as a yellow solid.

¹H NMR (CDCl₃, 500 MHz) δ 7.99 (dd, *J* = 8.3, 1.3 Hz, 1H), 7.66 – 7.63 (m, 2H), 7.59 (td, *J* = 7.6, 1.3 Hz, 1H), 7.45 (m, 1H), 7.34 (dd, *J* = 7.8, 1.1 Hz, 1H), 7.28 – 7.25 (m, 2H), 6.98 (d, *J* = 2.6 Hz, 1H), 6.89 (d, *J* = 9.0 Hz, 1H), 6.68 (dd, *J* = 9.2, 2.6 Hz, 1H), 4.43 (s, 2H), 4.17 (q, *J* = 7.1 Hz, 2H), 3.85 (s, 3H), 3.66 (s, 2H), 2.37 (s, 3H), 1.27 (t, *J* = 7.2 Hz, 3H);

¹³C NMR (CDCl₃, 126 MHz) δ 170.9, 169.2, 155.9, 149.3, 144.0, 136.0, 134.5, 134.0, 133.2, 132.6, 131.0, 130.6, 130.1, 129.2, 128.0, 125.1, 115.0, 112.4, 111.6, 101.2, 61.0, 55.7, 38.7, 30.5, 14.3, 13.4;

HRMS (ESI): calcd for C₂₈H₂₇N₂O₆ [M+H]⁺: 487.1864. Found 487.1857.

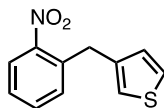


Product 3.81 Prepared according to the General Procedure B from the corresponding arylboronic neopentyl ester (58.2 mg, 0.20 mmol, 1.0 equiv.) and copper arylacetate salt (63.6 mg, 0.15 mmol, 0.75 equiv.), 10h. 41% yield by ¹H NMR using durene as internal standard. Isolated in 20% yield after purification by silica gel chromatography (19:1 CH₂Cl₂:MeOH) as a yellow solid.

¹H NMR (CDCl₃, 700 MHz) δ 7.96 (dd, *J* = 8.2, 1.3 Hz, 1H), 7.70 – 7.67 (m, 2H), 7.54 (td, *J* = 7.60, 1.34 Hz, 1H), 7.41 (m, 1H), 7.27 (m, 1H), 7.22 – 7.20 (m, 2H), 6.52 (m, 1H), 4.35 (s, 2H), 3.70 (q, *J* = 5.4 Hz, 2H), 3.62 (q, *J* = 6.16 Hz, 2H), 2.93 (t, *J* = 5.96 Hz, 1H), 1.78 (pent, *J* = 5.71 Hz, 2H);

¹³C NMR (CDCl₃, 126 MHz) δ 168.2, 149.2, 142.6, 134.9, 133.2, 132.6, 132.5, 129.1, 127.8, 127.3, 125.0, 59.8, 38.4, 37.2, 32.2;

HRMS (ESI): calcd for C₁₇H₁₇N₂O₄ [M-H]⁻: 313.1194. Found 313.1194.

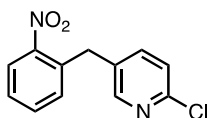


Product 3.83 Prepared according to the General Procedure A from the corresponding arylboronic neopentyl ester (98.0 mg, 0.50 mmol, 1.0 equiv.) and nitrophenylacetate salt (137.0 mg, 1.25 mmol, 1.25 equiv.), 24h. Isolated in 56% yield after purification by prep plate (20:1 to 15:1 hexane:EtOAc) as a light yellow oil.

¹H NMR (CDCl₃, 700 MHz) δ 7.92 (dd, *J* = 8.2, 1.3 Hz, 1H), 7.64 (td, *J* = 7.6, 1.2 Hz, 1H), 7.37 (m, 1H), 7.31 (m, 1H), 7.25 (m, 1H), 6.96 (m, 1H), 6.90 (dd, *J* = 5.0, 1.2 Hz, 1H), 4.30 (s, 2H);

¹³C NMR (CDCl₃, 126 MHz) δ 149.2, 138.8, 135.5, 133.1, 132.1, 128.3, 127.5, 125.9, 124.8, 122.2, 33.2;

HRMS (EI): calcd for C₁₁H₉NO₂S [M]⁺: 219.0354. Found 219.0351.

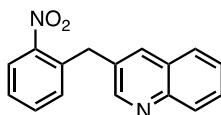


Product 3.85 Prepared according to the General Procedure A from the corresponding arylboronic neopentyl ester (45 mg, 0.20 mmol, 1.0 equiv.) and nitrophenylacetate salt (55 mg, 0.25 mmol, 1.25 equiv.), 7 h. 52% yield by ¹H NMR using durene as internal standard. Isolated in 58% yield after purification by silica gel chromatography (4:1 hexane:EtOAc) as a light yellow oil (90% pure, pyridyl homocoupling side-product present).

¹H NMR (CDCl₃, 498 MHz) δ 8.25 (m, 1H), 8.02 (m, 1H), 7.60 (m, 1H), 7.49 – 7.43 (m, 2H), 7.32 (m, 1H), 7.26 (m, 1H), 4.31 (s, 2H);

¹³C NMR (CDCl₃, 126 MHz) δ 149.88, 149.86, 139.1, 137.0, 134.0, 133.5, 133.3, 132.4, 128.2, 125.3, 124.2, 35.2;

HRMS (ESI): calcd for C₁₂H₁₀ClN₂O₂ [M+H]⁺: 248.0353. Found 248.0353.



Product 3.87 Prepared according to the General Procedure A from the corresponding arylboronic neopentyl ester (48.2 mg, 0.20 mmol, 1.0 equiv.) and nitrophenylacetate salt (54.8

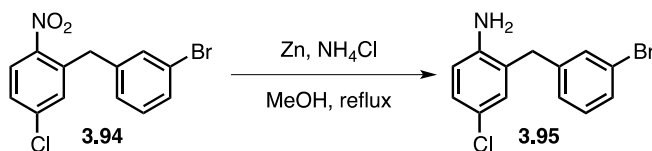
mg, 0.25 mmol, 1.25 equiv.), 9h. Isolated in 47% yield after purification by silica gel chromatography (2:1 to 1:1 Hexane:EtOAc) as a light yellow solid.

$^1\text{H NMR}$ (CDCl_3 , 700 MHz) δ 8.80 (d, $J = 2.4$ Hz, 1H), 8.08 (m, 1H), 8.01 (dd, $J = 8.3, 1.3$ Hz, 1H), 7.87 (m, 1H), 7.72 (m, 1H), 7.67 (m, 1H), 7.57 (td, $J = 7.7, 1.4$ Hz, 1H), 7.51 (m, 1H), 7.42 (m, 1H), 7.35 (m, 1H), 4.50 (s, 2H);

$^{13}\text{C NMR}$ (CDCl_3 , 126 MHz) δ 151.7, 149.1, 147.0, 135.1, 134.5, 133.4, 132.5, 131.6, 129.2, 129.2, 128.0, 128.0, 127.5, 126.9, 125.2, 36.0;

HRMS (ESI): calcd for $\text{C}_{16}\text{H}_{13}\text{N}_2\text{O}_2$ $[\text{M}+\text{H}]^+$: 265.0972. Found 265.0970.

3.7.4 Functionalization Procedures and Characterization Data

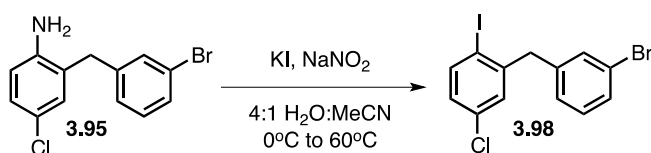


Product 3.95 Adapted from a literature procedure.¹²³ To a 200 mL RBF with stir bar, added diarylmethane (1.11 g, 3.4 mmol, 1.0 equiv.), zinc powder (1.67 g, 25.5 mmol, 7.5 equiv.), ammonium chloride (364 mg, 6.8 mmol, 2.0 equiv.), and 25 mL of methanol. The reaction was refluxed for 2 hours, upon which the reaction mixture was cooled and filtered through a plug of Celite, rinsing with EtOAc, and concentrated *in vacuo*. The residue was dissolved in EtOAc (130 mL) and sequentially washed with water (70 mL) and brine (70 mL). The organic layer was dried with Na_2SO_4 , and concentrated *in vacuo* to yield the title compound in 94% yield as a bright orange oil.

¹H NMR (CDCl₃, 498 MHz) δ 7.39 (m, 1H), 7.34 (m, 1H), 7.19 (t, *J* = 7.7 Hz, 1H), 7.11 (m, 1H), 7.08 (dd, *J* = 8.4, 2.5 Hz, 1H), 7.03 (m, 1H), 6.63 (d, *J* = 8.5 Hz, 1H), 3.84 (s, 2H), 3.56 – 3.44 (bs, 2H);

¹³C NMR (CDCl₃, 126 MHz) δ 143.2, 140.9, 131.4, 130.4, 130.2, 129.9, 127.8, 127.1, 125.7, 123.4, 123.0, 117.1, 37.4;

HRMS (EI): calcd for C₁₃H₁₁BrClN [M]⁺: 294.9763. Found 294.9762.

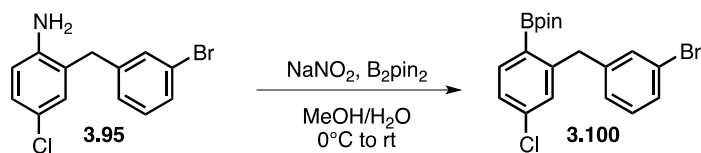


Product 3.98 Adapted from a literature procedure.¹²⁴ To a 0.5-dram vial charged with a stir bar was added the corresponding aniline (60 mg, 0.2 mmol, 1.0 equiv.), 0.5 mL H₂O, 0.5 mL conc HCl (aq.), and 0.5 mL MeCN. The reaction was cooled to 0°C, NaNO₂ (15 mg, 0.22 mmol, 1.1 equiv.) was added dropwise as a solution in H₂O (0.5 mL). KI (37 mg, 0.22 mmol, 1.1 equiv.) dissolved in H₂O, was added dropwise at 0°C which provided a red solution. The reaction was warmed to room temperature, and then heated to 60°C overnight. Additional EtOAc (50 mL) and water (30 mL) were added, followed by aq. satd. NaHCO₃ (20 mL) and 2M aq. Na₂S₂O₃ (5 mL). The organic layer was separated, washed with brine (30 mL), dried with Na₂SO₄, filtered, and concentrated *in vacuo* to provide the title compound in 78% yield as an amber oil.

¹H NMR (CDCl₃, 498 MHz) δ 7.78 (d, *J* = 8.5 Hz, 1H), 7.40 (m, 1H), 7.34 (m, 1H), 7.20 (t, *J* = 7.9 Hz, 1H), 7.12 – 7.09 (m, 2H), 6.96 (dd, *J* = 8.4, 2.5 Hz, 1H), 4.05 (s, 2H);

¹³C NMR (CDCl₃, 126 MHz) δ 144.6, 141.0, 140.6, 134.8, 132.0, 130.3, 130.2, 129.8, 128.6, 127.7, 122.8, 98.1, 45.9;

HRMS (EI): calcd for C₁₃H₉BrClI [M]⁺: 405.8621. Found 405.8620.

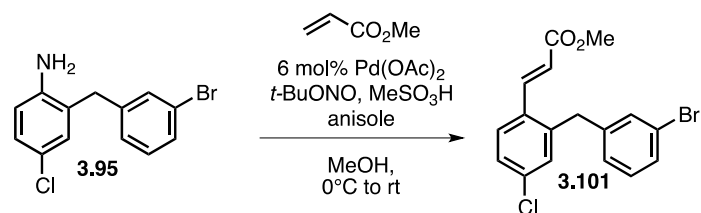


Product 3.100 Adapted from a literature procedure.¹²⁵ To a 1-dram vial charged with stir bar, was added the corresponding aniline (59 mg, 0.2 mmol, 1.0 equiv.), 0.5 mL MeOH, 0.75 mL 1M aqueous HCl, and 0.75 mL MeCN. The reaction was cooled to 0°C, and NaNO₂ (15 mg, 0.22 mmol, 1.1 equiv.) was added dropwise as an aqueous solution (0.25 mL). After stirring at 0°C for 20 minutes, B₂pin₂ (152 mg, 0.6 mmol, 3.0 equiv.) was added as a solution in MeOH (0.5 mL). The reaction warmed to room temperature and stirred for 3 hours, at which point H₂O (5 mL) and EtOAc (60 mL) were added. The organic layer was washed with sat. aqueous NaHCO₃ (30 mL) and brine (30 mL), then dried with Na₂SO₄, filtered, and concentrated *in vacuo*. Isolated in 55% yield after purification by silica gel chromatography (49:1 to 19:1 hexane:EtOAc) as a yellow oil.

¹H NMR (CDCl₃, 498 MHz) δ 7.76 (d, J = 8.0, 1H), 7.37 (m, 1H), 7.29 (m, 1H), 7.21 (m, 1H), 7.15 (m, 1H), 7.11 (m, 1H), 7.05 (m, 1H), 4.25 (m, 2H), 1.28 (s, 12H);

¹³C NMR (CDCl₃, 126 MHz) δ 148.7, 144.2, 138.0, 137.4, 132.2, 130.1, 129.9, 129.1, 127.6, 126.1, 122.5, 84.0, 40.5, 24.9, (*C-[B]* carbon could not be detected);

HRMS (EI): calcd for C₁₉H₂₁BBrClO₂ [M]⁺: 406.0507. Found 406.0513.



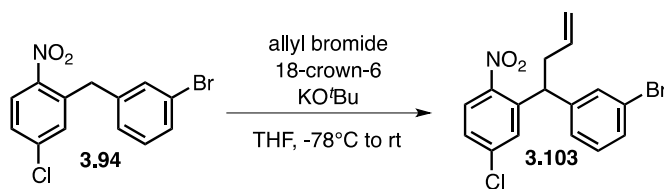
Product 3.101 Adapted from a literature procedure.¹²⁶ To a 1-dram vial charged with a stir bar was added the corresponding aniline (59.3 mg, 0.2 mmol, 1.0 equiv.) and 1.0 mL MeOH. This

solution was cooled to 0°C, and 90% *t*-BuONO (33 mL, 0.25 mmol, 1.25 equiv.) was added dropwise, resulting in a yellow suspension, and was stirred for an additional 30 minutes at 0°C. Methyl acrylate (40 mL, 0.44 mmol, 2.2 equiv.) in 0.8 mL MeOH, Pd(OAc)₂ (2.7 mg, 0.012 mmol, 0.06 equiv.), MeSO₃H (3.8 mg, 0.04 mmol, 0.20 equiv.) in 0.4 mL MeOH, and anisole (11 mL, 0.10 mmol, 0.5 equiv.) were sequentially added at 0°C. The reaction was warmed to RT and stirred until full conversion was observed by GC (~41 hours), at which point the reaction mixture was concentrated *in vacuo*. The residue was dissolved in EtOAc and sequentially washed with saturated aq. NaHCO₃ and brine. The organic layer was dried with Na₂SO₄, and concentrated *in vacuo*. Purification by silica-gel column chromatography (19:1 to 7:1 hexane:EtOAc) provided the title compound in 68% yield as a yellow oil.

¹H NMR (CDCl₃, 498 MHz) δ 7.90 (d, *J* = 15.7 Hz, 1H), 7.54 (s, *J* = 8.6 Hz, 1H), 7.36 (m, 1H), 7.29 – 7.26 (m, 2H), 7.19 – 7.15 (m, 2H), 7.06 (m, 1H), 6.32 (d, *J* = 15.7 Hz, 1H), 4.07 (s, 2H), 3.80 (s, 3H);

¹³C NMR (CDCl₃, 126 MHz) δ 166.9, 141.5, 140.9, 140.8, 136.1, 132.1, 131.7, 130.7, 130.3, 129.8, 128.2, 127.6, 127.4, 122.8, 120.3, 51.8, 38.4;

HRMS (EI): calcd for C₁₇H₁₅BrClO₂ [M+H]⁺: 364.9938. Found 364.9935.



Product 3.103 Adapted from a literature procedure.¹²² To a 2-dram vial charged with a stir bar was added nitroarene (98 mg, 0.3 mmol, 1.0 equiv.). The vial was sealed with a PTFE-lined cap, then evacuated and backfilled with N₂. THF (1 mL) was added and the solution was cooled to -

10°C. A solution of potassium *tert*-butoxide (51 mg, 0.45 mmol, 1.5 equiv.) and 18-crown-6 (79 mg, 0.3 mmol, 1.0 equiv.) in THF (1 mL) was added dropwise, maintaining the reaction at -10°C. An instant color change to a deep ink-blue occurs.

To a separate sealed 2-dram vial under N₂ was added allyl bromide (39 μ L, 0.45 mmol, 1.5 equiv.) and anhydrous THF (4 mL); this vial was cooled to -78°C. The nitroarene containing mixture was quantitatively transferred (via dropwise addition) to the allyl bromide solution. The reaction was warmed to room temperature and stirred 5 hours, then diluted with EtOAc (50 mL), deionized H₂O (40 mL) and brine (40 mL). The organic layer was separated and dried over Na₂SO₄, filtered, and concentrated *in vacuo*. Isolated in 72% yield after purification by silica gel chromatography (40:1 to 60:1 pentane:Et₂O) as an off-white solid.

¹H NMR (CDCl₃, 700 MHz) δ 7.90 (d, *J* = 8.6 Hz, 1H), 7.39 – 7.36 (m, 2H), 7.35 (m, 1H), 7.32 (m, 1H), 7.2 – 7.16 (m, 2H), 5.66 (m, 1H), 5.05 – 5.00 (m, 2H), 4.75 (t, *J* = 7.8 Hz, 1H), 2.83 – 2.70 (m, 2H);

¹³C NMR (CDCl₃, 176 MHz) δ 148.3, 143.9, 140.1, 139.3, 134.6, 131.3, 130.4, 130.38, 129.8, 127.8, 127.1, 126.2, 123.0, 118.3, 44.2, 39.7;

HRMS (APPI): calcd for C₁₆H₁₃BrClNO₂ [M]⁺: 364.9813. Found 364.9812.

REFERENCES

1. Seechurn, C. C. C. J.; DeAngelis, A.; Colacot, T. J., Introduction to New Trends in Cross-Coupling. In *New Trends in Cross-Coupling: Theory and Applications*, Colacot, T., Ed. The Royal Society of Chemistry: Cambridge, United Kingdom, 2015; pp 1-19.
2. Miyaura, N.; Suzuki, A., *Chem. Rev.* **1995**, *95*, 2457-2483.
3. Martin, R.; Buchwald, S. L., *Acc. Chem. Res.* **2008**, *41*, 1461-1473.
4. Chen, X.; Engle, K. M.; Wang, D. H.; Yu, J. Q., *Angew. Chem. Int. Ed.* **2009**, *48*, 5094-5115.
5. Tasker, S. Z.; Standley, E. A.; Jamison, T. F., *Nature* **2014**, *509*, 299-309.
6. Tollefson, E. J.; Hanna, L. E.; Jarvo, E. R., *Acc. Chem. Res.* **2015**, *48*, 2344-2353.
7. Smith, G. B.; Dezen, G. C.; Hughes, D. L.; King, A. O.; Verhoeven, T. R., *J. Org. Chem.* **1994**, *59*, 8151-8156.
8. Amatore, C.; Jutand, A.; Le Duc, G., *Chem. Eur. J.* **2011**, *17*, 2492-2503.
9. Torborg, C.; Beller, M., *Adv. Synth. Catal.* **2009**, *351*, 3027-3043.
10. Xu, S.; Kim, E. H.; Wei, A.; Negishi, E. I., *Sci. Technol. Adv. Mat.* **2014**, *15*, 044201.
11. Ruiz-Castillo, P.; Buchwald, S. L., *Chem. Rev.* **2016**, *116*, 12564-12649.
12. Lightowler, S.; Hird, M., *Chem. Mater.* **2004**, *16*, 3963-3971.
13. Lei, A.; Shi, W.; Liu, C.; Liu, W.; Zhang, H.; He, C., Oxidative Coupling - Bonding between Two Nucleophiles. In *Oxidative Cross-Coupling Reactions*, Wiley-VCH Verlag GmbH & Co. KGaA: 2016; pp 1-5.
14. Liu, C.; Zhang, H.; Shi, W.; Lei, A., *Chem. Rev.* **2011**, *111*, 1780-1824.
15. Shi, W.; Liu, C.; Lei, A., *Chem. Soc. Rev.* **2011**, *40*, 2761-2776.
16. Lei, A.; Liu, C.; Jin, L., *Synlett* **2010**, *2010*, 2527-2536.
17. Siemsen, P.; Livingston, R. C.; Diederich, F., *Angew. Chem. Int. Ed.* **2000**, *39*, 2632-2657.
18. Glaser, C., *Ber. Dtsch. Chem.* **1869**, *2*, 422-424.
19. Hay, A. S., *J. Org. Chem.* **1962**, *27*, 3320-3321.
20. Clifford, A. A.; Waters, W. A., *J. Chem. Soc.* **1963**, *0*, 3056-3062.
21. Bohlmann, F.; Schönowsky, H.; Inhoffen, E.; Gray, G., *Chem. Ber.* **1964**, *97*, 794-800.
22. Chan, D. M. T.; Monaco, K. L.; Wang, R.-P.; Winters, M. P., *Tetrahedron Lett.* **1998**, *39*, 2933-2936.

23. Evans, D. A.; Katz, J. L.; West, T. R., *Tetrahedron Lett.* **1998**, *39*, 2937-2940.
24. Lam, P. Y. S.; Clark, C. G.; Saubern, S.; Adams, J.; Winters, M. P.; Chan, D. M. T.; Combs, A., *Tetrahedron Lett.* **1998**, *39*, 2941-2944.
25. Herradura, P. S.; Pendola, K. A.; Guy, R. K., *Org. Lett.* **2000**, *2*, 2019-2022.
26. Wang, L.; Wang, M.; Huang, F., *Synlett* **2005**, 2007-2010.
27. King, A. E.; Brunold, T. C.; Stahl, S. S., *J. Am. Chem. Soc.* **2009**, *131*, 5044-5045.
28. King, A. E.; Ryland, B. L.; Brunold, T. C.; Stahl, S. S., *Organometallics* **2012**, *31*, 7948-7957.
29. Tromp, M.; van Strijdonck, G. P. F.; van Berkel, S. S.; van den Hoogenband, A.; Feiters, M. C.; de Bruin, B.; Fiddy, S. G.; van der Eerden, A. M. J.; van Bokhoven, J. A.; van Leeuwen, P. W. N. M.; Koningsberger, D. C., *Organometallics* **2010**, *29*, 3085-3097.
30. Cox, P. A.; Leach, A. G.; Campbell, A. D.; Lloyd-Jones, G. C., *J. Am. Chem. Soc.* **2016**, *138*, 9145-9157.
31. Ishiyama, T.; Murata, M.; Miyaura, N., *J. Org. Chem.* **1995**, *60*, 7508-7510.
32. Ishiyama, T.; Takagi, J.; Ishida, K.; Miyaura, N.; Anastasi, N. R.; Hartwig, J. F., *J. Am. Chem. Soc.* **2001**, *124*, 390-391.
33. Cho, J.-Y.; Tse, M. K.; Holmes, D.; Maleczka Jr., R. E.; Smith III, M. R., *Science* **2002**, *295*, 305-308.
34. Billingsley, K. L.; Barder, T. E.; Buchwald, S. L., *Angew. Chem. Int. Ed.* **2007**, *46*, 5359-5363.
35. Larsen, M. A.; Hartwig, J. F., *J. Am. Chem. Soc.* **2014**, *136*, 4287-4299.
36. Larsen, M. A.; Wilson, C. V.; Hartwig, J. F., *J. Am. Chem. Soc.* **2015**, *137*, 8633-8643.
37. Vantourout, J. C.; Law, R. P.; Isidro-Llobet, A.; Atkinson, S. J.; Watson, A. J., *J. Org. Chem.* **2016**, *81*, 3942-3950.
38. Tzschucke, C. C.; Murphy, J. M.; Hartwig, J. F., *Org. Lett.* **2007**, *9*, 761-764.
39. Sueki, S.; Kuninobu, Y., *Org. Lett.* **2013**, *15*, 1544-1547.
40. McGarry, K. A.; Duenas, A. A.; Clark, T. B., *J. Org. Chem.* **2015**, *80*, 7193-7204.
41. Marcum, J. S.; McGarry, K. A.; Ferber, C. J.; Clark, T. B., *J. Org. Chem.* **2016**, *81*, 7963-7969.
42. Vantourout, J. C.; Miras, H. N.; Isidro-Llobet, A.; Sproules, S.; Watson, A. J., *J. Am. Chem. Soc.* **2017**, *139*, 4769-4779.

43. Stevens, J. M.; MacMillan, D. W., *J. Am. Chem. Soc.* **2013**, *135*, 11756-11759.
44. Moon, P. J.; Halperin, H. M.; Lundgren, R. J., *Angew. Chem. Int. Ed.* **2016**, *55*, 1894-1898.
45. Weaver, J. D.; Recio, A., 3rd; Grenning, A. J.; Tunge, J. A., *Chem. Rev.* **2011**, *111*, 1846-1913.
46. Rodriguez, N.; Goossen, L. J., *Chem. Soc. Rev.* **2011**, *40*, 5030-5048.
47. Larrosa, I.; Cornella, J., *Synthesis* **2012**, *44*, 653-676.
48. Wei, Y.; Hu, P.; Zhang, M.; Su, W., *Chem. Rev.* **2017**, *117*, 8864-8907.
49. Richard, J. P., *Pure Appl. Chem.* **2011**, *83*, 1555-1565.
50. Li, T.; Huo, L.; Pulley, C.; Liu, A., *Bioorg. Chem.* **2012**, *43*, 2-14.
51. Jordan, F.; Patel, H., *ACS Catal.* **2013**, *3*, 1601-1617.
52. Staunton, J.; Weissman, K. J., *Nat. Prod. Rep.* **2001**, *18*, 380-416.
53. Nakamura, S., *Org. Biomol. Chem.* **2014**, *12*, 394-405.
54. Hara, N.; Nakamura, S.; Funahashi, Y.; Shibata, N., *Adv. Synth. Catal.* **2011**, *353*, 2976-2980.
55. Shang, R.; Xu, Q.; Jiang, Y. Y.; Wang, Y.; Liu, L., *Org. Lett.* **2010**, *12*, 1000-1003.
56. Goossen, L. J.; Lange, P. P.; Rodriguez, N.; Linder, C., *Chem. Eur. J.* **2010**, *16*, 3906-3909.
57. Bi, H. P.; Zhao, L.; Liang, Y. M.; Li, C. J., *Angew. Chem. Int. Ed.* **2009**, *48*, 792-795.
58. Boto, A.; Hernandez, R.; de Leon, Y.; Suarez, E., *J. Org. Chem.* **2001**, *66*, 7796-7803.
59. Huang, W.; Wang, M.; Yue, H., *Synthesis* **2008**, *2008*, 1342-1344.
60. Zuo, W.; Ahneman, D. T.; Chu, L.; Terrett, J. A.; Doyle, A. G.; MacMillan, D. W., *Science* **2014**, *345*, 437-440.
61. Lundgren, R.; Fahandej-Sadi, A., *Synlett* **2017**, *28*, 2886-2890.
62. Purser, S.; Moore, P. R.; Swallow, S.; Gouverneur, V., *Chem. Soc. Rev.* **2008**, *37*, 320-330.
63. Wang, J.; Sanchez-Rosello, M.; Acena, J. L.; del Pozo, C.; Sorochinsky, A. E.; Fustero, S.; Soloshonok, V. A.; Liu, H., *Chem. Rev.* **2014**, *114*, 2432-506.
64. Zhou, Y.; Wang, J.; Gu, Z.; Wang, S.; Zhu, W.; Acena, J. L.; Soloshonok, V. A.; Izawa, K.; Liu, H., *Chem. Rev.* **2016**, *116*, 422-518.
65. Neumann, C. N.; Ritter, T., *Angew. Chem. Int. Ed.* **2015**, *54*, 3216-3221.

66. Champagne, P. A.; Desroches, J.; Hamel, J. D.; Vandamme, M.; Paquin, J. F., *Chem. Rev.* **2015**, *115*, 9073-174.
67. Campbell, M. G.; Ritter, T., *Chem. Rev.* **2015**, *115*, 612-33.
68. Moon, P. J.; Yin, S.; Lundgren, R. J., *J. Am. Chem. Soc.* **2016**, *138*, 13826-13829.
69. Adolph, H. G.; Kamlet, M. J., *J. Am. Chem. Soc.* **1966**, *88*, 4761-4763.
70. Hine, J.; Mahone, L. G.; Liotta, C. L., *J. Am. Chem. Soc.* **1967**, *89*, 5911-5920.
71. Zhang, Z.; Puente, A.; Wang, F.; Rahm, M.; Mei, Y.; Mayr, H.; Prakash, G. K., *Angew. Chem. Int. Ed.* **2016**, *55*, 12845-9.
72. Fina, N. J.; Edwards, J. O., *Int. J. Chem. Kinet.* **1973**, *5*, 1-26.
73. Kabore, L.; Chebli, S.; Faure, R.; Larent, E.; Marquet, B., *Tetrahedron Lett.* **1990**, *31*, 3137-3140.
74. Weinberg, N. L.; Brown, E. A., *J. Org. Chem.* **1966**, *31*, 4054-4058.
75. Weinberg, N. L.; Brown, E. A., *J. Org. Chem.* **1966**, *31*, 4058-4061.
76. Weinberg, N. L.; Reddy, T. B., *J. Am. Chem. Soc.* **1968**, *90*, 91-94.
77. Weinberg, N. L., *J. Org. Chem.* **1968**, *33*, 4326-4329.
78. Gray, E. E.; Nielsen, M. K.; Choquette, K. A.; Kalow, J. A.; Graham, T. J.; Doyle, A. G., *J. Am. Chem. Soc.* **2016**, *138*, 10802-10805.
79. Zhao, X.; Zhang, Y.; Wang, J., *Chem. Commun.* **2012**, *48*, 10162-10173.
80. Jacobson, O.; Kiesewetter, D. O.; Chen, X., *Bioconjug. Chem.* **2015**, *26*, 1-18.
81. van der Born, D.; Pees, A.; Poot, A. J.; Orru, R. V. A.; Windhorst, A. D.; Vugts, D. J., *Chem. Soc. Rev.* **2017**, *46* (15), 4709-4773.
82. Searle, N. E.; Newman, M. S.; Ottmann, G. F.; Grundmann, C. F., *Org. Synth.* **1956**, *36*, 25.
83. Clark, J. D.; Shah, A. S.; Peterson, J. C., *Thermochim. Acta* **2002**, *392-393*, 177-186.
84. Ford, A.; Miel, H.; Ring, A.; Slattery, C. N.; Maguire, A. R.; McKervey, M. A., *Chem. Rev.* **2015**, *115*, 9981-10080.
85. Goldberg, N. W.; Shen, X.; Li, J.; Ritter, T., *Org. Lett.* **2016**, *18*, 6102-6104.
86. Tang, P.; Wang, W.; Ritter, T., *J. Am. Chem. Soc.* **2011**, *133*, 11482-11484.
87. Sladojevich, F.; Arlow, S. I.; Tang, P.; Ritter, T., *J. Am. Chem. Soc.* **2013**, *135*, 2470-2473.
88. Fujimoto, T.; Ritter, T., *Org. Lett.* **2015**, *17*, 544-547.

89. Paull, D. H.; Scerba, M. T.; Alden-Danforth, E.; Widger, L. R.; Lectka, T., *J. Am. Chem. Soc.* **2008**, *130*, 17260-17261.
90. Erb, J.; Alden-Danforth, E.; Kopf, N.; Scerba, M. T.; Lectka, T., *J. Org. Chem.* **2010**, *75*, 969-971.
91. Harsanyi, A.; Sandford, G.; Yufit, D. S.; Howard, J. A., *Beilstein J. Org. Chem.* **2014**, *10*, 1213-1219.
92. Qing, F.-L.; Guo, C.; Yue, X., *Synthesis* **2010**, *2010*, 1837-1844.
93. Su, Y. M.; Feng, G. S.; Wang, Z. Y.; Lan, Q.; Wang, X. S., *Angew. Chem. Int. Ed.* **2015**, *54*, 6003-6007.
94. Lloyd-Jones, G. C., *Angew. Chem. Int. Ed.* **2002**, *41*, 953-956.
95. Liu, Q.; Dong, X.; Li, J.; Xiao, J.; Dong, Y.; Liu, H., *ACS Catal.* **2015**, *5*, 6111-6137.
96. Yu, W.; Xu, X.-H.; Qing, F.-L., *New. J. Chem.* **2016**, *40*, 6564-6567.
97. Weinreb, S. M.; Nahm, S., *Tetrahedron Lett.* **1981**, *22*, 3815-3818.
98. Moon, P. J.; Fahandej-Sadi, A.; Qian, W.; Lundgren, R. J., *Angew. Chem. Int. Ed.* **2018**, DOI: 10.1002/anie.201800829.
99. Still, W. C.; Kahn, M.; Mitra, A., *J. Org. Chem.* **1978**, *43*, 2923-2925.
100. Leeper, F. J.; Rock, M.; Appleton, D., *J. Chem. Soc.-Perkin Trans. 1* **1996**, 2633-2642.
101. Morris, T. S.; Frommann, S.; Shechosky, S.; Lowe, C.; Lall, M. S.; GaussMuller, V.; Purcell, R. H.; Emerson, S. U.; Vederas, J. C.; Malcolm, B. A., *Bioorg. Med. Chem.* **1997**, *5*, 797-807.
102. Huang, Y. J.; Jiang, Y. B.; Bull, S. D.; Fossey, J. S.; James, T. D., *Chem. Commun.* **2010**, *46*, 8180-8182.
103. Matthew, S. C.; Glasspoole, B. W.; Eisenberger, P.; Crudden, C. M., *J. Am. Chem. Soc.* **2014**, *136*, 5828-5831.
104. Long, Y.-Q.; Jiang, X.-H.; Dayam, R.; Sanchez, T.; Shoemaker, R.; Sei, S.; Neamati, N., *J. Med. Chem.* **2004**, *47*, 2561-2573.
105. Gangjee, A.; Devraj, R.; Queener, S. F., *J. Med. Chem.* **1997**, *40*, 470-478.
106. Emmerich, J.; Hu, Q.; Hanke, N.; Hartmann, R. W., *J. Med. Chem.* **2013**, *56*, 6022-6032.
107. Moree, W. J.; Li, B. F.; Jovic, F.; Coon, T.; Yu, J.; Gross, R. S.; Tucci, F.; Marinkovic, D.; Zamani-Kord, S.; Malany, S.; Bradbury, M. J.; Hernandez, L. M.; O'Brien, Z.; Wen,

- J.; Wang, H.; Hoare, S. R.; Petroski, R. E.; Saccaan, A.; Madan, A.; Crowe, P. D.; Beaton, G., *J. Med. Chem.* **2009**, *52*, 5307-5310.
108. Barawkar, D. A.; Meru, A.; Bandyopadhyay, A.; Banerjee, A.; Deshpande, A. M.; Athare, C.; Koduru, C.; Khose, G.; Gundu, J.; Mahajan, K.; Patil, P.; Kandalkar, S. R.; Niranjana, S.; Bhosale, S.; De, S.; Mukhopadhyay, S.; Chaudhary, S.; Koul, S.; Singh, U.; Chugh, A.; Palle, V. P.; Mookhtiar, K. A.; Vacca, J.; Chakravarty, P. K.; Nargund, R. P.; Wright, S. D.; Roy, S.; Graziano, M. P.; Singh, S. B.; Cully, D.; Cai, T. Q., *ACS Med. Chem. Lett* **2011**, *2*, 919-923.
109. Calloway, N. O., *Chem. Rev.* **1935**, *17*, 327-392.
110. Rueping, M.; Nachtsheim, B. J., *Beilstein J. Org. Chem.* **2010**, *6*, DOI: 10.3762/bjoc.6.6.
111. Mo, X.; Yakiwchuk, J.; Dansereau, J.; McCubbin, J. A.; Hall, D. G., *J. Am. Chem. Soc.* **2015**, *137*, 9694-9703.
112. Vukovic, V. D.; Richmond, E.; Wolf, E.; Moran, J., *Angew. Chem. Int. Ed.* **2017**, *56*, 3085-3089.
113. Ueda, M.; Nakakoji, D.; Kuwahara, Y.; Nishimura, K.; Ryu, I., *Tetrahedron Lett.* **2016**, *57*, 4142-4144.
114. Wu, G.; Xu, S.; Deng, Y.; Wu, C.; Zhao, X.; Ji, W.; Zhang, Y.; Wang, J., *Tetrahedron* **2016**, *72*, 8022-8030.
115. Do, H. Q.; Chandrashekar, E. R.; Fu, G. C., *J. Am. Chem. Soc.* **2013**, *135*, 16288-16291.
116. Zhou, Q.; Cobb, K. M.; Tan, T.; Watson, M. P., *J. Am. Chem. Soc.* **2016**, *138*, 12057-60.
117. Storr, T. E.; Teskey, C. J.; Greaney, M. F., *Chem. Eur. J.* **2016**, *22*, 18169-18178.
118. Vasilopoulos, A.; Zultanski, S. L.; Stahl, S. S., *J. Am. Chem. Soc.* **2017**, *139*, 7705-7708.
119. Zhang, W.; Chen, P.; Liu, G., *J. Am. Chem. Soc.* **2017**, *139*, 7709-7712.
120. Bull, D. J.; Fray, M. J.; Mackenny, M. C.; Malloy, K. A., *Synlett* **1996**.
121. Xu, Z.; Wang, Q.; Zhu, J., *Angew. Chem. Int. Ed.* **2013**, *52*, 3272-3276.
122. Shang, R.; Huang, Z.; Chu, L.; Fu, Y.; Liu, L., *Org. Lett.* **2011**, *13*, 4240-4243.
123. Tsukinoki, T.; Tsuzuki, H., *Green Chem.* **2001**, *3*, 37-38.
124. Lesueur, W.; Solari, E.; Floriani, C.; Chiesi-Villa, A.; Rizzoli, C., *Inorg. Chem.* **1997**, *36*, 3354-3362.
125. Xue, D.; Zhao, C.-J.; Jia, Z.-H.; Wang, C.; Xiao, J., *Synlett* **2014**, *25*, 1577-1584.
126. Callonnec, F. L.; Fouquet, E.; Felpin, F.-X., *Org. Lett.* **2011**, *13*, 2646-2649.

127. Yin, G.; Kalvet, I.; Englert, U.; Schoenebeck, F., *J. Am. Chem. Soc.* **2015**, *137*, 4164-4172.